Mineral Reconnaissance Programme Report

D. Slater
Programme Manager
Mineral Reconnaissance Programme
British Geological Survey
154 Clerkenwell Road
London EC1R 5DU

Uned Arolwg Daearegol Cymru
Wales Geological Survey Unit
Bryn Eithyn Hall
Llanfarian
Aberystwyth SY23 4BY

No. 73

Platinum-group element mineralisation in the Unst ophiolite, Shetland

Mineral Reconnaissance Programme

Report No. 73

Platinum-group element mineralisation in the Unst ophiolite, Shetland

Geochemistry
A. G. Gunn, BA, MSc
R. C. Leake, BSc, PhD

Mineralogy
M. T. Styles, BSc, PhD

Contributor
J. H. Bateson, BSc, MIMM

Mineral Reconnaissance Programme Reports

Bibliographic reference
Gunn, A. G., Leake, R. C., and Styles, M. T. 1985. Platinum-group element mineralisation in the Unst ophiolite, Shetland. *Mineral Reconnaissance Programme Rep. Br. Geol. Surv.,* No. 73.

CONTENTS

APPENDICES

FIGURES

TABLES

PLATE

SUMMARY

The ophiolitic basic and ultrabasic rocks of the island of Unst, Shetland comprise a sequence of harzburgites, dunites, clinopyroxene-rich cumulates, and gabbro, within tectonic blocks that have been thrust over a migmatite complex during the Lower Palaeozoic. Concentrations of chromite are found in the harzburgite and dunite, and to a small extent in the pyroxene cumulate rocks. They occur as disseminations, sometimes forming millimetre scale layers, and as more massive schlieren and pods of chromitite. Five alteration or hydrothermal events have been recognised in the ultrabasic rocks. These comprise early pervasive serpentinisation, later fracture controlled serpentinisation, veining and pervasive carbonation, minor late serpentine veining and talc-carbonate alteration controlled by fault zones.

Exploration for platinum group element (PGE) mineralisation was carried out using a combination of drainage, overburden and rock sampling. Analyses of PGE were obtained by fire assay followed by either neutron activation analysis or flameless atomic absorption spectrometry, and up to 20 other elements were determined by X-ray fluoresence analysis.

Panned concentrate samples were taken from 73 drainage sites distributed throughout the complex. Ir, the only PGE determined in all samples, showed a greater concentration in samples derived from the harzburgite unit than those from other units. Low amplitude anomalies are present in three discrete areas in the harzburgite but the maximum level of 210 ppb Ir is associated with a sample derived from a prominent N-S zone of faulting and hydrothermal activity markedly discordant to the regional trend of layering in the harzburgite and dunite. This discordant zone, which extends for at least 7 km, is also marked by samples containing enrichments in Fe, Co, Ni, Cu and As. The highest Cr levels are associated with an area in the north of the harzburgite with no previous history of chromite working but where many locally derived pieces of chromitite float have been discovered. Relatively high Cr levels are also associated with the area of dunite containing the greatest concentration of visible chromite and old workings.

A technique of collecting panned heavy mineral concentrates from overburden samples was adopted as a reconnaissance exploration technique after orientation sampling in the harzburgite unit at Cliff, an area with high PGE levels in chromitite and associated dunite. Systematic sampling in the Cliff area outlined a zone of coincident Pd, Pt and Rh enrichment near to but separate from the chromite workings known to be enriched in PGE. In contrast the distribution of Ru was entirely different with scattered low amplitude anomalous zones and a maximum anomaly 300m from the chromite-rich zone. Reconnaissance lines were sampled at other locations within the harzburgite, dunite and cumulate units. Low amplitude Pd and Pt anomalies were detected within the dunite unit, especially in a traverse across the trace of the prominent N-S fault zone at Helliers Water, adjacent to the outcrop of the cumulate unit. In general the overburden data suggest some association between PGE enrichment and enhanced levels of Ni relative to typical silicate levels apparent when expressed as the ratio Ni/MgO.

Rock samples were collected from all parts of the complex, including most of the main chromitite workings. Very high levels of all PGE occur in samples of chromitite, chromite-rich dunite and dunite from the Cliff area, with a strong

positive intercorrelation between all PGE. The proportions of the various PGE are very similar to those present in deposits in major layered basic/ultrabasic complexes like Bushveld and Stillwater, with strong relative enrichment in Pd and Pt. These PGE proportions are completely different from the Ru-Ir-Os dominant assemblage typical of ophiolitic rocks. Associated with high levels of PGE are enrichments in Ni, Cu, As, Sb and Te. There is no correlation with Cr and some samples of chromitite from the Cliff area contain only background levels of PGE.

High to moderate levels of PGE with the same proportions of elements as the Cliff samples also occur in samples of chromitite and serpentinised dunite from the dunite unit and in samples of pyroxenite from the cumulate unit. In contrast PGE-rich samples of chromitite from the harzburgite unit near Harold's Grave have entirely different proportions of PGE with Ru and Ir in greatest abundance. This PGE distribution is similar to that in some background samples of harzburgite and closely resembles the pattern found in typical ophiolites. The PGE in the Harold's Grave samples do not exhibit the Ni enhancement noted in the Cliff PGE mineralisation.

In samples from the Cliff area the platinum-group minerals (PGM) sperrylite, stibiopalladinite, hollingworthite, laurite and possibly irarsite have been identified, mostly as grains less than 10 microns in size. In chromite-rich rocks these minerals occur within chlorite haloes around chromite, in the blackened altered rims of chromite grains and in interstitial Ni-rich serpentine/carbonate intergrowths in association with pentlandite, orcellite and other Ni sulphides and arsenides, sometimes spatially related to chlorite-carbonate-magnetite veins. They also occur as fine grains within magnetite rims around chromite and in magnetite or carbonate veins in dunite. The Ni sulphide/arsenide assemblage associated with the PGM is characteristic of serpentinisation at temperatures less than 500°C, well below the range of magmatic conditions. A hydrothermal origin for the PGE mineralisation is proposed, probably related to the second phase of serpentinisation. This involved the redistribution of Ni accompanied by the introduction of As, Sb and Te probably with a structural control. Pre-existing concentrations of chromite may have acted as a precipitation barrier causing rich PGM deposition in the alteration haloes around chromite grains.

Continuous borehole or trench sections through mineralised zones are required to assess the economic significance of the PGE mineralisation. Nevertheless the high levels of PGE attained and the evidence of widespread occurrence of the Cliff-type PGE enrichment are favourable indications. The PGE enrichments found in the cumulate complex are of potential interest as they may originally have been of magmatic origin. Larger tonnage targets may therefore be present in this unit compared with the likely size of structurally-controlled mineralisation elswhere in the complex.

INTRODUCTION

Basic and ultrabasic rocks occupy an area of about 60 km^2 in the central and eastern parts of Unst, the most northerly of the Shetland Islands. The island has had a long history of extraction of chromite ore. Between 1820 and 1945 some 50000 tons of ore were produced, mostly from the area immediately to the north of Baltasound (Figure 1), with the Hagdale quarry responsible for more than 60% of the total output (Rivington 1953). The exhaustion of near-surface deposits
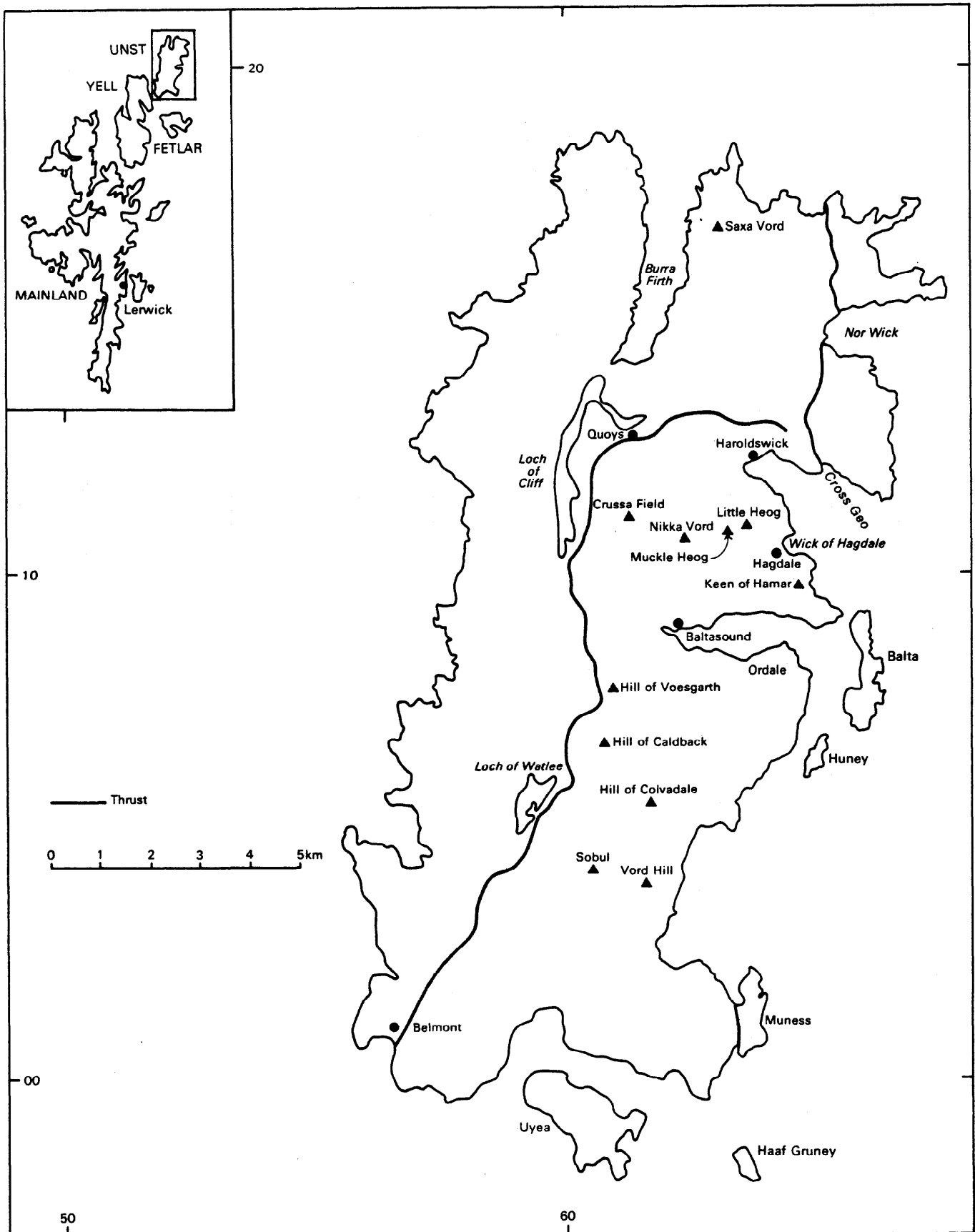
Fig. 1   Unst: Location Map

3

was responsible for the cessation of production after the second world war. Since that time various investigations have been directed towards the detection of additional chromite deposits and there have been a number of scientific studies of the mineralisation.

Previous investigations

In the early 1950's a resistivity survey and a programme of trenching and drilling was carried out by the United Steel Company to search for extensions of the worked-out bodies but this failed to identify further economic chromite concentrations. In the early 1970s Noranda undertook a programme of exploration for Cu and Ni on Unst and over a small part of the adjacent island of Fetlar (Longlands 1974). Soil and rock samples were collected systematically from Nikka Vord and the Heogs south to Baltasound (Figure 1), along the west thrust contact of the complex, over the gabbro contact south of Baltasound and over the small area of ultrabasic rocks at Muness (Figure 2). Follow-up trenching and detailed sampling were carried out over an east-west trending area 1200m x 200m, with coincident low amplitude Cu, Co and Ni anomalies, located to the south of the Heogs. Only minor amounts of Ni-Fe sulphide mineralisation and traces of native copper were observed in the rocks within this area. Brzozowski (1977) examined the potential application of VLF electromagnetic methods to the location of chromite and other mineralisation. This work, in combination with a geochemical soil survey, suggested the presence of at least one unexposed chromite pod and also of nickeliferous sulphide mineralisation on the southern slopes of Nikka Vord. None of these targets was investigated by drilling. A further investigation into the use of geophysical techniques in the detection of chromite was carried out as part of the Mineral Reconnaissance Programme by B.G.S./I.G.S. (Johnson et al 1980). Detailed magnetic, VLF-EM, IP and gravity surveys were carried out around the old chromite workings south of Muckle Heog. Shallow boreholes were drilled to investigate the source of positive gravity anomalies but in only two cases were minor concentrations of chromite intersected. A study of the chromite chemistry and general geology of the complex was carried out on behalf of the E.E.C. (Prichard 1982) but this did not lead to the identification of any specific targets for concealed chromite mineralisation.

Phillips (1927) speculated on the possible presence of platinum in association with the chromite ores of Unst. Concentrate samples from the vanning tables at the chromite mills were analysed and found to contain 1 dwt of the platinum-group metals per ton (1.8g/tonne) and the presence of Pt, Pd, Ir and Os-Ir was established. Subsequently Hitchen (1929) analysed similar samples but found only 4.8 grains of platinum-group metals per long ton (0.4g/tonne). The local sources of these metals were not identified. More recently platinum-group minerals (PGM) were identified in samples of chromitite from two localities (Prichard et al 1981). Microprobe analyses of the three PGM grains detected showed two to be laurite (RuS_2) and the other Os-Ir alloy. All grains were surrounded by chromite, one located adjacent to a nickel sulphide grain.

Scope of present investigations

The work described in this report was carried out as part of a wider programme to evaluate areas in Britain favourable for the occurrence of platinum-group element (PGE) mineralisation and to develop methods for the detection of such mineralisation. Particular attention was directed to Unst because of the known occurrence of PGMs and because exposure was relatively good compared with most other areas of similar rock in Britain. Initial work consisted of
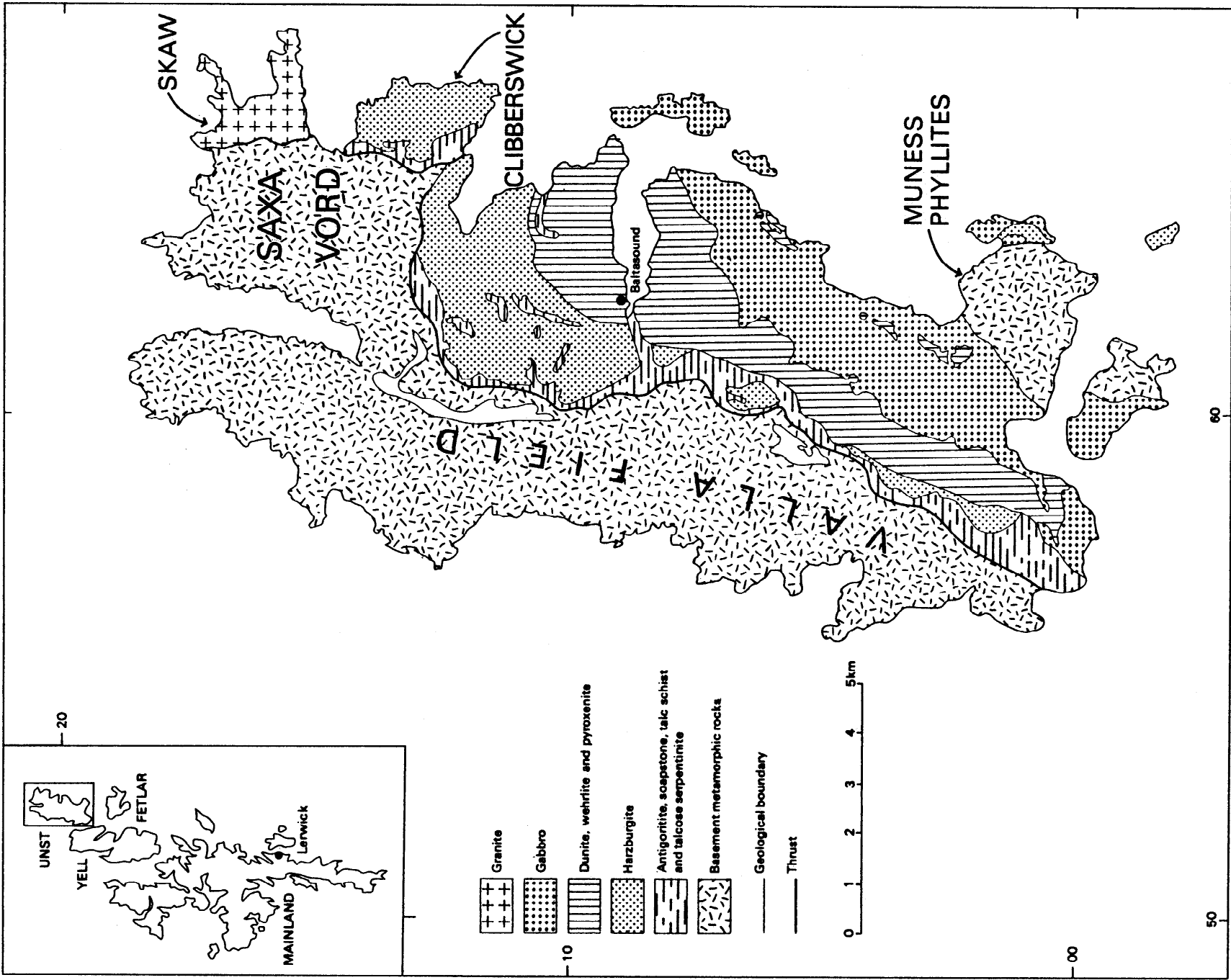
Unst: Simplified Geology

Legend:
- Granite
- Gabbro
- Dunite, wehrlite and pyroxenite
- Harzburgite
- Antigorite, soapstone, talc schist and talcose serpentinite
- Basement metamorphic rocks
- Geological boundary
- Thrust

Fig. 2

familiarisation with the geology of Unst, under the guidance of Hazel Prichard of the Open University, and the collection of reconnaissance drainage and rock samples from the whole area. Chemical analyses for PGEs in drainage samples suggested that the complex was relatively enriched in these elements compared with other areas of Britain investigated and analyses of some samples of chromitite from the dumps of old workings, especially in the Cliff area (Figure 3), showed extremely high levels of all PGEs to be present. The Cliff area was selected as the location of an orientation survey to investigate the behaviour of the PGEs in the secondary environment, to develop a method for the detection of PGE mineralisation in areas of no exposure and to investigate possible controls of the mineralisation. A method of overburden sampling was adopted and utilised systematically in the undisturbed ground surrounding the old workings. Detailed geological mapping of the Cliff area, supported by photogeological interpretation, geochemical mapping from the overdurden data and petrographical study of rock and ore samples was carried out to assist in investigation of mineralisation controls. Shallow diamond drilling into bedrock was also carried out in a few localities in the Cliff area to establish relationships between overburden and bedrock geochemistry. Subsequently overburden sampling on reconnaisance lines was extended to several other localities within the complex (Figure 3). The drainage survey was also extended to provide a more detailed coverage especially of the northern part of the complex. A short examination of the exploration possibilities of the island of Fetlar was also carried out but after the discovery of a mantle of drift of exotic origin over much of the island this was abandoned.

Physiography

The topography of the basic-ultrabasic complex is undulating with generally smooth, gentle slopes except for the prominent east-west ridge of Muckle Heog and Little Heog(Figure 1) up to 140m above sea level to the north of Baltasound. Exposure of the complex is variable but in some areas, eg to the south of Baltasound, poor. In the north of the complex, such as around Cliff, upstanding areas with moderately good exposure alternate with lower areas where it is absent except in streams. In these areas overburden is usually around 1m in thickness and comprises locally derived solifluxion debris probably reflecting a periglacial environment. Thicker accumulations of overburden occupy the flat ground on either side of Baltasound and to the west of Haroldswick(Figure 1). Glacial striae appear to be rare in the area. Drainage from the basic-ultrabasic rocks is by small streams flowing radially from the areas of higher gound on either side of Baltasound.

Observations during orientation drainage and overburden sampling on the island of Fetlar show that in many areas the ultramafic rocks are covered by a mantle of grey clay of varying thickness containing exotic fragments of black schist and other metasedimentary rocks. Panned concentrate samples of stream sediment and also of the clay show high concentrations of such minerals as red garnet and zircon which are not found in the basic-ultrabasic rocks. This material is glacial till derived from the area to the east now largely beneath the sea. Such material is not widely present in Unst but drainage samples suggest that it may occur in parts of the extreme south of the island.

6
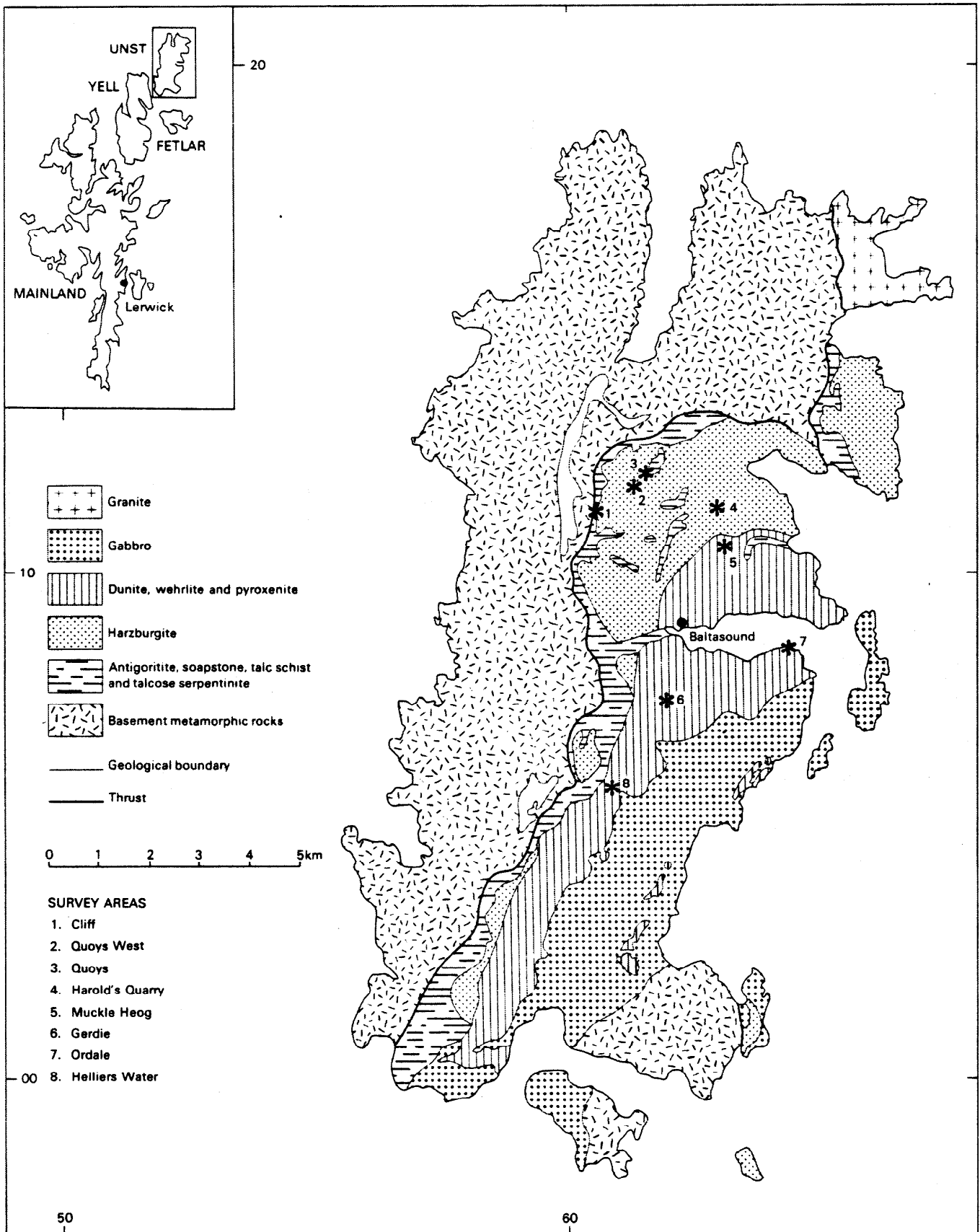
Fig. 3

Location of survey areas

Legend:

- Granite
- Gabbro
- Dunite, wehrlite and pyroxenite
- Harzburgite
- Antigoritite, soapstone, talc schist and talcose serpentinite
- Basement metamorphic rocks

— Geological boundary

—— Thrust

0 1 2 3 4 5km

SURVEY AREAS

1. Cliff
2. Quoys West
3. Quoys
4. Harold's Quarry
5. Muckle Heog
6. Gerdie
7. Ordale
8. Helliers Water

Inset map labels: UNST, YELL, FETLAR, MAINLAND, Lerwick

Map labels: Baltasound

GEOLOGY

General geology of Unst and Fetlar

The earliest accounts of the geology of Unst are by Heddle (1879a and 1879b), but the first detailed studies were conducted by Phillips (1927) and Read (1934). These authors presented geological maps, together with descriptions of the metamorphic and tectonic history supported by some chemical and mineralogical data. Flinn (1958,1970) refined Read's geological interpretation and extended them to Fetlar, presenting a model for the structure of the two islands involving successive emplacement of nappes.

Read recognised several distinct tectonic blocks within Unst, each separated by major structural dislocations trending approximately north-south and each differing in metamorphic history from its neighbours. The Valla Field block (Figure 2) forms the whole of the western part of Unst and is bounded to the east by a major dislocation which is marked by the central valley of the island. The rocks of this unit comprise coarsely crystalline metasediments, migmatites, pelites and limestones which have been correlated with the Moinian and Dalradian of the mainland of Scotland (Flinn et al 1972). The main outcrop of basic and ultrabasic rocks forms the block to the east of the Valla Field block and is described in detail below. The Saxa Vord block (Figure 2) is located in the extreme north of the island to the east of the Valla Field block and consists dominantly of non- migmatitic pelitic schists. Thrust over this to the east is the Skaw granite block (Figure 2) of microcline augen granite. The Saxa Vord block is similarly overlain by the Clibberswick block (Figure 2) of ultrabasic rocks which is also thrust over the main block of basic-ultrabasic rocks to the south. In the extreme SE of the island is the Muness phyllite block (Figure 2) which comprises low grade chlorite-sericite phyllites and the complex tectonised Muness basic-ultrabasic rocks.

Following on from Read's work, Flinn suggested that the rocks of Unst and Fetlar represent a pile of nappes separated by imbricate or schuppen zones resting on a migmatite basement. The age of the basic-ultrabasic rocks is uncertain though the timing of nappe emplacement from the greenschist metamorphism associated with this episode has been dated by the K-Ar method on micas from beneath the nappes at ca. 425 Ma. A similar K-Ar whole rock age was reported for a schist from the Muness phyllites (Miller and Flinn 1966). The migmatisation event in the basement rocks upon which the nappes rest has been dated at 526 Ma in the similar succession found on the east Mainland of Shetland (Flinn and Pringle 1976).

Geology of the basic-ultrabasic rocks

The first detailed examinations of the igneous complex were undertaken by Amin (1954) and Flinn (1970). Amin(1954) recognised a layer of dunitic composition between the olivine-rich peridotite to the the west and the diopside-rich pyroxenite to the east which were originally described by Phillips (1927). The interpretation of these rocks as part of an ophiolite was first suggested by Garson and Plant (1973). The presence of four major units within the lower nappe on Unst, comprising harzburgite, overlain in turn by dunite, pyroxenite and wehrlite and gabbro, is consistent with an ophiolitic origin for these rocks as defined at the G.S.A. Penrose Conference (Anonymous 1972). The Unst sequence does not represent the complete assemblage developed at an oceanic spreading centre as there are no mafic volcanic rocks or associated sediments present but

Prichard (1982) reports the presence of dolerite dykes within the gabbro on the east coast of the island which she suggests are the base of a sheeted dyke complex. The incomplete preservation of the sequence is a common feature of ophiolitic rocks and can be readily explained by dismemberment before or during emplacement as nappes onto the continental margin. Geological observations during this work and the interpretation of the chemistry of the overburden samples suggest that a simple ophiolitic model is inadequate and the relationship between the units is probably more complex. The dunite unit appears to grade southwards from Baltasound with increasing amounts of clinopyroxene into wehrlite or interlayered dunite and clinopyroxenite. On the other hand the gabbro is in contact with a well defined cumulate complex around Ordale, consisting of alternating horizons of pyroxenite, wehrlite and dunite but there appears to be a structural discordance between the two cumulate sequences. The trend of the cumulate rocks south of Baltasound is roughly east-west, parallel to the rocks further north, but the Ordale rocks trend NNE which is also the orientation of discordant dykes of pyroxenite at Swinna Ness.

The harzburgite unit

The rocks of this unit consist predominantly of varying proportions of serpentine and chlorite with relicts of original olivine and pyroxene or pseudomorphs after these minerals. According to Brzozowski (1977) the original mineral proportions in the unaltered predominant rock type are approximately by volume 60% olivine, 30-35% enstatite, 5% chrome spinel and up to 5% diopside. A typical specimen of least altered rock from the Cliff area consists of large grains (up to 4mm diameter) of olivine with 5-10% of interstitial pyroxene in granular aggregates of orthopyroxene and its alteration products up to 2mm in diameter. Minor clinopyroxene and scattered grains of chromite showing peripheral to extensive blackening are also present. The intensity of serpentinisation can be highly variable within the scale of a thin section and late serpentine veins also cut the rock. The harzburgite unit reaches its maximum outcrop width to the north of Baltasound (Figure 2) wedging out to the south against the basal thrust contact to the west. Along this basal zone extensive alteration has destroyed original textures and the rocks are largely converted to massive or schistose serpentinite. This alteration, within the zone stretching south from Caldback, makes recognition of the original nature of serpentinite very difficult though it appears that the majority of the ultrabasic rock was originally harzburgite.

Variations in the concentration of olivine and pyroxene locally give rise to near vertical banding within the harzburgite on the scale of <1cm to ca. 2m in width. North of Baltasound the trend of this banding is consistently 070-090° which is sub-parallel to the trend of the junction with the overlying dunite unit. South of Baltasound the trend of this banding is generally 040-050°. Lenses of serpentinised dunite from a few metres to several hundred metres across are scattered throughout the harzburgite. They are generally lensoid but sometimes more irregular in shape and are discordant to the harzburgite layering. Other dunite bodies are more elongate and are clearly concordant with the harzburgite layering. Dunites of this type are concentrated in certain zones within the harzburgite, becoming increasingly abundant immediately adjacent to the boundary with the dunite unit. These dunite lenses may contain chromite as massive pods and schlieren, thin discontinuous layers or as weak disseminations. Other dunite lenses, especially those with discordant trend or more irregular shape, contain little chromite.

Harzburgite that has not suffered significant serpentinisation can be distinguished chemically from the dunites as shown in table 1 by relatively higher levels of Al, Si, Ca and V, elements which reflect the presence of pyroxene in the harzburgite. Other elements are very similar though there are differences between the chemistry of the dunite within harzburgite and the dunite unit which are discussed below.

Table1. Average composition of ultramafic rocks

	Harzburgite		Dunite(H)		Dunite	
	Mean	Range	Mean	Range	Mean	Range
$Na_2O\%$	<0.01		<0.01		<0.01	
$MgO\%$	42.79	41.65-43.75	45.43	44.24-46.90	42.31	41.16-43.50
$Al_2O_3\%$	0.59	0.48- 0.74	0.37	0.30- 0.67	0.35	0.30- 0.39
$SiO_2\%$	42.28	41.51-43.32	39.96	38.78-43.47	39.13	38.95-39.30
Sppm	106	72- 136	148	97- 246	460	254- 719
$K_2O\%$	<0.01		<0.01		<0.01	
$CaO\%$	0.60	0.46- 0.81	0.14	0.09- 0.22	0.10	0.02- 0.19
$TiO_2\%$	<0.01		<0.01	<0.01- 0.01	<0.01	
Vppm	27	24- 32	15	9- 25	15	9- 20
Crppm	1862	1667- 2173	1734	1245- 2294	1945	891- 3373
$MnO\%$	0.15	0.14- 0.15	0.15	0.13- 0.16	0.15	0.10- 0.19
$Fe_2O_3\%$	10.06	9.75-10.33	10.04	9.69-10.50	11.79	10.96-12.81
Coppm	104	103- 107	107	96- 116	124	108- 139
Nippm	2264	2192- 2345	2493	2315- 2657	2278	1786- 3104
Cuppm	<1		2	<1- 5	84	14- 183
Znppm	25	24- 26	22	10- 26	25	17- 33
Asppm	2	<1- 4	2	<1- 6	1	<1- 7
Sbppm	1	<1- 2	1	<1- 3	4	3- 4
Teppm	1	<1- 2	<1		<1	
Bippm	<1	<1- 1	1	<1- 2	<1	
Ruppb	24	<10- 70	7	<10- 12	8	<10- 20
Rhppb	<5		<5		4	<5- 10
Pdppb	7	<5- 10	5	<5- 12	31	<5- 180
Irppb	<10		<10		<10	
Ptppb	8	<10- 15	<10		13	<10- 60
No. of samples	4		6		9	

$Fe_2O_3\%$ = Total Fe expressed as ferric oxide
Dunite(H) = dunite within harzburgite unit

The dunite unit

The junction between the dunite and harzburgite units is steeply dipping and commonly marked by interdigitation of the two rock types. Away from the contact zone, according to Brzozowski (1977), the typical rock of the unit comprises, by volume, 85-95% olivine, often partly or completely altered to mesh serpentine, chlorite, tremolite and magnetite, with up to 15% chrome spinel and minor interstitial sulphide. Many rock samples have small relics of olivine, rarely up to 40%, and exhibit a ghost dunite texture of granular olivine grains, around 1mm in size, outlined by trails of magnetite along original grain boundaries and fractures. Chromite is always present, often in grains around 1-2mm, with peripheral or sometimes extensive blackening and a halo of chlorite. A few dunites contain pseudomorphs after initial orthopyroxene in minor amounts

that are now composed of serpentine and magnetite. Other than the interlayering of dunite and harzburgite in the contact zone the only other planar fabric in the unit are discontinuous bands rich in chromite which trend parallel to the contact zone. South of Baltasound the dunite appears to grade into wehrlite and whether any distinct contact exists between the two is not known. Dunite also occurs in the strip extending south from Caldback through the centre of the island and is particularly conspicuous near Watlee where exposures show chromite rich layers trending at roughly 090°, sharply discordant to the layering of the nearby serpentinised harzburgite and cumulate rocks. Chromite in schlieren and podiform bodies is widespread within the dunite unit but is concentrated around the dunite-harzburgite contact zone on Nikka Vord in the north and in series of bodies near Sobul Hill in the south of the island.

Chemically the dunite differs from the harzburgite in its lower Al, Si, Ca and V levels as described above. There are also differences in chemistry between dunite within harzburgite and that making up the dunite unit with higher levels of Fe and correspondingly lower levels of Mg and Ni in the latter. In addition there are significantly higher levels of S, Co and Cu associated with rocks from the dunite unit.

The pyroxenite/wehrlite unit

This unit forms an irregular belt to the south and east of the dunite unit, stretching from the Keen of Hamar in the north to the south coast of the island. The boundary between this unit and the dunite is unclear since the dunite appears to grade upwards into a unit with on average wehrlitic composition over several hundred metres across strike. The long overburden traverse running north from Gerdie (Figure 43) shows a progressive and stepwise increase in Ca reflecting the amount of clinopyroxene present. This suggests that a distinct contact may not be present. In addition there is a well defined layered cumulate complex consisting of alternations of wehrlite, clinopyroxenite and dunite which is exposed near Ordale and also discontinuously to the west of the gabbro (Figure 2) southwards through the island. The discordant trend of layering in the Ordale cumulate rocks compared with the layering in the nearby dunite suggests that either intrusive or tectonic contacts occur. In the layered rocks pyroxenite grades through a narrow mixed zone into serpentinite with scattered clinopyroxene grains. Within the cumulate complex at Ordale there are bodies of coarse-grained pyroxenite some of which are discordant to the layering of the adjacent rocks. These consist of clinopyroxene grains up to 5mm in size with interstitial spaces filled with serpentine and fine magnetite after olivine and less commonly saussuritized plagioclase. A few grains of black chrome spinel are also present. At Swinna Ness pyroxenite dykes up to 10m wide intrude the dunite. Similarly a major discordant pyroxenite body can be traced northwards from the Hill of Colvadale for about 1 km. The diopside of the pyroxenites is often altered to tremolite and serpentine while in some wehrlites olivine grains appear to have crystallised earlier than the pyroxene.

The average of analyses of samples of the main varieties of the cumulate complex from Ordale are shown in table 2. The composition of the dunite layers appears richer in Al, Si, Ca, Ti and Cr and poorer in Mg and Ni than either the average of the dunite unit or of dunite within harzburgite. This can partly be explained by the presence of a small but significant amount of clinopyroxene within the dunite of the cumulate complex but there must also be a difference in the composition of olivine. The significantly higher Cr content of the dunite from the cumulate complex is of particular interest since it suggests that the concentration of chromite within the dunite unit is by a different process than

occurring in the cumulate rocks. This is in accord with the different minor element composition of the chromite deduced from the analysis of panned overburden samples derived from the same Ordale area. Within the rocks of the cumulate complex there is a progressive increase from dunite to wehrlite to pyroxenite in Na, Al, Si, Ca, and Ti and corresponding decrease in Mg, Fe, Ni and Zn.

Table 2. Average composition of units of cumulate complex and gabbro

	Dunite		Wehrlite		Pyroxenite		Gabbro	
	Mean	Range	Mean	Range	Mean	Range	Mean	Range
Na$_2$O	0.00		0.01	0.00- 0.02	0.29	0.08- 0.61	2.20	0.26- 5.54
MgO%	41.93	37.86-46.84	32.34	26.50-40.16	22.78	20.21-26.74	7.40	5.82-10.43
Al$_2$O$_3$	0.56	0.33- 0.64	0.93	0.70- 1.24	1.55	0.90- 2.35	14.76	12.65-16.87
SiO$_2$	44.59	40.94-46.93	48.51	46.80-49.46	52.10	50.26-53.49	43.25	38.66-47.90
Sppm	334	49- 923	106	41- 218	115	46- 265		27-2.45%
K$_2$O%	0.00		0.00		0.04	0.00- 0.11	0.05	0.01- 0.20
CaO%	0.86	0.16- 2.06	9.04	3.29-13.50	16.63	9.54-19.69	9.52	2.65-11.71
TiO$_2$%	0.01	0.00- 0.01	0.01	0.01- 0.02	0.04	0.03- 0.04	1.34	0.36- 1.83
Vppm	30	20- 38	64	37- 85	90	57- 107	400	189- 875
Crppm	4578	2100- 7817	3779	2251- 5060	4914	3080- 7048	260	57- 357
MnO%	0.14	0.06- 0.17	0.08	0.05- 0.11	0.08	0.02- 0.12	0.20	0.15- 0.27
Fe$_2$O$_3$%	9.63	8.38-11.11	6.45	5.07- 7.79	4.31	3.59- 5.81	15.86	8.60-20.77
Coppm	114	90- 140	81	64- 100	45	41- 49	58	49- 75
Nippm	1267	846- 1867	732	537- 1011	431	331- 738	44	17- 79
Cuppm	4	<1- 14	6	1- 15	69	12- 190	116	6- 218
Znppm	24	20- 27	16	10- 24	10	5- 15	82	53- 97
Asppm	65	1- 230	10	3- 14	1	<1- 2	3	<1- 12
Sbppm	2	<1- 5	2	<1- 3	3	2- 5	3	<1- 6
Teppm	<1	<1- 3	1	<1- 2	<1		<1	
Bippm	1	<1- 4	1	<1- 3	1	<1- 2	<1	<1- 1
Ruppb	9	<10- 20	15	10- 20	10	<10- 18	<10	<10- 17
Rhppb	3	<5- 6	5	<5- 7	<5		<5	
Pdppb	18	<5- 40	27	20- 35	58	15- 200	6	<5- 17
Irppb	<10		<10		<10		<10	
Ptppb	13	<10- 25	27	10- 40	40	<10- 100	6	<5- 10
No. of samples	7		3		5		6	

The gabbro unit

This unit consists predominantly of a pyroxene gabbro which has been altered to a mixture of actinolite, after the pyroxene, and saussuritised plagioclase. The contact with the underlying cumulate pyroxenites is in places tectonic but in others it intrudes these rocks and contains xenoliths of them. The gabbro is typically massive, although slight variation in the proportions of the two main constituent minerals locally produce layering. The layers may have sharp or diffuse boundaries and vary in thickness from a few cm up to 1m. In the SE part of the island there are horizons containing discontinuous lenses of high level pyroxenite and wehrlite. Chemically the gabbro is highly variable in composition (table 2) especially in terms of Na, Ca, V and Fe levels

Chromite mineralisation

Chrome spinels occur throughout the ultrabasic rocks of the complex in a wide variety of forms. In the harzburgite chromite is a ubiquitous accessory mineral, generally in grains up to 2mm in diameter but occasionally segregated into discontinuous bands, often parallel to the foliation of the harzburgite. Within some dunite lenses within the harzburgite and in the massive dunite chromite occurs as a) a disseminated accessory, b) in millimetre scale bands and c) in massive schlieren up to 10cm thick which may locally develop into larger massive pods of chromitite or a series of broader parallel veins. In the chromitites which are loosely described as rocks with abundant chromite, generally greater than 80%, chromite grains are usually equant and somewhat rounded ranging in size from 1mm to 2cm. The grains are typically extensively fractured and the subgrains may be pulled apart slightly. The unaltered parts of chromite grains are a reddish-brown colour in transmitted light but there is always some blackening around the margins and along fractures while in some altered samples the chromites are completely black. Where the amount of interstitial material is relatively small it is entirely chlorite but where interstices are larger chlorite occurs adjacent to the chromite with a central mass of serpentine or magnesite probably formed as a replacement of serpentine. The purple Cr-bearing chlorite type kammererite is often present. A range of textural types is found within the chromitites with local development of nodular and layered varieties together with the more widely distributed massive type. Inclusions of olivine, pargasite, diopside, nickel sulphide minerals, PGM and native Zn have been identified within chromite grains (Prichard 1983). The largest chromite deposits occur as a series of near vertical lenses orientated E-W in the north and NE-SW in the south of the island, either in alignment or as en-echelon clusters. These directions are parallel to the compositional layering in the adjacent harzburgite or cumulate rocks. The largest deposits near the harzburgite- dunite boundary on Nikka Vord are around 20m in diameter, while in the south of the island around Sobul they are 2-3m thick. Within the harzburgite unit most deposits are small, of the order of 3m x 10m although the working at Quoys (Figure 1) is much larger, 10 x 75m.

Post consolidation tectonism exerts considerable control over the form of the massive chromite pods. Contacts with the host serpentinite are sometimes slickensided and the mineralisation is often displaced or terminated by late shears or faults as can be seen in some of the quarries on Nikka Vord. In particular, an old working SW of Muckle Heog [46273 121050] shows discontinuous massive chromite lenses with sharp contacts in a sheared and fractured dunite host.

Sulphide mineralisation

Ni-Fe sulphides are widespread in small amounts in association with chromitites from several parts of the complex and also occur disseminated in dunite and pyroxenite. Brzozowski(1977) observed a complex paragenetic sequence of sulphide minerals which he interpreted as an original high temperature magmatic assemblage which was then substantially modified during serpentinisation, talc-carbonate formation and finally supergene alteration. Cu and Co-rich sulphides are locally important, especially in the eastern area of Nikka Vord and around Hagdale.

Alteration

All rock types show various stages of alteration but these are most obvious within dunites and are therefore described in terms of this rock type initially. The stages which have been recognised are described in turn below.

1. The early serpentinisation is essentially a static hydration of olivine to produce serpentine, sometimes leaving olivine relics and a distinct "ghost" dunite fabric. The serpentine is often fine-grained pale green or greenish brown and has areas and trails of fine magnetite along original grain boundaries and fractures.

2. A second phase of alteration comprises the recrystallisation of serpentine to coarser colourless crystals that in some specimens can be seen to be spreading out from fractures. Further recrystallisation leaves islands of first stage green-brown serpentine within the coarser colourless serpentine. Locally this stage may have taken place within a shear stress regime giving foliated serpentinite. The completion of this stage is a coarse-grained serpentinite with no trace of original rock texture remaining. The formation of many veins of magnetite accompanies this alteration stage.

3. The recrystallised serpentinites are often cut by carbonate veins (magnesite). The timing of this phase is difficult to assign but it probably postdates serpentine recrystallisation though it could be synchronous with the later phase of that alteration. The extent of the carbonate varies from a few cross-cutting veins to very extensive alteration of a large proportion of the rock to carbonate.

4. Some veins of serpentine cut across the carbonate veins and reflect the continuing solution and reprecipitation of serpentine in a low temperature environment.

5. Talc carbonate rocks are the most altered variety in the area. They are composed of magnesite and talc with scattered chromite grains. Most rocks have a well developed schistosity with slight augening around chromites and some of the larger carbonate grains. This phase of alteration has completely obliterated direct evidence of the original rock type, though the presence of chromite indicates an ultramafic parent. The distribution of these rocks are clearly related to shear zones.

The chemical differences between the various alteration assemblages formed from an original dunitic parent in the Cliff area are summarised in table 3.

Table 3 Comparison of composition of altered varieties of dunite

	Fresh		Relic oliv.		Serpentine		Carbonate		Talc + carb.		Talc
	Mean	S. D.	Mean	S. D.	Mean	S. D.	Mean	S. D.	Mean	S. D.	
MgO%	45.43		44.43	1.85	43.53	2.36	42.85	2.16	36.84	2.91	30.42
Al_2O_3	0.37		0.41	0.05	0.54	0.18	0.55	0.20	0.42	0.09	0.55
SiO_2	39.96		42.38	2.00	44.80	1.16	43.29	2.26	47.13	3.59	53.83
Sppm	148		306	116	126	71	74	25	119	62	82
CaO%	0.14		0.17	0.09	0.29	0.44	0.35	0.32	0.16	0.08	0.09
Vppm	15		19	2	21	6	21	7	18	3	19
Crppm	1734		2998	1787	1702	475	1896	964	1940	1061	1898
MnO%	0.15		0.11	0.04	0.09	0.04	0.15	0.04	0.15	0.03	0.19
Fe_2O_3	10.04		9.39	0.52	8.98	0.85	8.78	0.82	10.30	0.85	12.43
Coppm	107		113	5	105	13	95	12	99	18	151
Nippm	2493		3038	552	2712	1047	2520	464	2356	365	3363
Cuppm	6		87	62	61	146	10	11	9	5	10
Znppm	16		17	4	19	5	14	8	18	6	36
Asppm	10		61	78	22	18	6	4	22	50	<1
Ruppb	7		52	44	26	45	11	7	17	18	15
Rhppb	<5		21	24	16	44	5	6	4	2	<5
Pdppb	5		231	243	233	686	21	37	34	65	8
Irppb	<10		7	4	8	11	<10		<10		<10
Ptppb	<10		151	156	108	249	16	28	21	35	<10
Ni/MgO			68	12	62	22	59	9	65	16	111
No. samp.	6		5		11		7		11		1

"Fresh" samples contain significant proportion of relic olivive.
"Relic oliv." samples contain some relic olivine.
"Serpentine" samples contain no olivine but can have either stage 1 or 2 type serpentine.
"Carbonate" samples contain significant amount of carbonate in association with serpentine.
"Talc + carb" samples contain a significant amount of talc and carbonate.
"Talc" sample is made up almost exclusively of talc and carbonate.

Some clear chemical trends with increasing alteration are discernible from the data presented in table 3. Mg shows a progressive decrease as the intensity of alteration increases while Si shows a corresponding increase especially with the occurrence of talc. Ca shows an increase with the presence of carbonate but a decrease with the occurrence of talc. Mn shows an increase with the occurrence of carbonate. Fe increases only with the occurrence of talc and Co, Ni and Ni/MgO are relatively high only in the most talcose sample. Many elements, especially Cr, PGE, S and As are unrelated to the degree of alteration. The significance of this is discussed below. Cu is relatively depleted in the talcose samples relative to other elements with which it is generally associated ie PGE, As and Ni.

The initial serpentinisation of harzburgite produces brown-green serpentine after olivine and distinct orthopyroxene bastite pseudomorphs of serpentine with trails of fine magnetite parallel to the c-axis of the original orthopyroxene. Further recrystallisation produces mottled serpentinites with coarse serpentine and aggregates of coarser magnetite with a less distinct shape. The most recrystallised rocks have diffuse areas of magnetite concentration and probably represent altered harzburgite as this feature is not seen in the serpentinised

dunites.

Within the chromitites the various stages of alteration are less distinct than in the previously described rocks. The least altered chromitites show blackening only along cracks and interstitial chlorite and a green-brown type serpentine of the type found in stage 1 alteration of dunite. With increasing alteration the chromite rims are also blackened and blackening along cracks is wider so that some subgrains are completely altered. Chlorite is more abundant relative to serpentine and coarse discordant veins of chlorite also occur. In some examples the intsertitial serpentine is replaced by magnesite probably originating at the same time as the carbonation of the serpentinites. The most altered examples have chromite grains which are completely black. The grains are fractured and pulled apart while the chlorite may exhibit some preferred orientation.

Structure

Structurally the main block of basic-ultrabasic rocks can be divided into 5 sectors. The northernmost sector comprises the harzburgite and dunite to the north of the Baltasound inlet. Here the trend of layering is around east-west with a bend to E-N-E in the south-east. The sector south of the inlet comprises dunite and wehrlite, which are very poorly exposed but with layering probably around E-N-E, and the Ordale cumulate complex which trends roughly NE. The cumulate complex also occurs at Swinna Ness on the north of the Baltasound inlet where it is also sharply discordant to the layering in the dunite and harzburgite units. The cause of this discordance is not clear and could be intrusive or tectonic or a combination of the two. SW of this is a sector of complex geology and juxtaposition of the gabbro against several other rock types in the vicinity of Helliers Water but with a general N-N-E trend. The sector to the south of this, east of Watlee Burn in Mid Unst, dunite is exposed which shows layers of chromite trending around east-west This direction is sharply discordant to the trend of the adjacent cumulate rocks and the contact of the gabbro. In the southernmost sector a NNE trend of layering and of chromite lens orientation is again dominant. The anomalous layering trend in the Watlee sector is more likely to represent an original feature of the dunitic rocks against which the cumulate and gabbro units have been emplaced discordantly rather than an isolated block which has been rotated from an original NNE orientation as has been suggested by Prichard(1983).

Faulting and alteration zones

Several major lineaments can be seen on the aerial photographs to cross the complex, some of which clearly represent major fault zones. In the ultrabasic rocks they are usually marked by the development of extreme alteration to produce talc-magnesite-chlorite rock. Along the basal thrust contact zone there is also extensive development of antigorite serpentinite as in the Belmont area in the south of the island. East of the Loch of Cliff (Figure 1) the basal thrust is marked by a 10m thick zone of pink-brown weathering talcose rocks, irregularly foliated with a north-south trend and dipping eastwards at moderate angles. Away from the basal thrust there are several elongate and irregular belts of talcose serpentinites which weather in to form relatively low ground littered with pink-brown flaggy or schistose float material. The direction of foliation within these zones is often variable either parallel or oblique to the lineament and often discordant to the local direction of layering in the fresher ultrabasic rocks nearby. A conspicuous belt of talcose schists runs westwards from Hagdale Wick. Several directions of lineament are discernable on air photographs as described below with reference to the detailed study of the area

16

around the old workings at Cliff. Their origin is clearly related to the nappe emplacement events during the latter part of the geological history of the complex.

Detailed geology of Cliff area

A geological map of the Cliff area based on field observations, photogeological interpretation and geochemical data is shown in Figure 4. Locations in the area are made with reference to the grid surveyed for the overburden sampling programme which is shown in Figure 14. The old chromite workings are shown on Figure 4 and also on Figure 14 where they are characterised by letter A to F. Pit F is situated ca 250m WNW of the other group close to the basal thrust of the complex. No chromite ore is visible in situ in any of the workings but examination of dump material which appears to represent the bulk of material extracted from the pits allowed the recognition of two principal textural varieties. The more common type consists of disseminated or blebby chromite in complex bands within massive serpentinised dunite. The other type is much more massive in character with conspicuous coatings and veinlets of the purple chlorite kamererite and hosted by a foliated serpentinite rich in talc and carbonate. Away from the area of the old workings small pieces of chromite float were discovered at several locations. Two main areas were identified with distinct concentrations: (1) within a broad zone of carbonated serpentinite around 00 450S and (2) within a poorly exposed area around 450E 300S. In the first area no in situ mineralisation was discovered though exposure is very poor while in the second there were a number of old exploration trenches but no in situ mineralisation.

The main chromite workings at Cliff are located within a poorly exposed elongate zone measuring 400m x 150m which, on the basis of outcrop evidence and the results of drilling a number of auger holes to bedrock, consists largely of serpentinized dunite with sporadic small lenses of harzburgite. Within the zone and also marginal to it there are areas of flaggy or schistose talc-carbonate rich rocks which have characteristic pink-brown weathered surfaces the extent of which are difficult to define because of poor exposure. The foliation within these zones is generally near vertical at about 70° while the less altered rocks nearby exhibit more variable foliation orientations. Petrographic examination of rock and core samples from this zone reveals variable and complex alteration assemblages. Serpentinisation has destroyed all original olivine and other silicate crystals but poorly preserved pseudomorphs in a distinctive mottled variety found in the boreholes suggest a harzburgite precursor also to be present.

Chromite, other than a fine-grained accessory, is observed in this zone only as a few impersistent lenses and bands of disseminated material. A conspicuous example occurs around 185E 70S, where an irregular band, up to 2.5cm wide, can be traced intermittently over 5 metres, trending 70-75° and occasionally offset by N-S shears.

The northern edge of the above dunitic zone is partly defined by a major fault trending 70° which can be traced westwards as far as the Loch of Cliff. It intersects and displaces the basal thrust. Further east the dunitic zone is defined by a pair of parallel faults trending about 40°. Elswhere the boundaries of the zone cannot be located accurately because of lack of exposure but their approximate position can be defined geochemically.
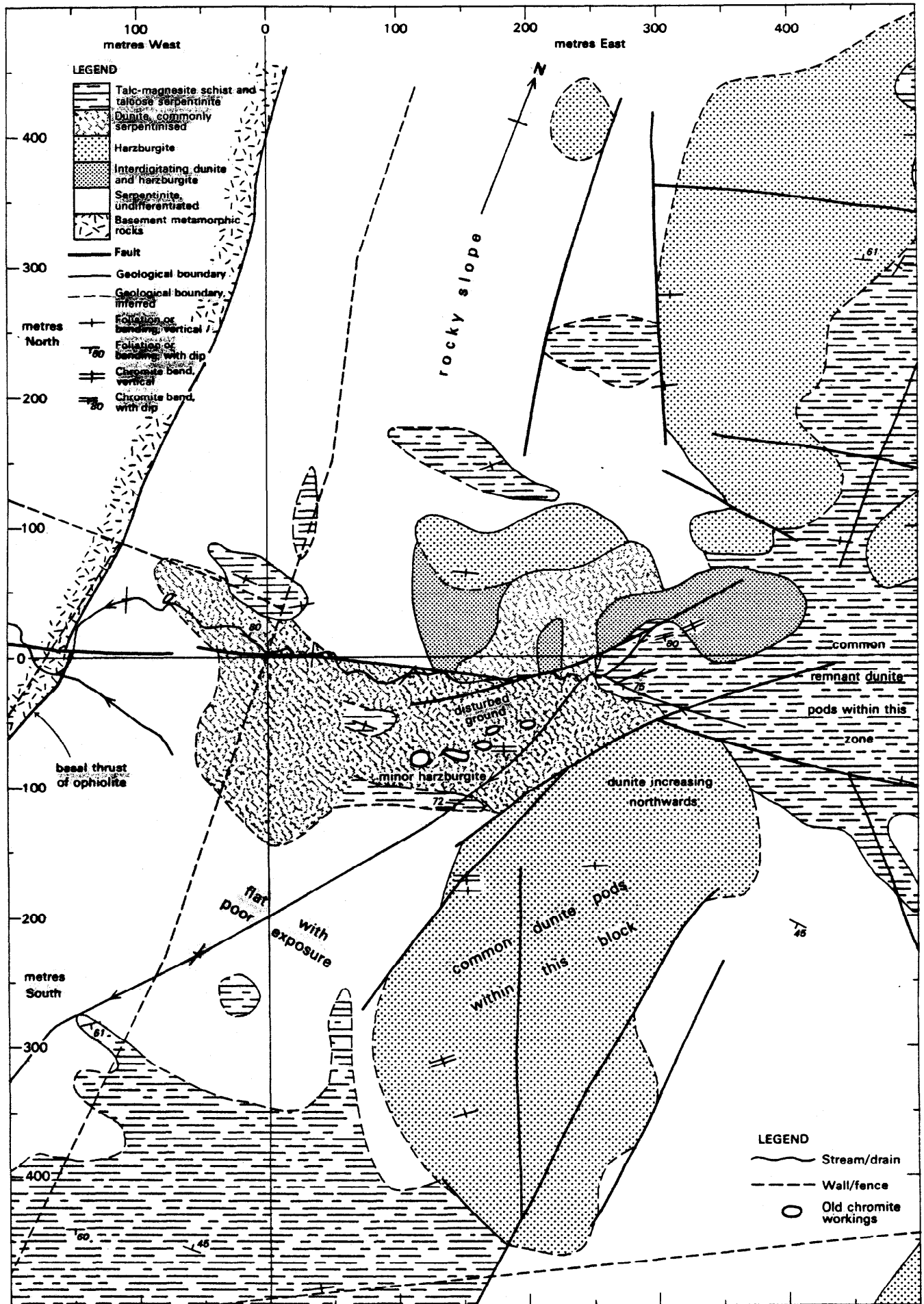
Fig. 4

Geology of Cliff area

To the north and south of the dunitic zone there are prominent blocks of massive harzburgite which form elevated well exposed ridges. Foliation in these rocks is generally weak, but is locally well developed with a near vertical attitude consistently striking at 060-070°. Dunite pods of variable shape and size but commonly 10-20m in largest dimension, are widespread, particularly in the southern block. They occupy relatively depressed zones between harzburgite outcrops and have characteristic well-jointed, nearly flat weathering surfaces. Chromite stringers and impersistent bands of fine disseminated or blebby grains (< 1cm) are quite widespread in these pods trending 50-60° and may be traced over distances of up to 1 m. Between the dunitic zone and the northern harzburgite block is a poorly exposed area of pod-like interdigitations of harzburgite and dunite with locally well developed foliation which may be transitional between the two.

The area to the east of the main dunitic zone is very poorly exposed with few inconspicuous outcrops of talc-magnesite schist and talcose serpentinite. In addition there a impersistent outcrops of dunite which have escaped the pervasive talc carbonate alteration and occasional small masses of harzburgite interlayered with the dunite. The foliation in these relics is concordant with the regional foliation of ca. 075° but the foliation within the talc carbonate rocks is more variable. Similar material extends northwards in an elongate zone marking the trace of a major fault roughly parallel to the basal thrust. Foliation within this zone is often parallel to its trend. The same fault extends south of the dunitic zone marking the eastern boundary of the southern harzburgite block but talc carbonate alteration appears much less abundant in float within this zone. Another major zone of talc carbonate alteration occurs in the SW of the area with borders which are mostly ill defined because of lack of exposure. In this zone the foliation is generally similar to the regional trend of layering but with a more variable and generally lower angle of dip.

Four major lineament directions can readily be identified in the Cliff area and also more widely in the harzburgite unit. These trend roughly at 0°, 30-40°, 70° and 150° respectively. Of these the 0° trend is most conspicuous and since this is parallel to the trend of the basal thrust it is probable that these structures are associated with the nappe emplacement event. The age relationships between the various fault groups is difficult to decipher because of poor exposure but but some movement along the 70° must have postdated the nappe emplacement as the basal thrust is displaced. The main 70° fault cutting the Cliff area is significant as it separates two contrasting zones and may in part be relatively early. To the south is the main dunitic zone containing the chromite workings which passes southwards into harzburgite, deduced in the flat grassy area from rock fragments in the pits and the chemistry of the overburden samples. North of the fault the terraine is quite different with much more exposure and the transitional interdigitating harzburgite and dunite zone passes into harzburgite which has been less altered than to the south. The distribution pattern of chromite-rich and other overburden samples and the presence of the small chromite pit in the west of the dunitic zone suggest that the zone may have been displaced northwards along a north trending fault by up to 50m but it is not possible to recognise the line of such a structure in this poorly exposed ground.

EXPLORATION

Analytical methods

In the absence of quantitative PGE data on rock samples from the Unst ophiolite and particularly because nothing was known about the abundance and behaviour of PGE in the secondary environment there was a requirement to obtain high quality analyses to detection limits of a few ppb in order to establish a sound database. To obtain the necessary sensitivity a fire assay stage is needed in the first instance to concentrate the PGE into a simpler matrix than the original sample. An additional advantage of this procedure is that it allows the analysis of a relatively large volume of sample thereby reducing the effect on precision of subsampling. A fire assay method using nickel sulphide as the collector was utilised in order to effect preconcentration of all six PGE and also Au (Robert et al 1971). 50g of sample powder were fused at 1100°C and the resulting slag refused to ensure complete extraction of the PGE from chromite-rich matrixes (Robert et al 1977). The two nickel sulphide buttons were then crushed, dissolved in acid and the insoluble precious metals collected by filtration.

In the early stages of the programme samples were analysed by I.C.I. at Billingham with a neutron activation following the double nickel sulphide fusion (Hoffman et al 1978). The determination of Au and Ir is the most sensitive by this method and detection limits of less than 1ppb were readily obtained on all samples. Doubt has been expressed (Robert et al 1971) about the possible incomplete collection of Au by the nickel sulphide method. However it was possible in drainage samples to verify relatively high levels of both Au and Ir by non destructive neutron activation analysis. Rh determination is also relatively sensitive and a detection limit of 1ppb was normally achieved. For Os and Ru the method is less sensitive and the detection limits are more variable, dependent on the background counts from the sample matrix after fire assay. For Os the reported detection limits were in the range 2-10ppb and for Ru they were normally between 5 and 20ppb, but exceptionally up to 80ppb. For Pt and Pd major interference problems were encountered due primarily to the high background counts produced by Cr in many samples. In addition samples with enhanced levels of As, Sb and Cu gave rise to specific peak interference problems. Reported detection limits for Pt and Pd were therefore highly variable but generally within the range 10-40ppb, though occasionally as high as 500ppb.

The precision of the data provided by this method has not been assessed in detail but general figures of total subsampling plus analytical precision can be given for Os, Ir and Ru in overburden samples and all PGE in rock samples from a comparison of replicate analyses. For overburden samples total precision for Os and Ir is 20-25% and for Ru 48% from 3 to 7 samples. Figures for Rh are not available because of the low levels present in the overburden samples relative to detection limit and for Pt and Pd the elevated and variable detection limits make estimates of precision impossible. For rock samples with higher levels of PGE in many cases precision levels are better. Total precision for Os, Ru and Pt is between 7 and 11% for 3 to 5 samples. For Ir a figure of 21% was obtained from 4 replicate analyses and for Rh a figure of 40% was obtained for the same number of samples.

A suite of samples of various types from Unst and other parts of Britain were analysed by essentially the same fire assay + neutron activation method in a Canadian laboratory (X-ray Assay laboratories Ltd., Ontario). Agreement between the two labs was relatively good for Ir and Rh. Ru agreement was next best,

while Au, Pt and Os were only moderately good. Comparisons of Pd data were of doubtful value because of variable detection limit problems. Extreme discrepancies were noted in two samples for Pd and in one for Pt. A small number of check analyses for Pt and Pd were performed mostly on high PGE samples using a fire assay with fusion at 1050°C, lead collection and a flameless atomic absorption finish. This work was carried out by Alfred H. Knight International Ltd. of Merseyside, England. Reasonable agreement between the two methods was obtained, but the AAS finish gave much improved limits of detection for Pt and Pd relative to NAA. Checks on high levels of Pt and Pd were also made by XRF at M. E. S. A., Long Eaton, Nottingham.

Subsequently as a result of the severe problems encountered with the determination of Pt and Pd an alternative analytical procedure was adopted and all overburden samples from the Cliff area and other parts of the harzburgite unit were analysed by this method. The nickel sulphide fire assay stage was coupled with the determination of the individual PGE by AAS using electrothermal atomisation (graphite furnace). This method has been described by Haines and Robert (1982) who assessed optimum determination conditions and interference problems. In the present work which was carried out by Alfred H. Knight International , following a double fusion of a 25g sample and dissolution of the buttons, the PGE sulphides were dissolved in hydrochloric acid and hydrogen peroxide to provide solutions for the flameless AAS determinations. Detection limits of 5 ppb for Pd and Rh and of 10 ppb for Ru, Pt and Ir were obtained with this method. Os was not determined because of the extremely poor sensitivity of the AAS finish. No serious interference effects were noted and there was generally close agreement with Pt and Pd data derived from the Pb fire assay method described below. Haines and Robert (1982) report high precision (<10%) and accuracy for all 5 PGE determined by this method on 3 samples, one of which was rich in chromite.

In the later detailed studies and in most of the reconnaissance traverses a lead fire assay method was utilised for the determination of Pt and Pd. This approach is simpler than the NiS fire assay and because of lower cost allowed data to be obtained from more sites than would have otherwise been possible. The method involves fusion of a 25g sample at 1050°C using lead and gold as collectors for the PGE. After cupellation to remove the lead, Pt and Pd are determined by flameless AAS in the solution obtained by dissolving the gold prill in aqua regia. This method has been widely used and thoroughly tested and a high reliance can be placed on data so derived as the recovery of the PGE is quantitative and the AAS determinations highly sensitive, giving detection limits of 5 and 10 ppb for Pd and Pt respectively.

Multielement geochemical data were obtained on all samples by X. R. F. at Midland Earth Science Associates (M. E. S. A.), Long Eaton , Nottingham. The list of elements determined varies according to sample type and progress of the investigation.

Drainage geochemistry

Drainage samples were obtained from 73 sites in Unst and 2 in Fetlar. The location of the sites in Unst is shown in Figure 5. Only two samples were taken on Fetlar because of the widespread presence of drift of exotic origin covering the ultrabasic rocks. This can be illustrated by the K levels in the Fetlar samples which at 1.18% and 0.97% K_2O respectively are much higher than any from Unst (maximum 0,29% K_2O%). Accordingly these will not be considered further. At each site suspended matter and panned concentrate samples were obtained as described in Leake and Smith (1975). The concentrate samples were panned to constant volume from a standard original minus 2mm sediment volume. To obtain a large concentrate the process was repeated 2 or 3 times. The mean levels of elements from samples derived from the different geological units of the complex are compared in table 4.

Table 4 Average composition of drainage panned concentrates

	harzburgite		Clibberswick		dunite		wehrlite etc		gabbro	
	Mean	S. D.	Mean	S. D.	Mean	S. D.	Mean	S. D.	Mean	S. D.
MgO%	15.84	7.27	23.11	3.13	13.89	2.38	14.16	1.59	10.96	2.96
Al₂O₃%	6.41	1.22	-	-	8.37	1.41	6.48	1.56	12.93	4.23
SiO₂%	18.66	4.60	-	-	12.93	2.13	19.14	1.10	44.55	2.85
Sppm	151	133	158	43	150	35	850	1780	206	95
CaO%	0.98	0.45	1.41	0.95	0.56	0.18	5.19	3.15	15.02	1.64
TiO₂%	0.37	0.10	-	-	0.25	0.01	0.38	0.12	0.63	0.82
Vppm	752	85	-	-	748	43	623	19	213	115
Cr%	16.28	6.37	4.33	1.87	20.34	2.97	12.56	4.39	1.49	1.00
MnO%	0.34	0.02	-	-	0.32	0.02	0.46	0.07	0.17	0.05
Fe₂O₃%	22.90	5.60	12.07	1.37	29.70	3.57	24.81	7.28	6.46	3.51
Coppm	358	99	173	29	349	44	377	92	64	16
Nippm	1752	591	1401	227	1868	217	1798	834	177	36
Cuppm	31	5	21	3	80	11	63	25	27	4
Znppm	1446	544	526	182	1108	273	968	377	123	60
Asppm	6	7	16	11	1	3	16	13	1	2
Ruppb	41.5	10.3	-	-	26.6	21.4	-	-	-	-
Rhppb	8.5	2.3	-	-	3.3	0.8	3.8	0.5	<1	
Osppb	17.8	11.6	-	-	9.3	6.7	<2-4.4		-	-
Irppb	12.9	5.9	-	-	6.5	2.0	4.4	1.8	0.5	0.3
Auppb	1.0	0.5			4.2	8.9	0.8	0.6	13.7	17.6
No. samples	41(9)		6		11(7)		7(3)		5	

Samples derived from the gabbro are clearly distinguished by their relatively high Si contents and low levels of Cr, Ni and Zn. Samples derived from the wehrlite and other cumulate rocks are characterised by much higher Ca contents than those derived from the other ultrabasic rocks, though in other respects they are similar. Compared with the harzburgite, samples derived from the dunite unit have higher levels of Cr, Fe and Cu and lower levels of Mg, Ca, Ti and Zn. Similar relationships particularly for Ca and Cu contents are also shown in the corresponding rock data set (Table 1). The compositions of samples derived from the Clibberswick block of harzburgite are significantly different from those derived from the main body of harzburgite in having much lower Cr, Fe, Co and Zn levels and higher Mg levels. These chemical differences are compatible with the interpretation of the Clibberswick mass of harzburgite as a separate block
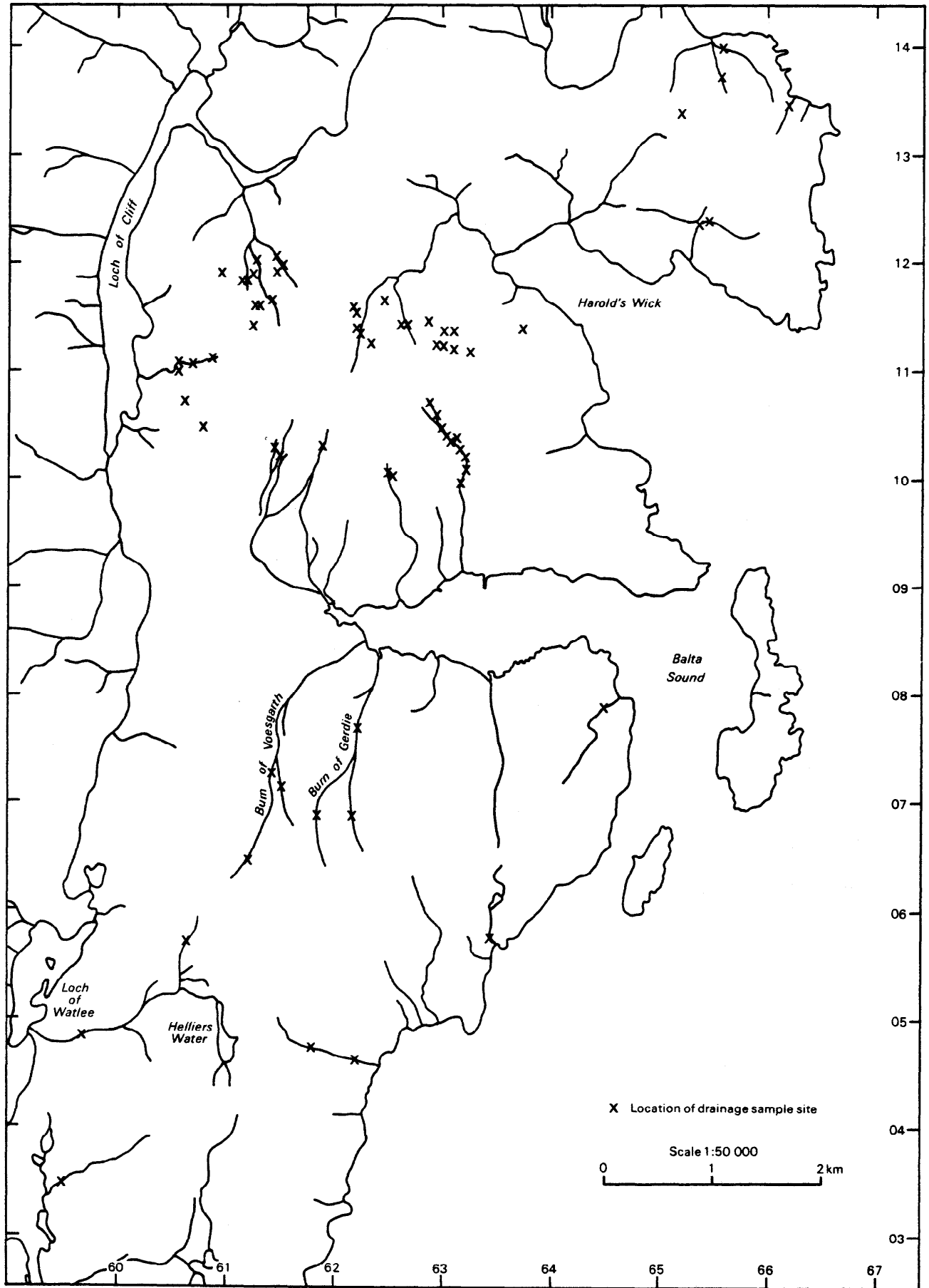
Fig.5   Distribution of drainage sample sites

thrust over the main body of harzburgite.

Maps showing the distribution of samples with relatively high levels of Cr, Fe, Co, Ni, Cu, As, Au and Ir for the complete drainage data set are shown in figures 6-13. Samples with highest levels of Cr are derived from the upper reaches of Mill Burn (Figure 6), to the south-west of Quoys talc quarry. As boulders and small pieces of massive chromite float are common in that area it is likely that some previously undiscovered chromite mineralisation is present. Slightly lower levels of Cr are present in samples from the stream draining south from between Muckle Heog and Nikka Vord and further west, the area with most visible chromite concentrations and old chromite workings. One sample from the Cliff area also contains similar amounts of chromium. Samples with the highest levels of iron follow a roughly north-south linear trend from Burn of Voesgarth in the south to Dale in the north (Figure 7). In these samples the Fe enrichment is not accompanied by similarly high Cr levels, indicating that additional iron in the form of oxide is present. The linear trace of the anomalies suggests that a major structure which has been the locus of hydrothermal activity cuts the complex. Other relatively Fe-rich samples occur in the upper part of the stream south of Muckle Heog. There is a very close correlation between the most Co-rich samples (Figure 8) and those richest in Cr, with the exception of the sample from the Burn of Voesgarth where an additional source of Co, perhaps related to sulphide, is possibly present. The distribution of the most Ni-rich samples are shown in Figure 9. They are concentrated along the same linear zone as for Fe, from north of Helliers Water to Dale , in the Cliff area and on the edges of the group of Cr-rich samples to the south-west of Quoys. Cu-rich samples (Figure 10) are concentrated in the dunite unit to the south of Muckle Heog and also along a roughly north-south line from the Burn of Voesgarth southwards. The extent of the Cu anomalies along this line is greater than the Ni anomalies. The highest levels of As also occur in samples derived from the roughly north-south trending zone running northwards from the Burn of Voesgarth and from the northern part of the Clibberswick block. Other less rich samples occur in the Cliff area, south of Quoys and near Ordale (Figure 11). The As-rich samples from the Clibberswick block are unlike the rest in that other elements such as Fe, Co and Ni which are commonly associated with As are, in fact, present in low concentrations. The distribution of Au-rich samples is shown in Figure 12. Anomalous samples are widely scattered and do not correlate with other elements. The two samples from the eastern part of the gabbro may indicate that that part of the complex shows some general enrichment in Au. Ir is the only PGE determined in all the drainage samples and Figure 13 shows the distribution of samples with higher levels of Ir. It is apparent that all the relatively Ir-rich samples are confined to the harzburgite unit but with a sporadic distribution. The Quoys West area shows the greatest concentration of relatively anomalous samples but the maximum anomaly of 210 ppb is derived from the area of the north-south linear zone of anomalies of several elements near Nikka Vord. There is insufficient data to be able to plot distributions of Ru, Rh or Os-rich samples.

24

Fig.6   Cr in drainage samples

Cr

● ⩾ 21.5   < 25%

★ ⩾ 25%

X Location of drainage sample site

Scale 1:50 000

25

Fig. 7   **Fe in drainage samples**

Fe as Fe$_2$O$_3$

● ⩾27%

X Location of drainage sample site

Scale 1:50 000

0   1   2 km
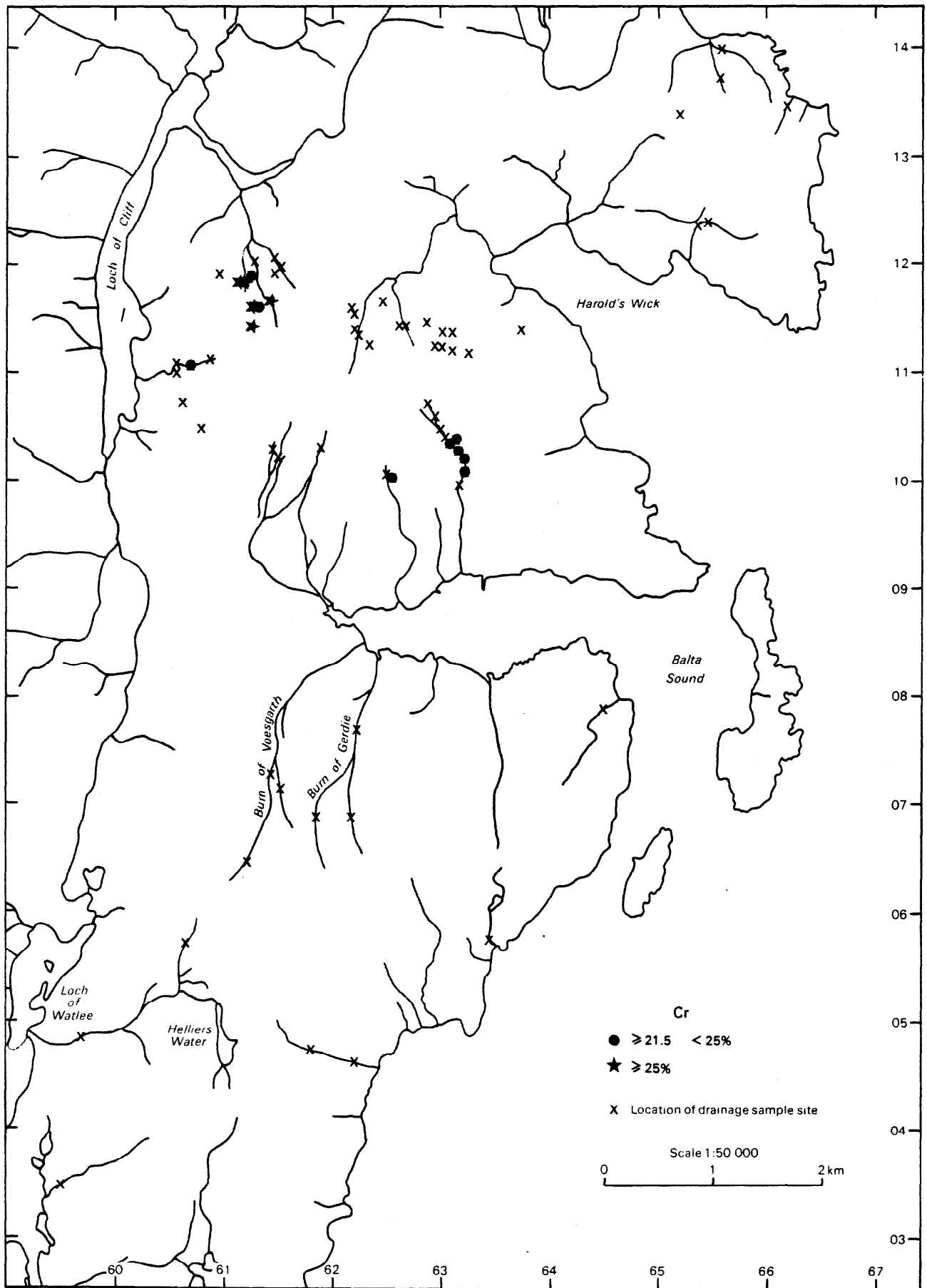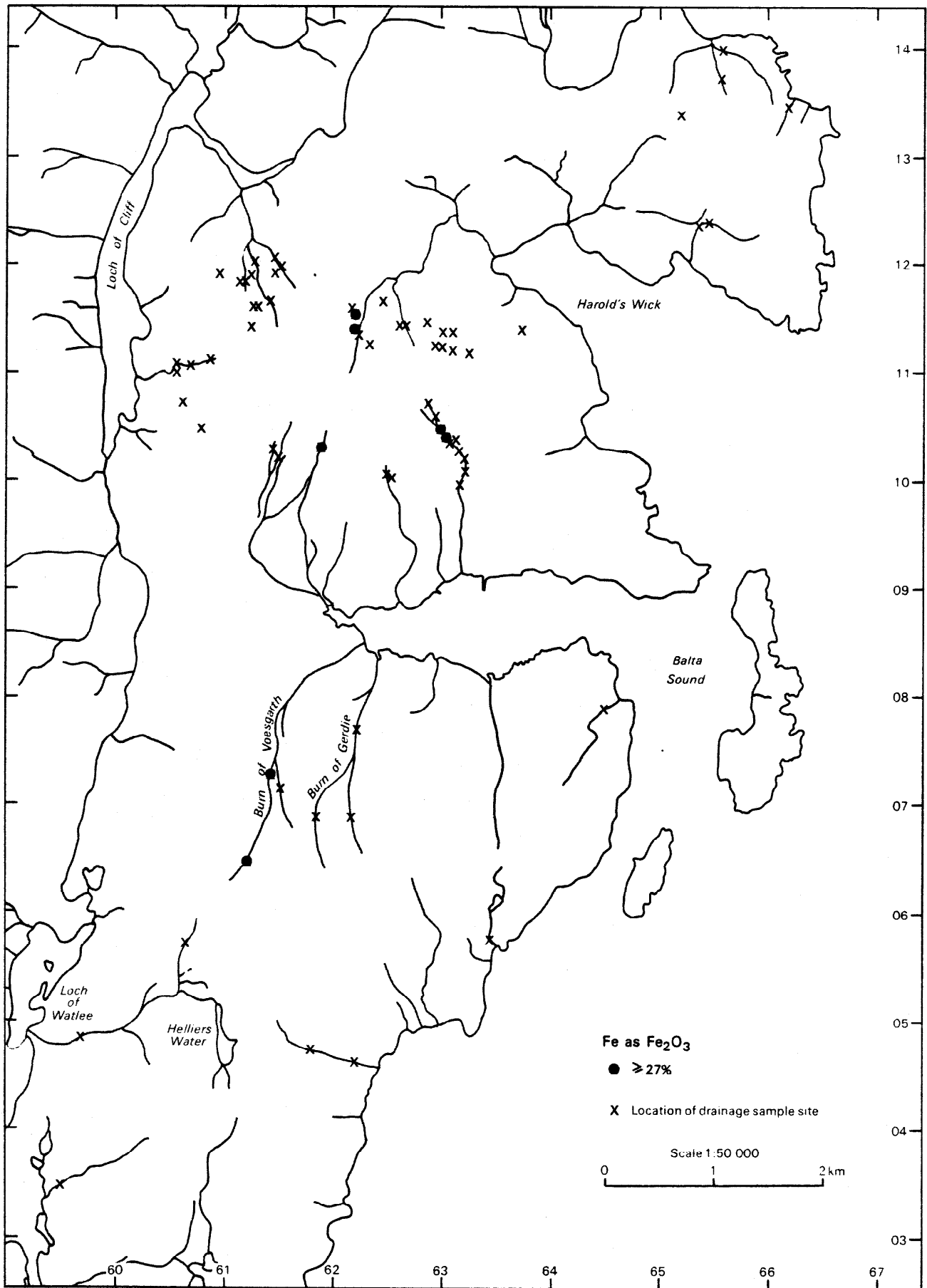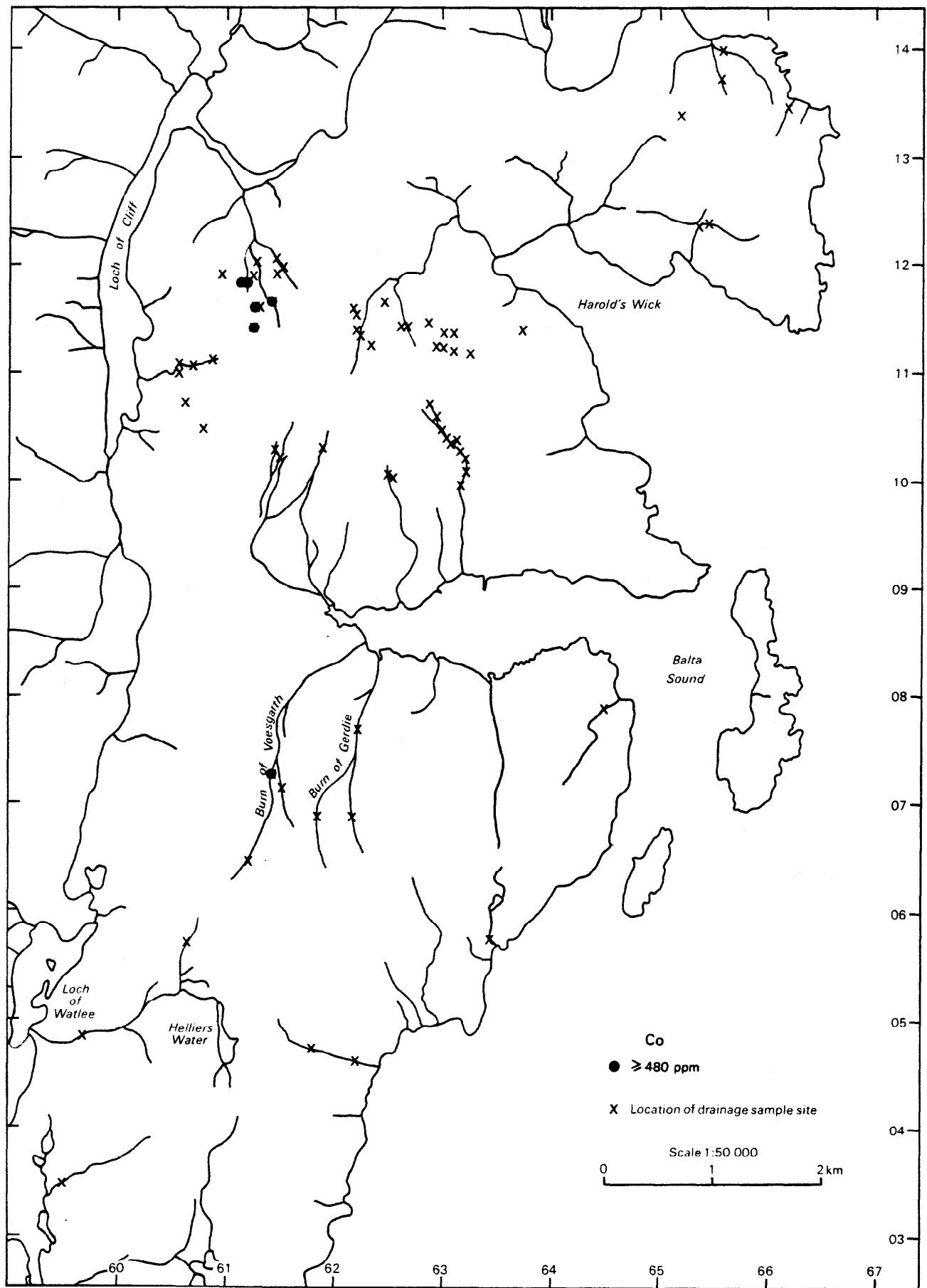
Fig.8   Co in drainage samples

Co

● ≥ 480 ppm

X   Location of drainage sample site

Scale 1:50 000

0   1   2 km

Loch of Cliff

Harold's Wick

Balta Sound

Burn of Voesgarth

Burn of Gerdie

Loch of Watlee

Helliers Water
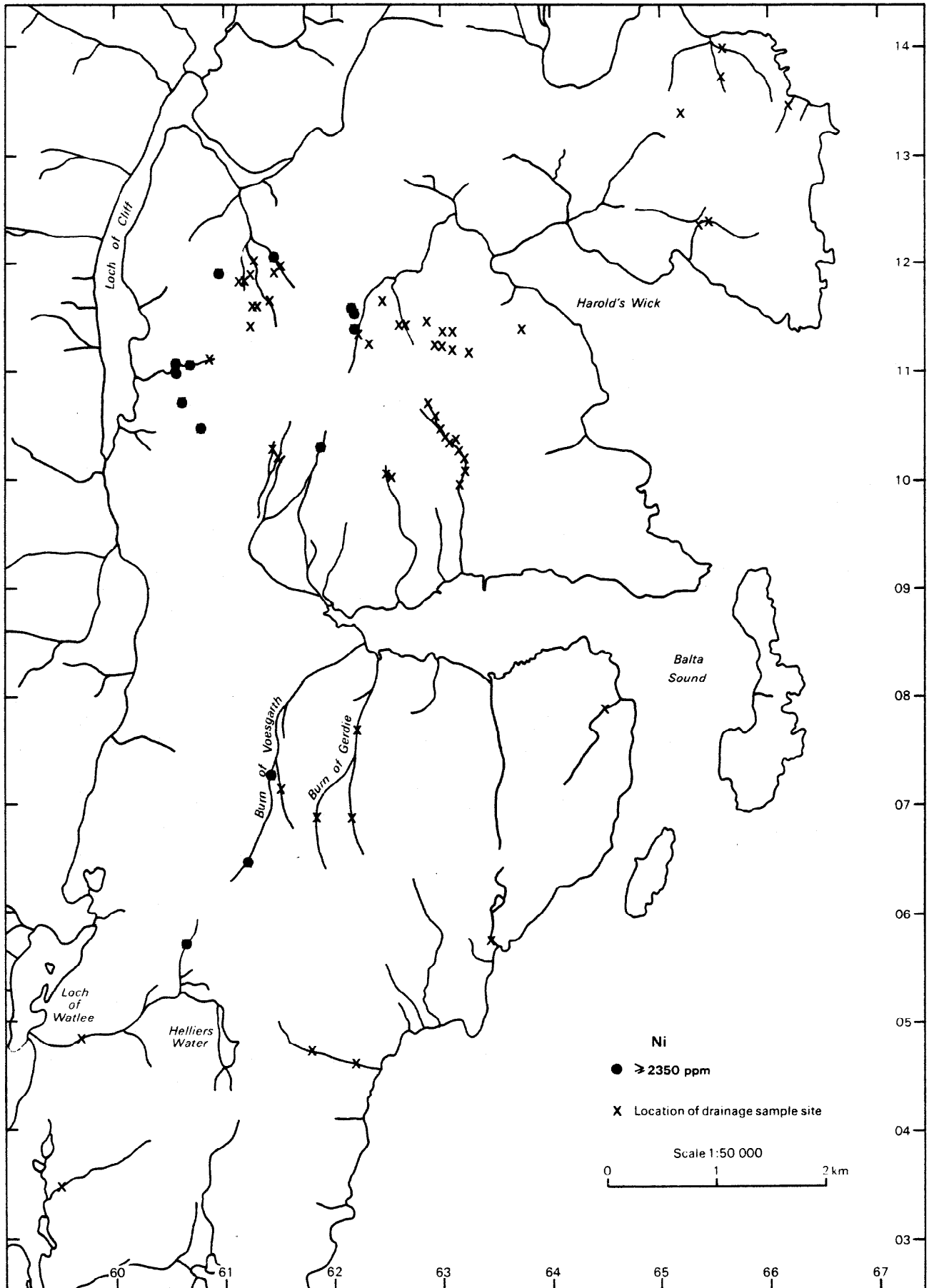
Fig.9 Ni in drainage samples

Ni

● ≥ 2350 ppm

X Location of drainage sample site

Scale 1:50 000

0   1   2 km

Loch of Cliff

Harold's Wick

Balta Sound

Burn of Voesgarth

Burn of Gerdie

Loch of Watlee

Helliers Water
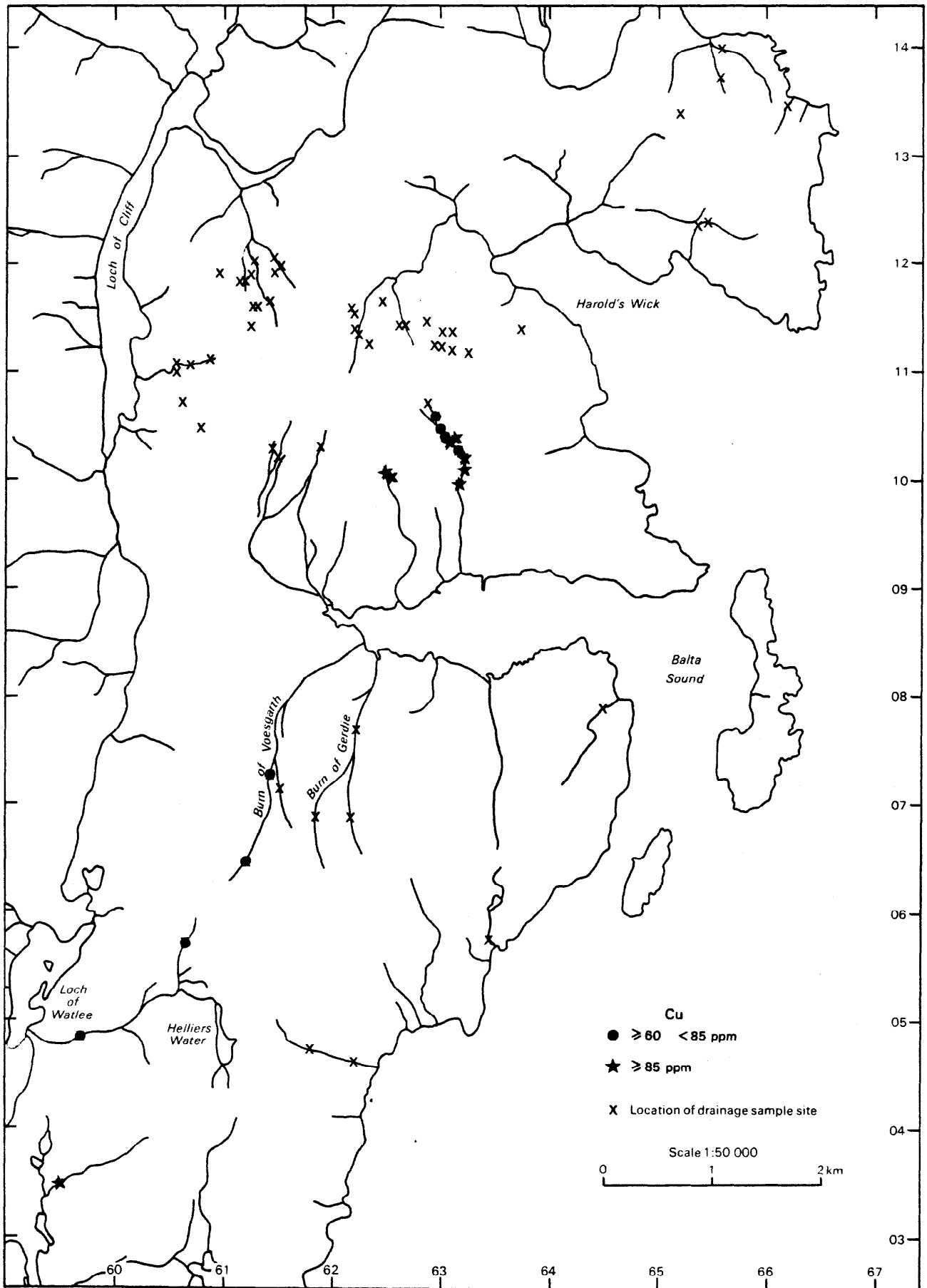
Fig.10   Cu in drainage samples

29
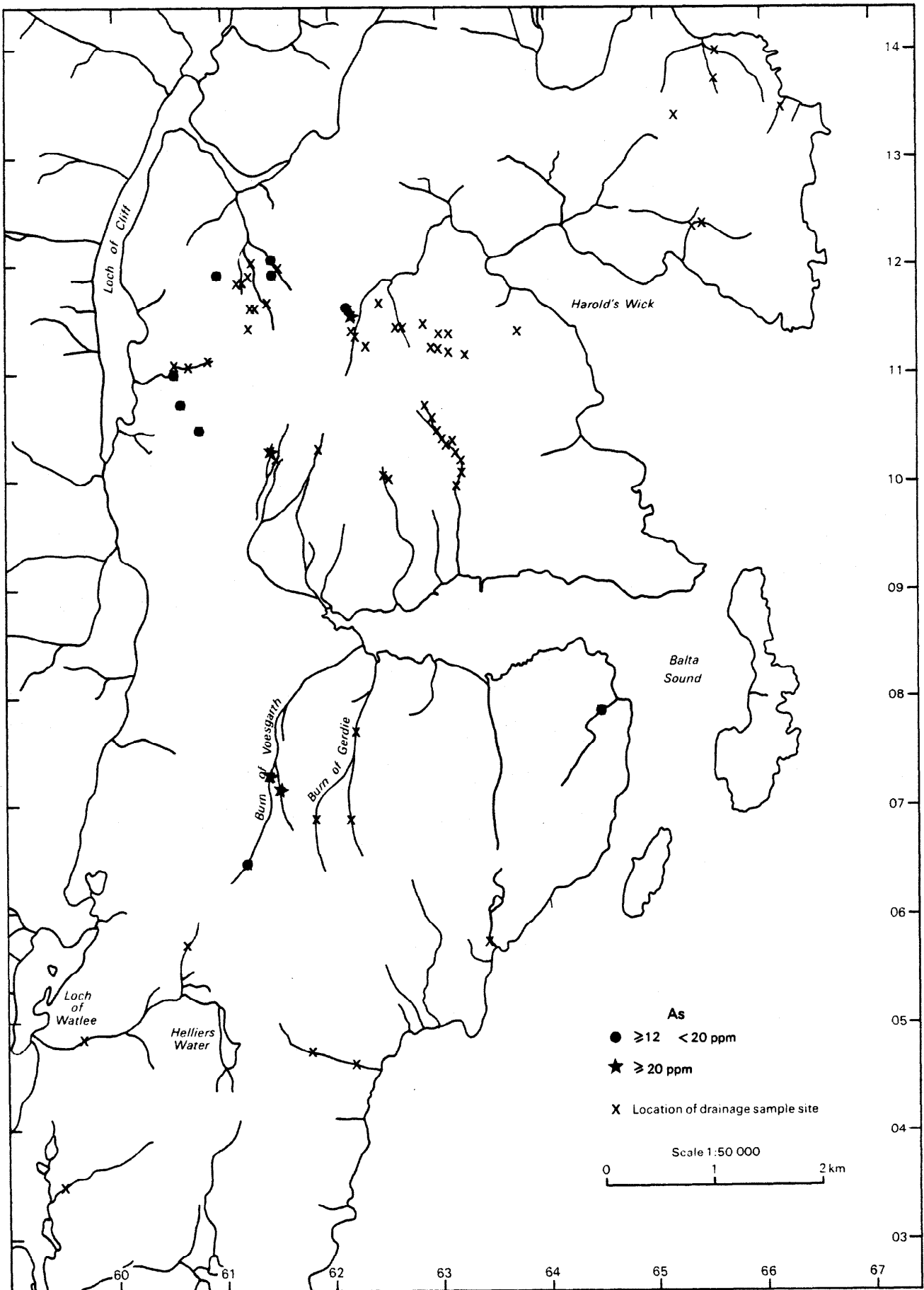
Fig.11   As in drainage samples
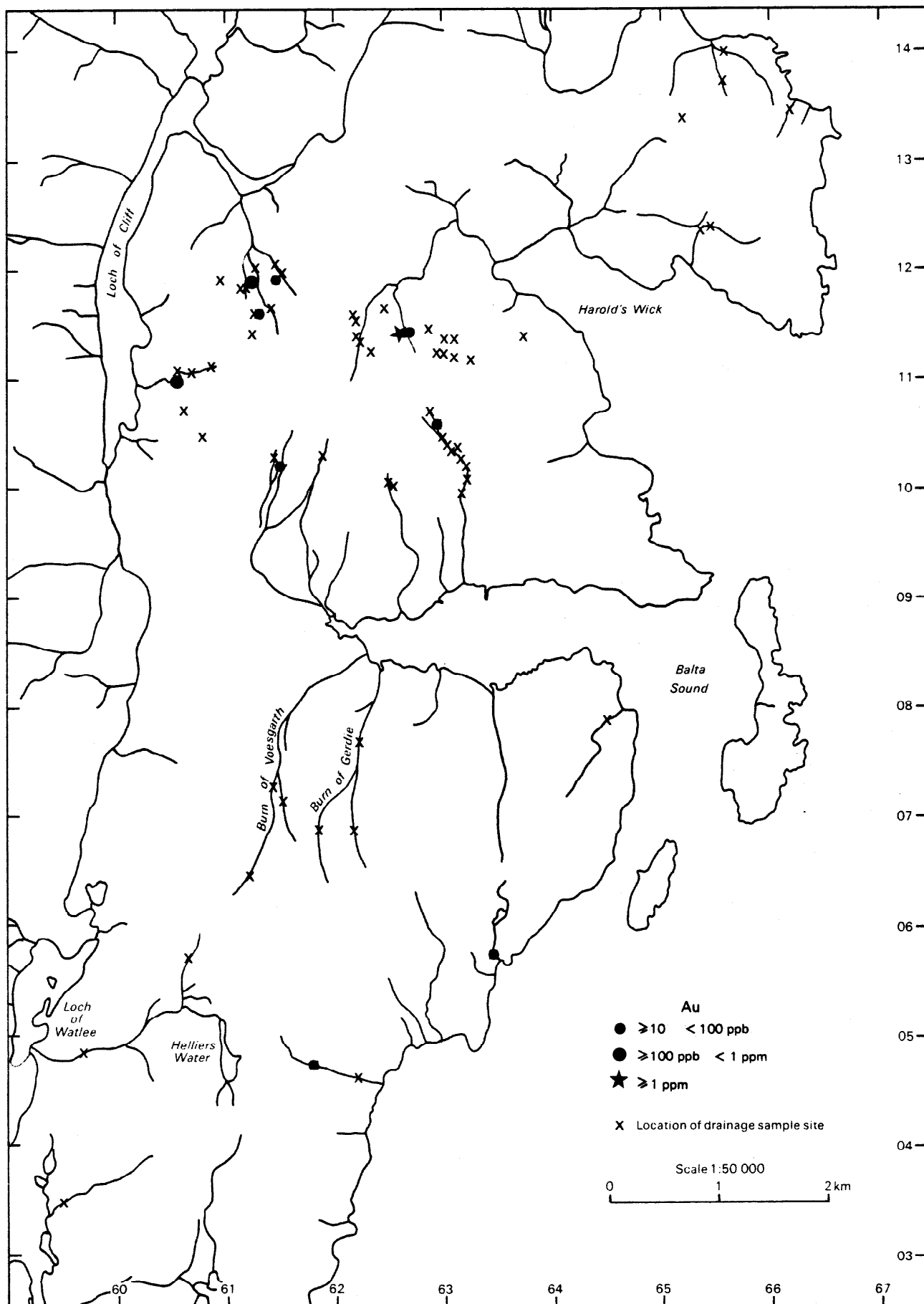
Fig.12   Au in drainage samples

Legend on map:

Au
- ● ⩾10   < 100 ppb
- ● ⩾100 ppb   < 1 ppm
- ★ ⩾1 ppm

X   Location of drainage sample site

Scale 1:50 000

0   1   2 km

Map labels: Loch of Cliff, Harold's Wick, Balta Sound, Burn of Voesgarth, Burn of Gerdie, Loch of Watlee, Helliers Water
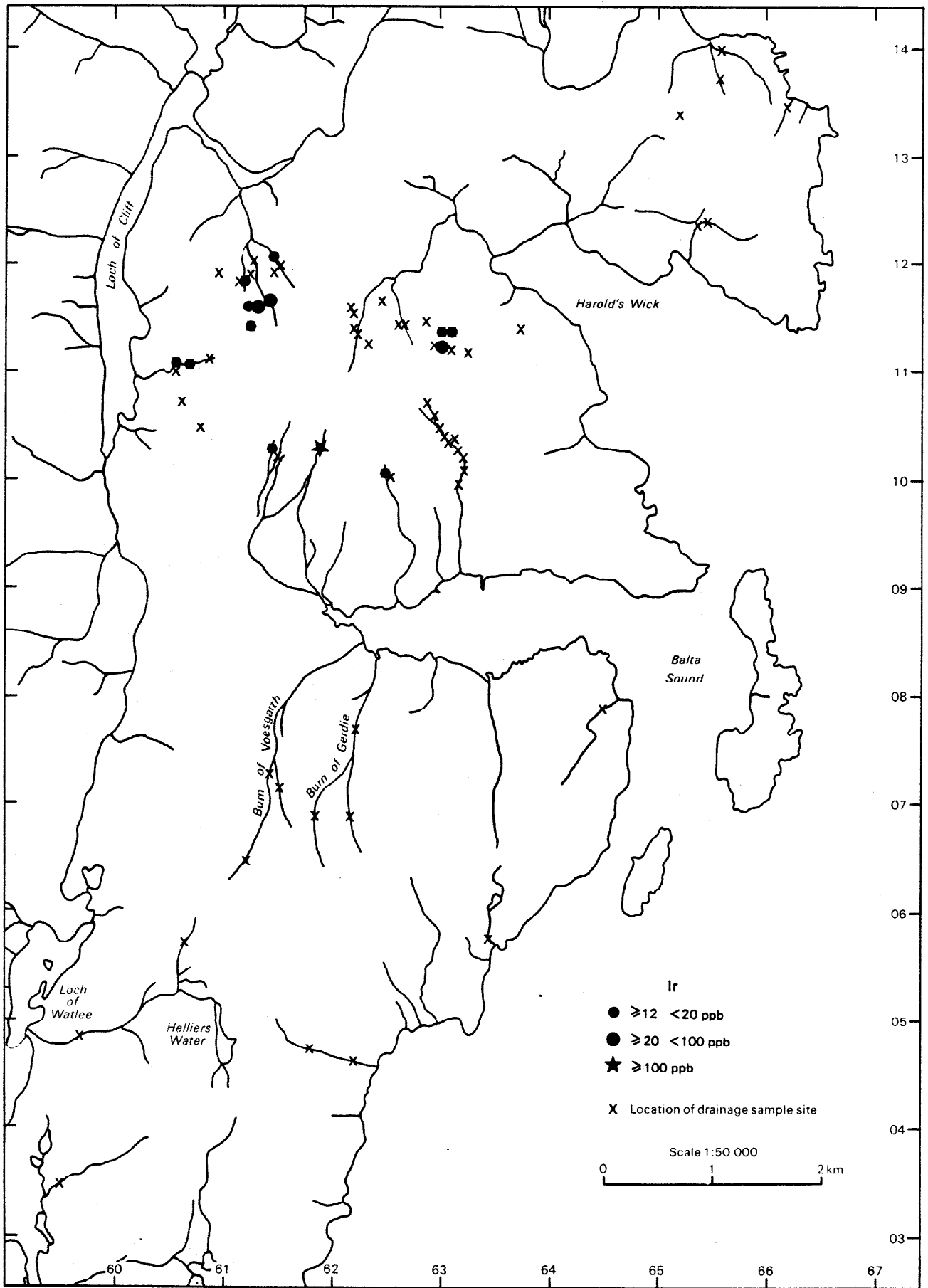
Fig.13   Ir in drainage samples

Labels on map:
- Loch of Cliff
- Harold's Wick
- Balta Sound
- Burn of Voesgarth
- Burn of Gerdie
- Loch of Watlee
- Helliers Water

Legend:
Ir
● ≥12 <20 ppb
● ≥20 <100 ppb
★ ≥100 ppb

X Location of drainage sample site

Scale 1:50 000
0   1   2 km

Overburden sampling

Orientation

An orientation study of overburden sampling methods was carried out in the vicinity of the old chromite workings at Cliff as samples from the dumps had shown the highest levels of PGE. Because of widespread ground disturbance due to previous trenching operations it was not possible to sample immediately adjacent to the workings but a series of pits were sampled both close to and remote from the apparent zone of mineralisation. Previous experience suggested that sieving of the samples to produce a minus 85 mesh BSS fraction (<180 micrometer) could be ineffective as PGE may be associated with chromite of mostly coarser grain size. Panning of the overburden to provide a concentrate of the same type as obtained from the drainage was carried out. In addition a water suspended fraction sample was also collected since if PGE were present as very fine discrete grains they may be lost during the panning process. Material was taken from the orientation pits as located in Figure 14. Sampling intervals and chemical analyses of the panned concentrate samples are shown in table 5.

Table 5 Analyses of pit profile samples

		MgO%	CaO%	Cr%	Fe$_2$O$_3$%	Co	Ni	Cu	Zn	As
1	15-30cm	17.8	2.05	10.99	12.9	253	791	19	1055	0
	30-60cm	18.1	2.06	9.14	19.6	245	1505	23	894	0
	60-80cm	20.7	2.14	7.47	19.6	219	1716	25	714	0
5	15-30cm	30.6	0.92	5.30	11.5	166	1668	15	560	0
	30-60cm	28.6	1.28	5.28	12.9	176	1714	16	541	3
	60-75cm	30.3	0.97	4.36	15.9	167	2215	21	406	5
6	15-30cm	16.6	2.31	7.62	12.9	186	851	21	756	0
	30-60cm	26.5	1.72	5.88	16.8	194	1804	23	572	2
	60-75cm	29.1	1.32	4.84	13.4	154	1632	20	449	5
8	15-30cm	32.8	0.78	3.15	17.7	181	2951	24	274	12
	30-60cm	33.8	0.77	2.97	17.2	179	3077	23	245	12
	60-75cm	34.1	0.75	2.98	21.5	204	3358	26	271	20
9	15-30cm	32.2	1.00	5.05	12.8	166	1817	17	458	7
	30-60cm	34.3	0.84	3.53	14.9	133	2063	18	292	9
	60-75cm	38.8	0.45	2.14	11.1	114	2119	13	126	12

The results show a tendency for Cr and associated Zn levels to decrease with depth probably due to the greater proportion of rock fragments making up the original sample before panning. In contrast there is an increase in Ni levels with depth and in some cases a marked increase from the uppermost sample to the next. As and Cu also show increases down the profile but other element distributions are less regular. Because of the big differences in Ni contents in some samples from the 15-30cm to 30-60cm levels in the pits, which may be the result of leaching, the 30-60cm level was chosen as a standard sampling depth.

A general comparison of the panned concentrate sample and the equivalent suspended solid sample from the same site is shown in table 6. Cr and Zn show the greatest enrichment in the concentrate relative to the water suspended
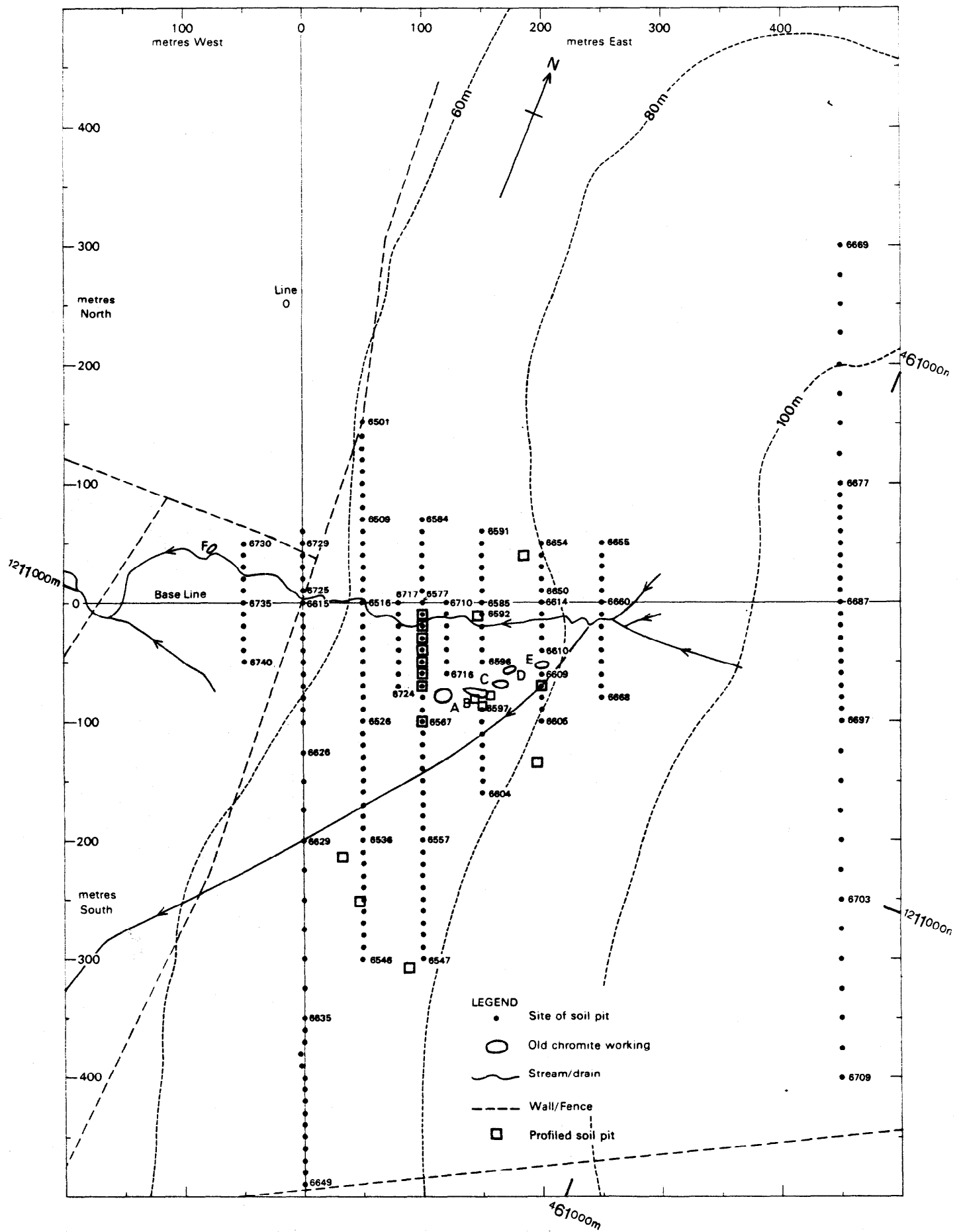
Fig. 14   Distribution of overburden sample sites in Cliff area

LEGEND

●   Site of soil pit

⬭   Old chromite working

〰   Stream/drain

- - -   Wall/Fence

▢   Profiled soil pit

fraction samples. This is a consequence of a combination of the relatively coarse grain size of most of the chromite and the concentration of chromite as a heavy mineral during panning. The vast majority of Zn in these samples must be accommodated in chromite to account for the similarity in behaviour. In contrast Fe shows a much smaller degree of concentration in the panned samples which indicates a significant amount of mobilisation of the element derived from the weathering of the common silicates and perhaps some sulphides in the secondary environment. The lower but still significant Mg content of the concentrates is a reflection of the silicate content of the concentrates which are still present in substantial amounts in consequence of the incomplete degree of panning employed. The elements Cu and As are present in broadly similar amounts in both sample types. Of the PGE Rh, Pd and Pt are significantly richer in the panned samples than the water suspended fraction samples which indicates that in spite of the fine grain size of the PGMs the panning procedure is not losing a large proportion of these elements. The enrichment factor is much less than for Cr however, indicating that PGE cannot be largely included within chromite grains. The enrichment factor for Ru in the panned concentrates is anomalously low and a reason for this is unclear. Data from the two sample types from line 150E at Cliff, which traverses the zone of old chromite workings, is shown in Figure 15 as a profile plot. This shows similar patterns for Fe, Ni, Ni/MgO but with the peak amplitude of suspended fraction samples generally less than in the corresponding panned samples. For other elements like Cr and Co the anomalies present in the panned sample data do not appear in the corresponding suspended fraction samples.

Table 6 Comparison of panned concentrate and water suspended fractions

	Water suspended fraction			Panned concentrate		
	Mean	S. D.	Range	Mean	S. D.	Range
MgO%	34.28	2.27	29.37-39.90	23.55	5.91	13.09-36.24
Sppm	237	85	118- 436	79	31	41- 181
CaO%	0.47	0.15	0.20- 0.77	1.40	0.46	0.25- 1.99
Cr%	0.22	0.06	0.12- 0.39	8.27	3.85	2.78-17.31
Fe₂O₃%	9.79	1.94	5.16-15.51	15.82	2.65	11.57-24.00
Coppm	99	17	63- 143	222	61	126- 357
Nippm	2191	332	1667-2941	1645	413	992- 2696
Cuppm(6)	16	4	13- 21	22	3	18- 27
Znppm	42	3	38- 45	838	361	604- 1564
Asppm	3	3	<1- 10	5	7	<1- 10
Ruppb(6)	40	32	10- 100	56	29	20- 100
Rhppb(6)	<5			13	10	<5- 27
Pdppb(6)	17	10	<5- 30	83	72	5- 200
Ptppb(6)	8	3	<10- 10	60	67	<10- 180

No. of samples 40 or 6 as shown

Comparative data for different sample types from two sites with anomalous PGE levels are shown in table 7. In addition to the panned concentrate and water suspended fraction samples a minus 85 B.S.S mesh sieved sample of the type commonly used for geochemical soil surveys is included together with the analysis of the minus 100 B.S.S. fraction (<150 micrometer) of the panned concentrate sample.
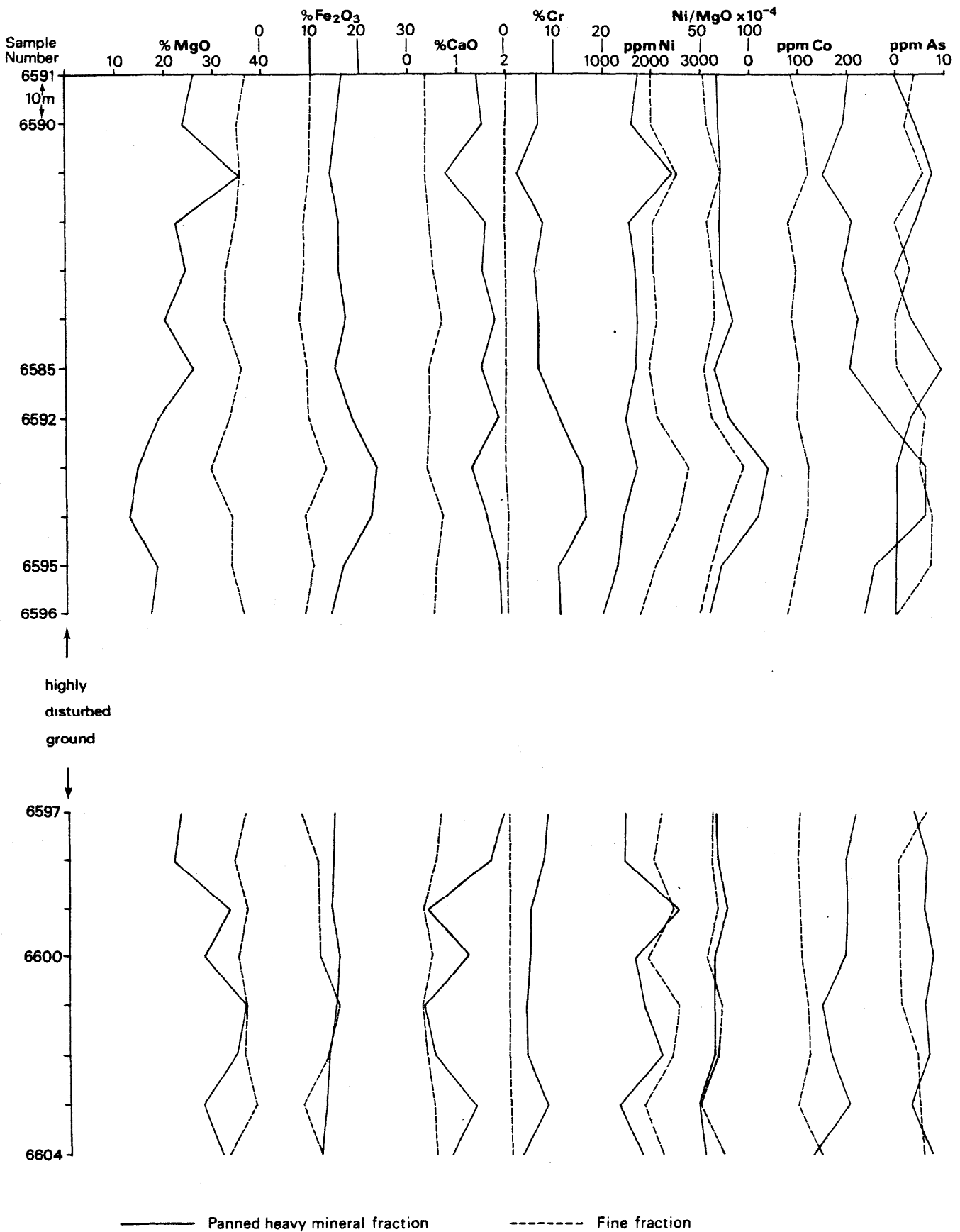
Fig. 15   Comparison of element distributions in fine and panned heavy
mineral fractions of overburden samples from line 150E at Cliff

Table 7 Comparison of overburden sample types from two anomalous sites

| | Sample 6571 | | | | Sample 6573 | | | |
	A	B	C	D	A	B	C	D
MgO%	33.36	30.95	21.40	18.64	34.63	32.68	26.53	22.39
CaO%	0.50	0.63	1.98	3.34	0.41	0.29	1.08	2.20
Sppm	159	184	68	67	147	222	61	64
Cr%	0.19	0.20	8.34	7.10	0.28	0.16	7.75	8.45
Fe_2O_3%	7.86	7.87	16.57	15.84	6.03	8.89	14.32	14.61
Coppm	120	108	233	212	110	103	209	240
Nippm	2719	2480	1677	1462	2346	2637	1991	1593
Cuppm	21	20	25	24	21	17	22	23
Znppm	48	45	689	830	52	38	666	969
Asppm	12	3	10	2	8	7	<1	<1
Ruppb	-	30	100	-	-	30	60	-
Rhppb	-	<5	27	-	-	<5	8	-
Pdppb	70	30	200	340	20	25	110	150
Ptppb	30	10	180	290	10	10	30	300

Sample A -85mesh fraction, B water suspended fraction, C panned concentrate
Sample D -100mesh fraction of panned concentrate.

In general the compositions of the -85mesh and water suspended fraction samples from one site are very similar as are the two panned concentrate samples. The levels of PGE are significantly higher in the panned concentrate samples than the other sample types and there is also a significant upgrading of the levels in the -100 mesh fraction of the concentrate. Since the -100 mesh fraction of the concentrate samples comprises only between 13 and 23% of the total it is probable that some of the PGEs in these two samples must be present as inclusions in larger grains even allowing for the likely subsampling precision. The only example where the difference is compatible with presence entirely in the fine fraction is Pt in sample 6573.

The above data indicate that the panned concentrate of an overburden sample is likely to be the most effective sample type for exploration for PGE in areas of poor exposure. This sample type has other practical advantages for exploration because it can be examined directly using a binocular microscope in the field. Observations made in this way suggest that variations in the proportions of coarse to fine grained chromite could be important in the detection of concealed massive chromitite. Other readily identified minerals like the purple Cr-chlorite kammererite, oxide gossan after sulphide, different types of serpentine and secondary nickel minerals could also be important indications of proximity to chromite or PGE mineralisation.

Overburden survey of Cliff area.

A grid of overburden samples was collected at the 30-60cm depth interval from pits in the vicinity of the old chromite workings in the Cliff area as shown in Figure 14. The samples were analysed for a range of elements by X.R.F. and, subsequently, selected samples were analysed for PGE by nickel sulphide fire assay with a furnace AAS finish as described above. Maps showing the distribution of the elements Mg, Si, Ca, Cr, Fe, Co, Ni, Zn, As, Sb, Te and Bi, Ru, Rh, Pd, Ir, Pt and the ratio Ni/MgO are shown in Figures 16-32. The chemical data are plotted in class interval form with levels chosen mostly from the breaks in slope of cumulative frequency plots included with each map.

Fig. 16   MgO in panned overburden samples from Cliff area

LEGEND
- Site of soil pit
- Old chromite working
- Stream/drain
- Wall/Fence

⊙ < 17%
• ≥ 17 < 33%
● ≥ 33%
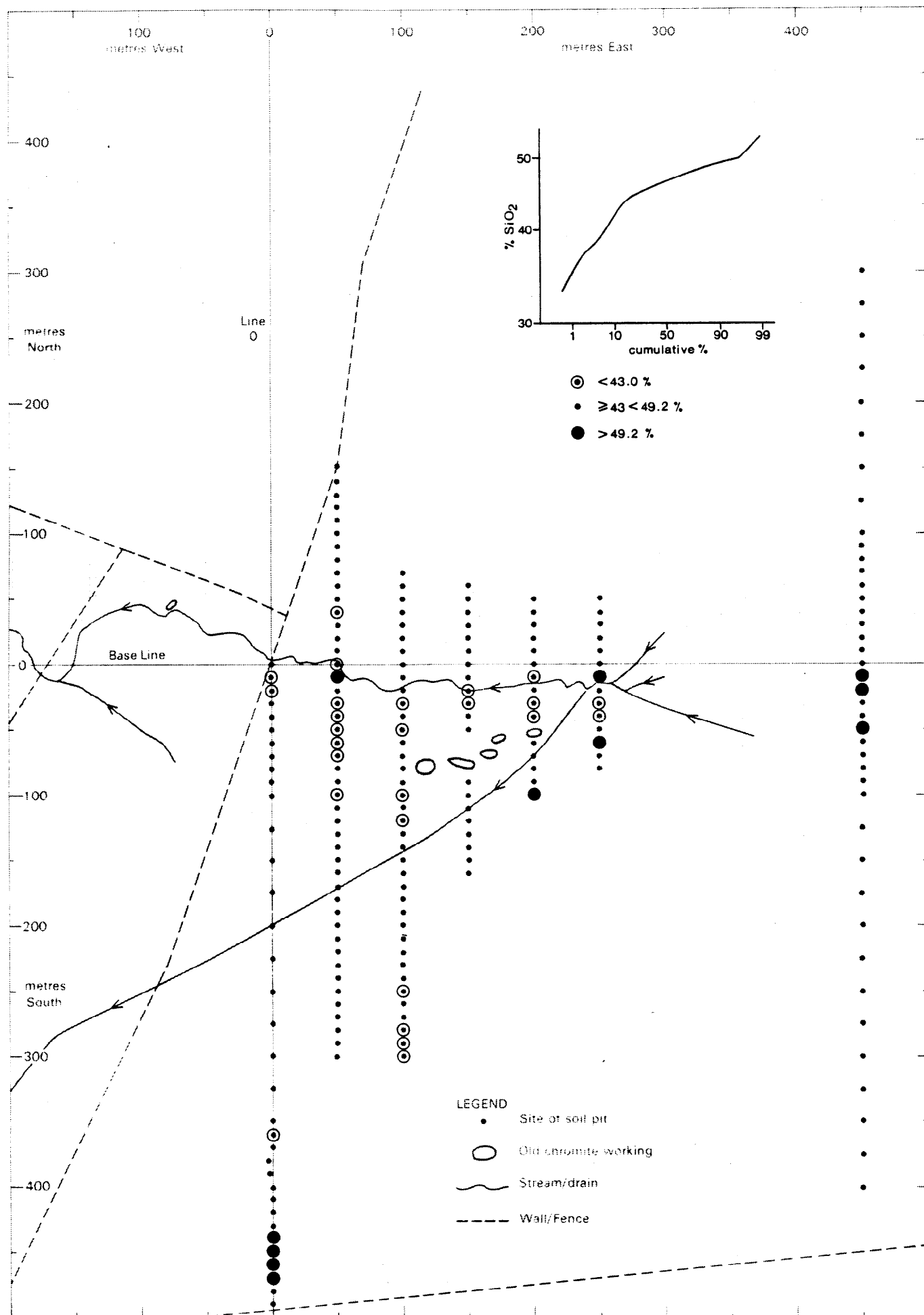
Fig. 17 SiO$_2$ in panned overburden samples from Cliff area

Fig. 18   CaO in panned overburden samples from Cliff area

Inset axis labels:
% CaO: 2.0, 1.0, 0.5, 0.1
Cumulative %: 1, 10, 50, 90, 99

⊚ < 0.62%
• ≥ 0.62% ≤ 1.8%
● > 1.8%

LEGEND
• Site of soil pit
⬭ Old chromite working
〜 Stream/drain
--- Wall/Fence

100 metres West   0   metres East
100   200   300   400

metres North: 400, 300, 200, 100
Line 0
Base Line
0
metres South: 100, 200, 300, 400
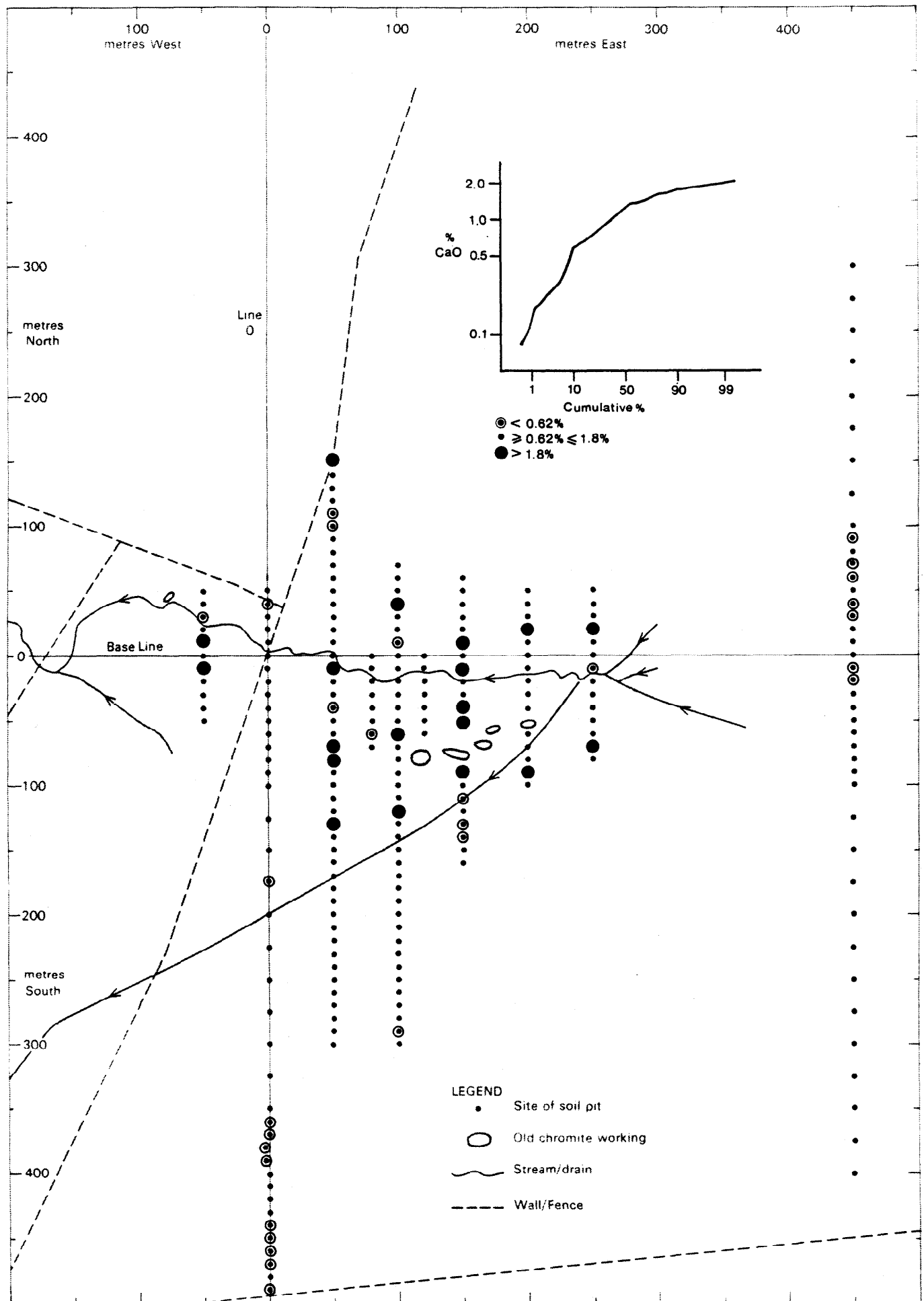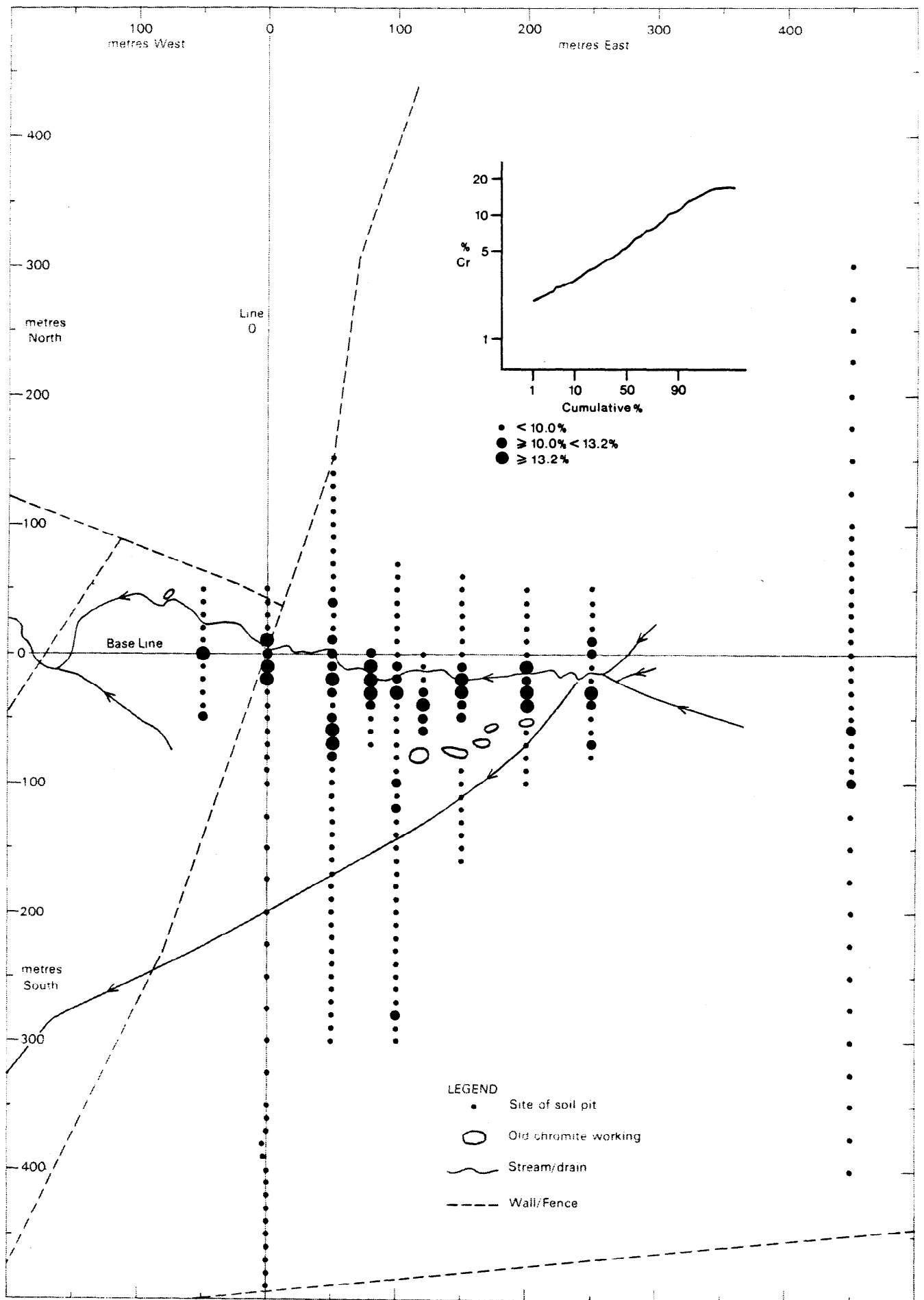
Fig. 19.   Cr in panned overburden samples from Cliff area
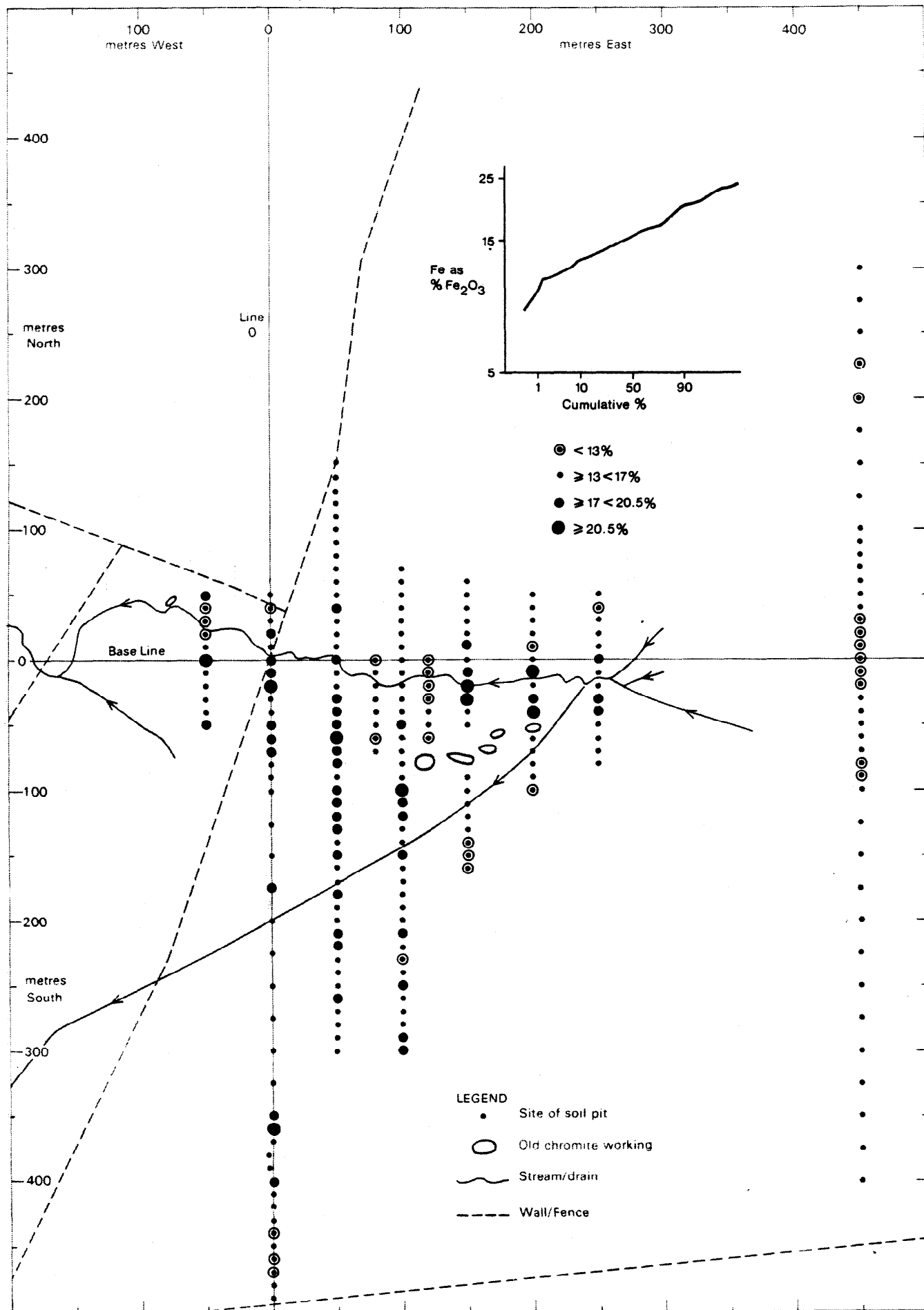
Fig. 20   Fe in panned overburden samples from Cliff area

Legend content within figure:

- ⊙ < 13%
- · ≥ 13 < 17%
- ● ≥ 17 < 20.5%
- ● ≥ 20.5%

Inset graph axis: Fe as % Fe_2O_3 ; Cumulative %

LEGEND

- · Site of soil pit
- ⬭ Old chromite working
- ～ Stream/drain
- – – Wall/Fence
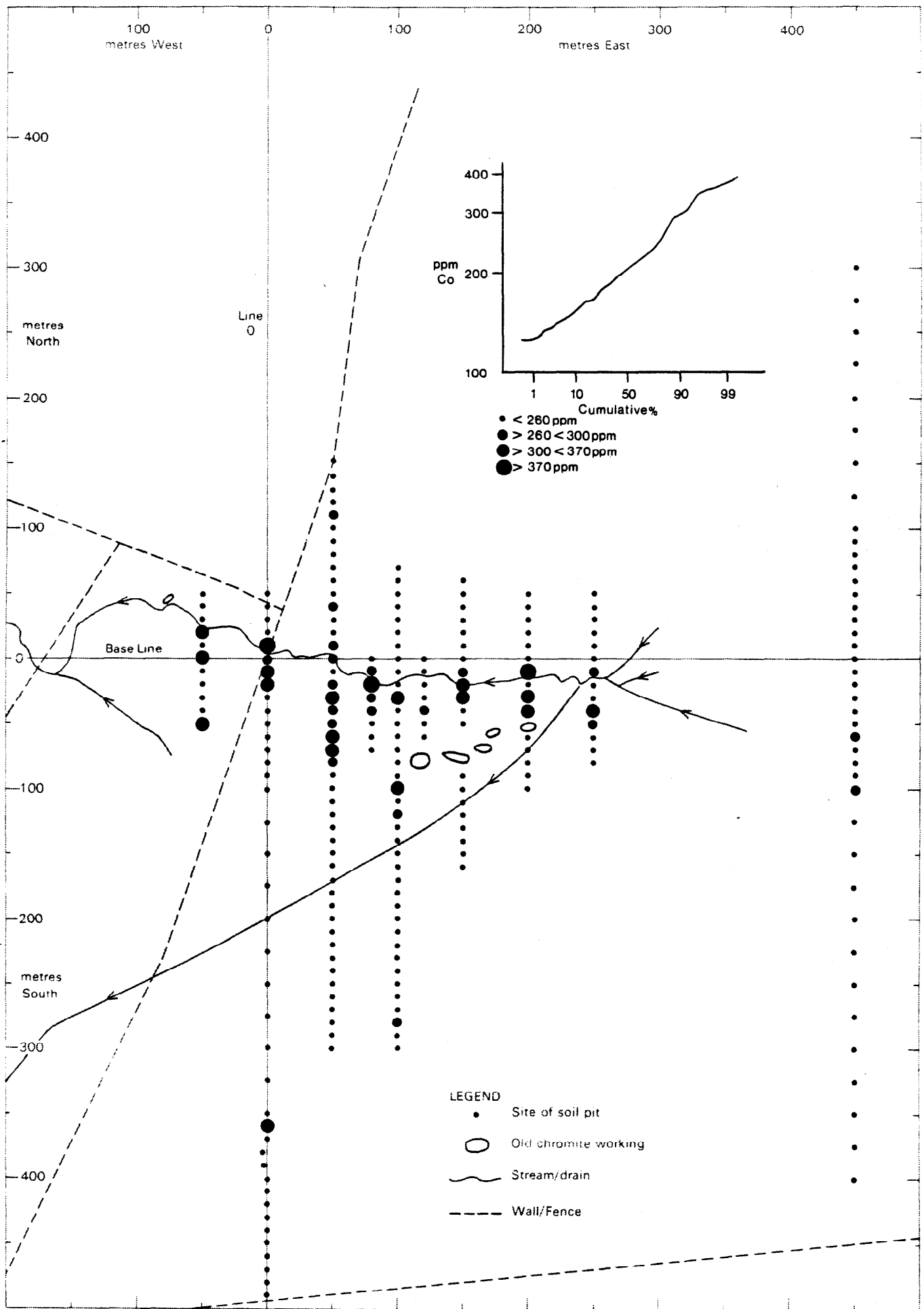
Fig. 21　　　　Co in panned overburden samples from Cliff area
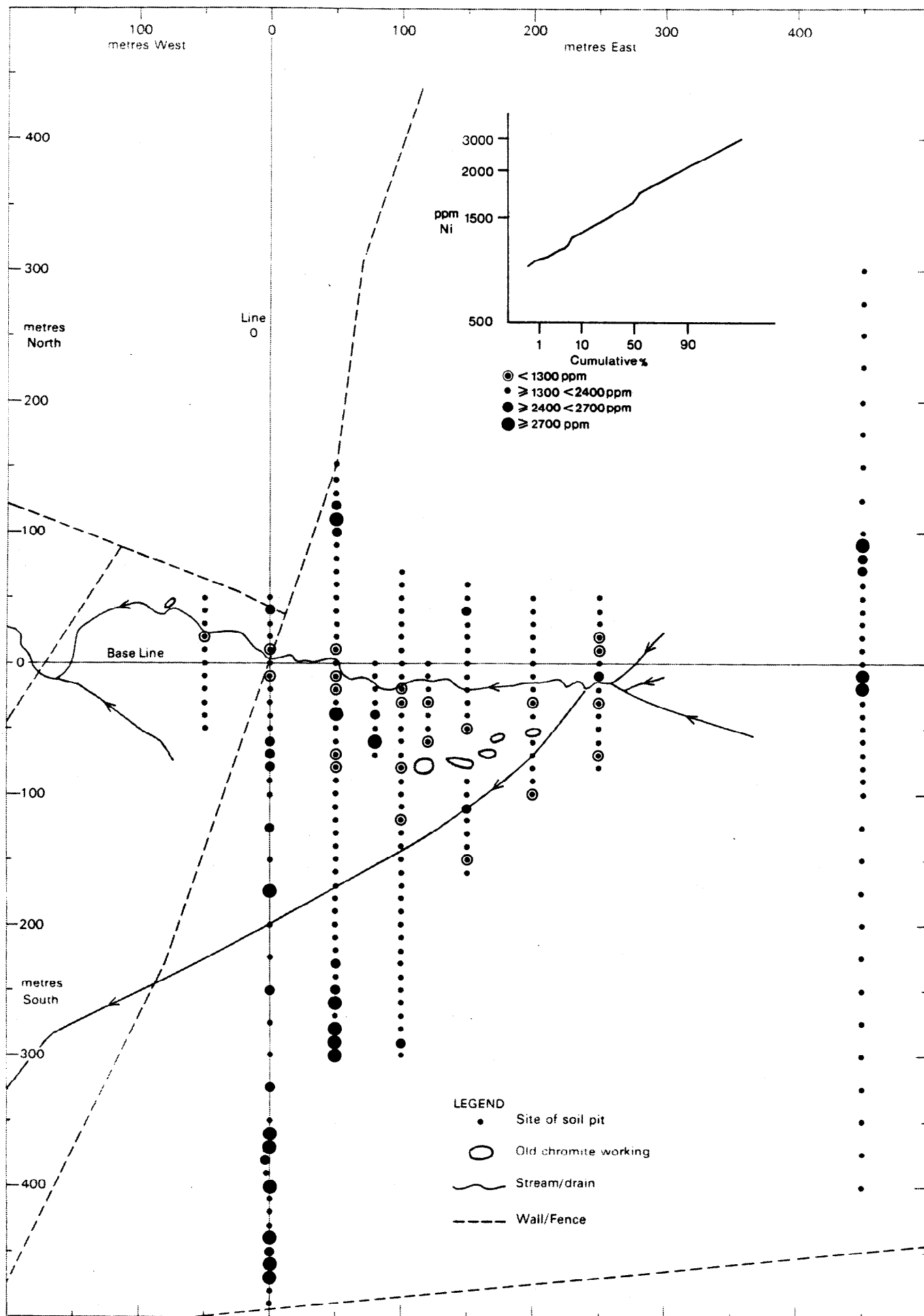
Fig. 22   Ni in panned overburden samples from Cliff area
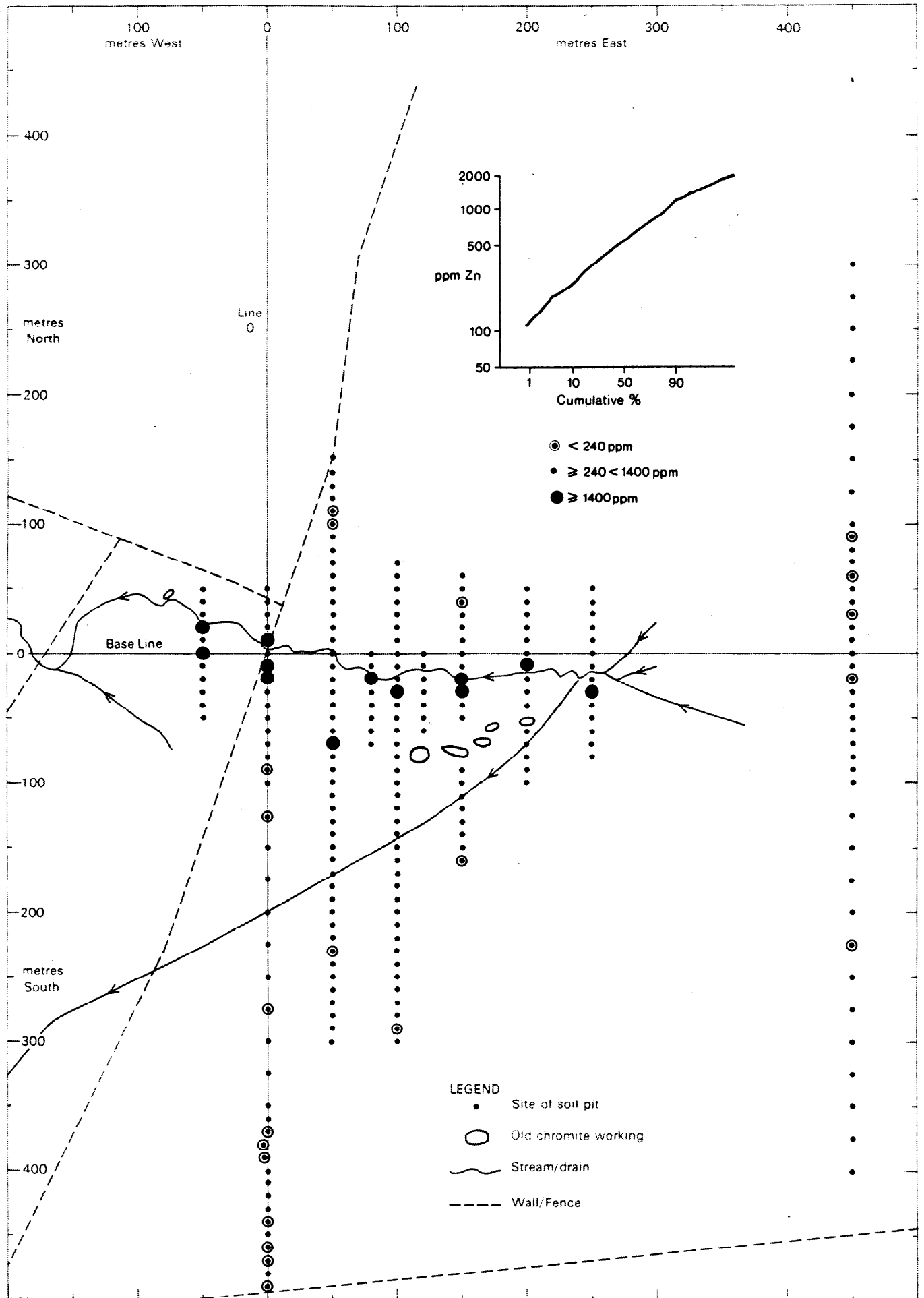
Fig. 23   Zn in panned overburden samples from Cliff area
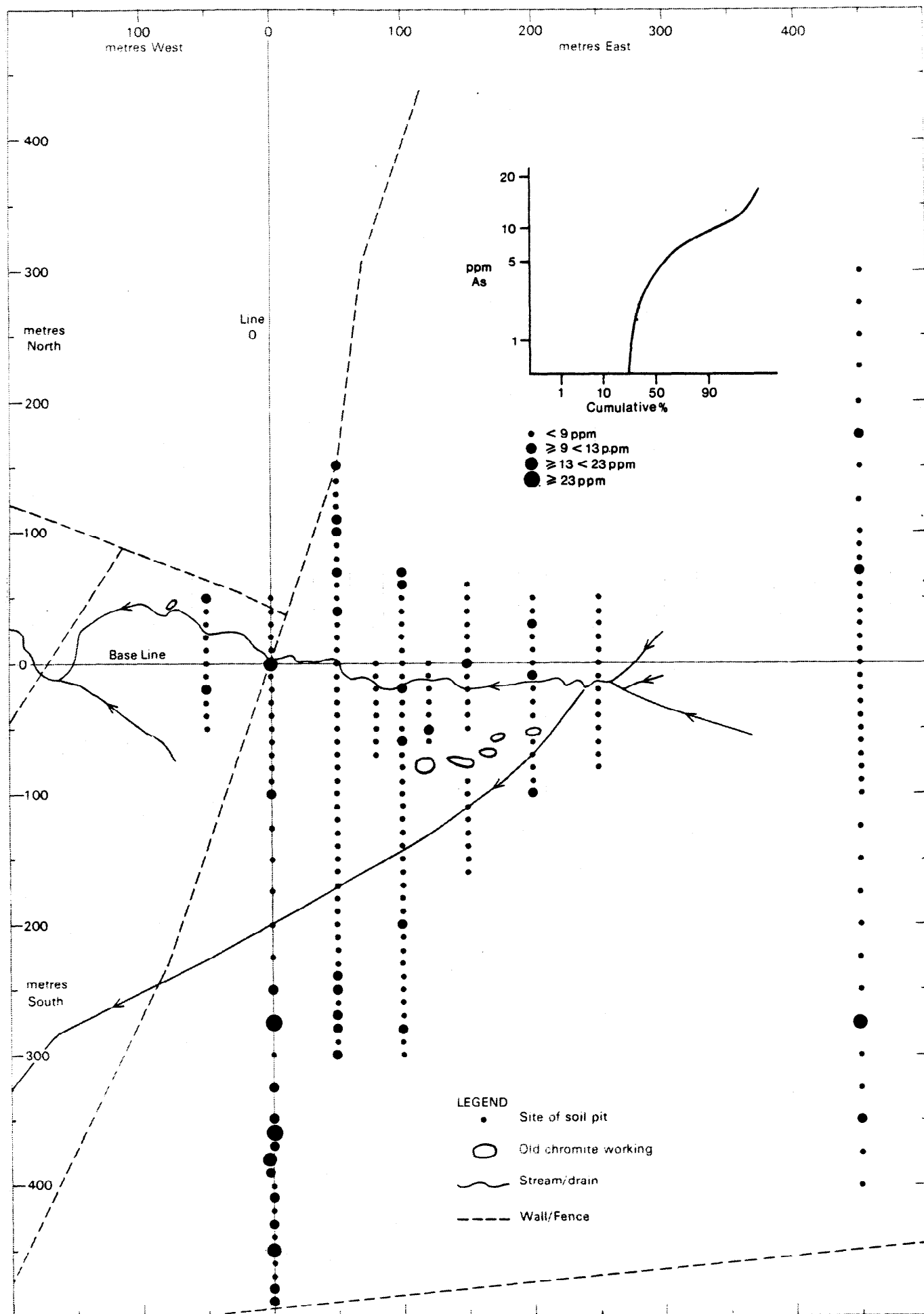
Fig. 24 As in panned overburden samples from Cliff area
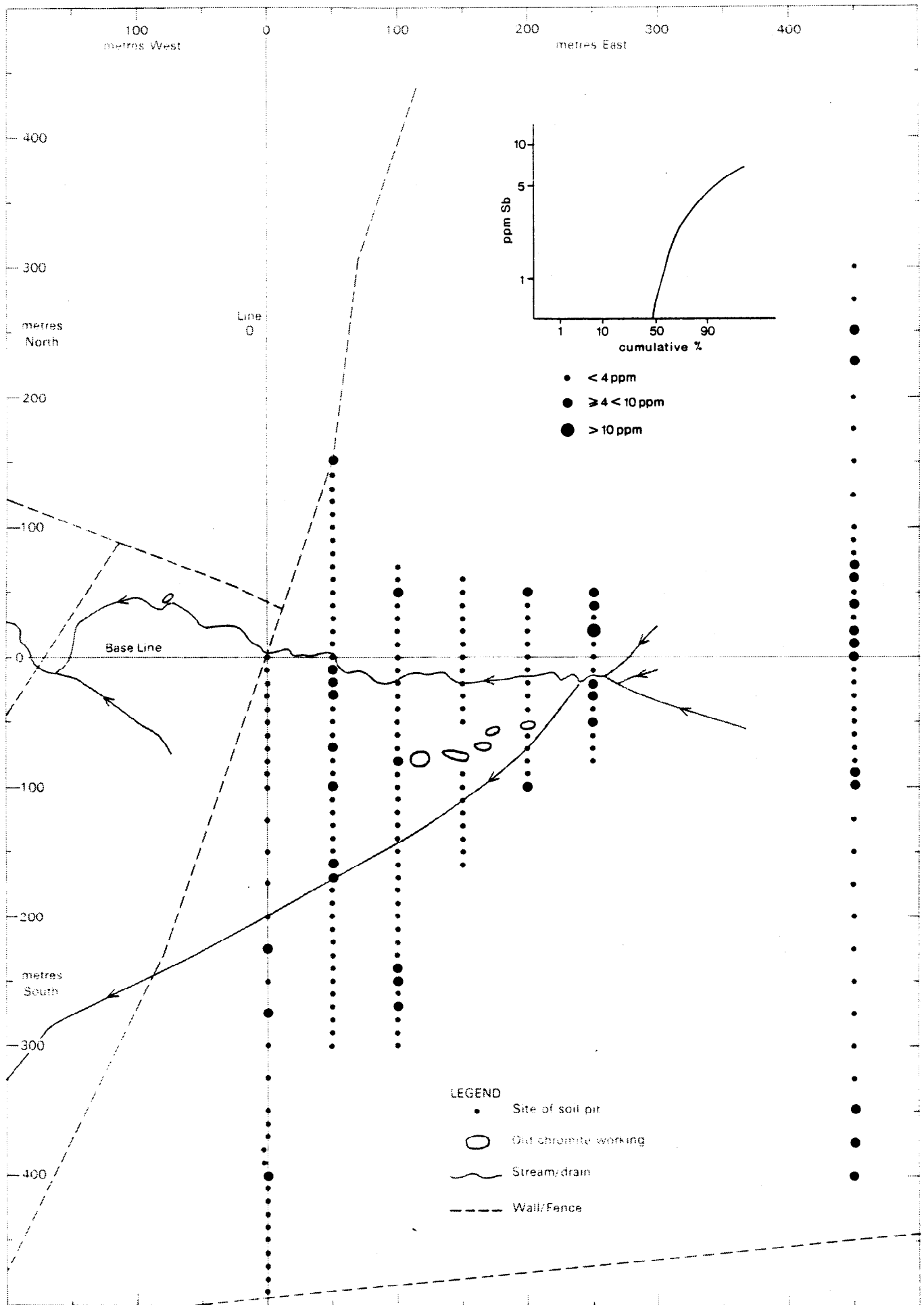
Fig. 25   **Sb in panned overburden samples from Cliff area**
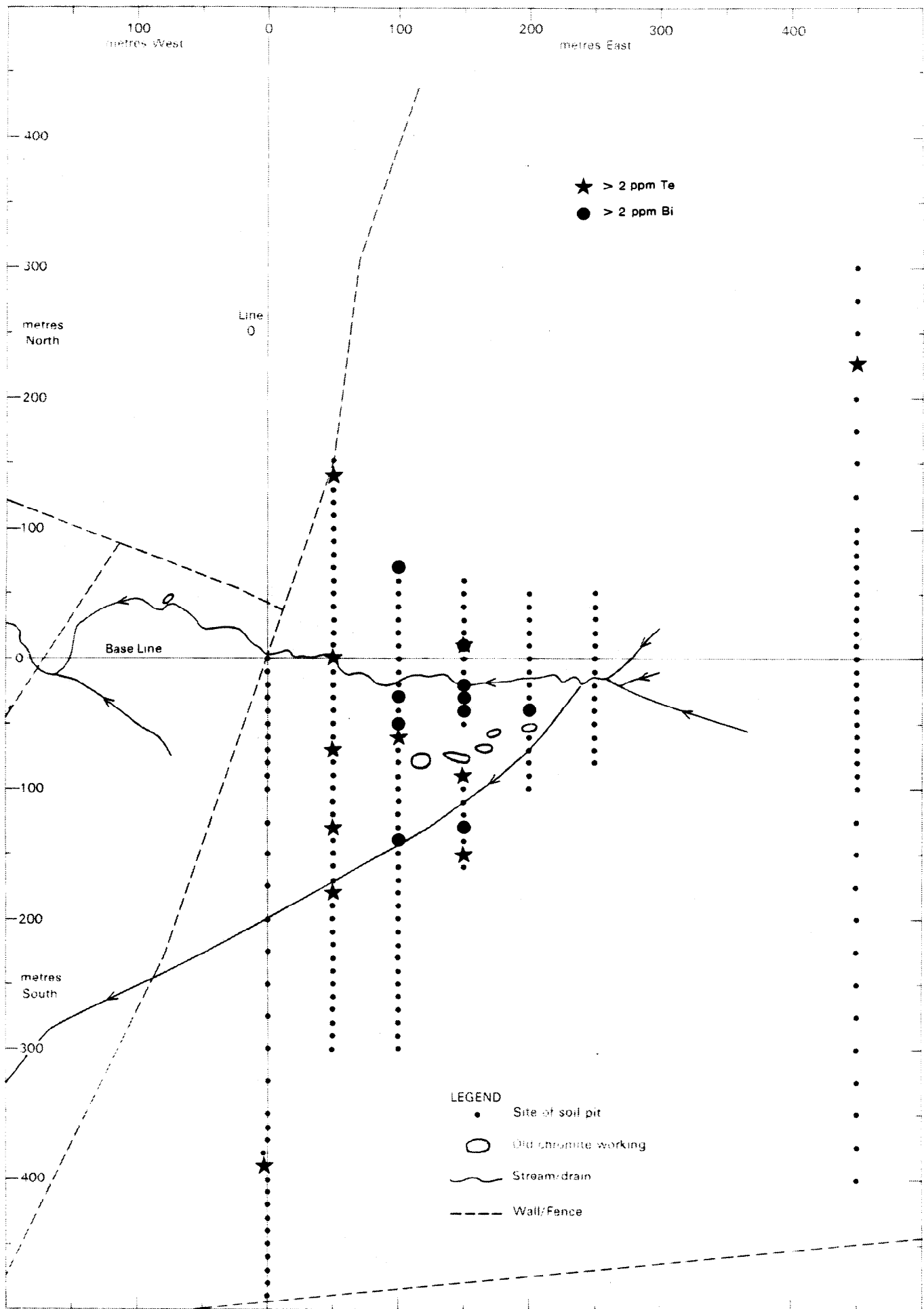
Fig. 26　　　　Te and Bi in panned overburden samples from Cliff area
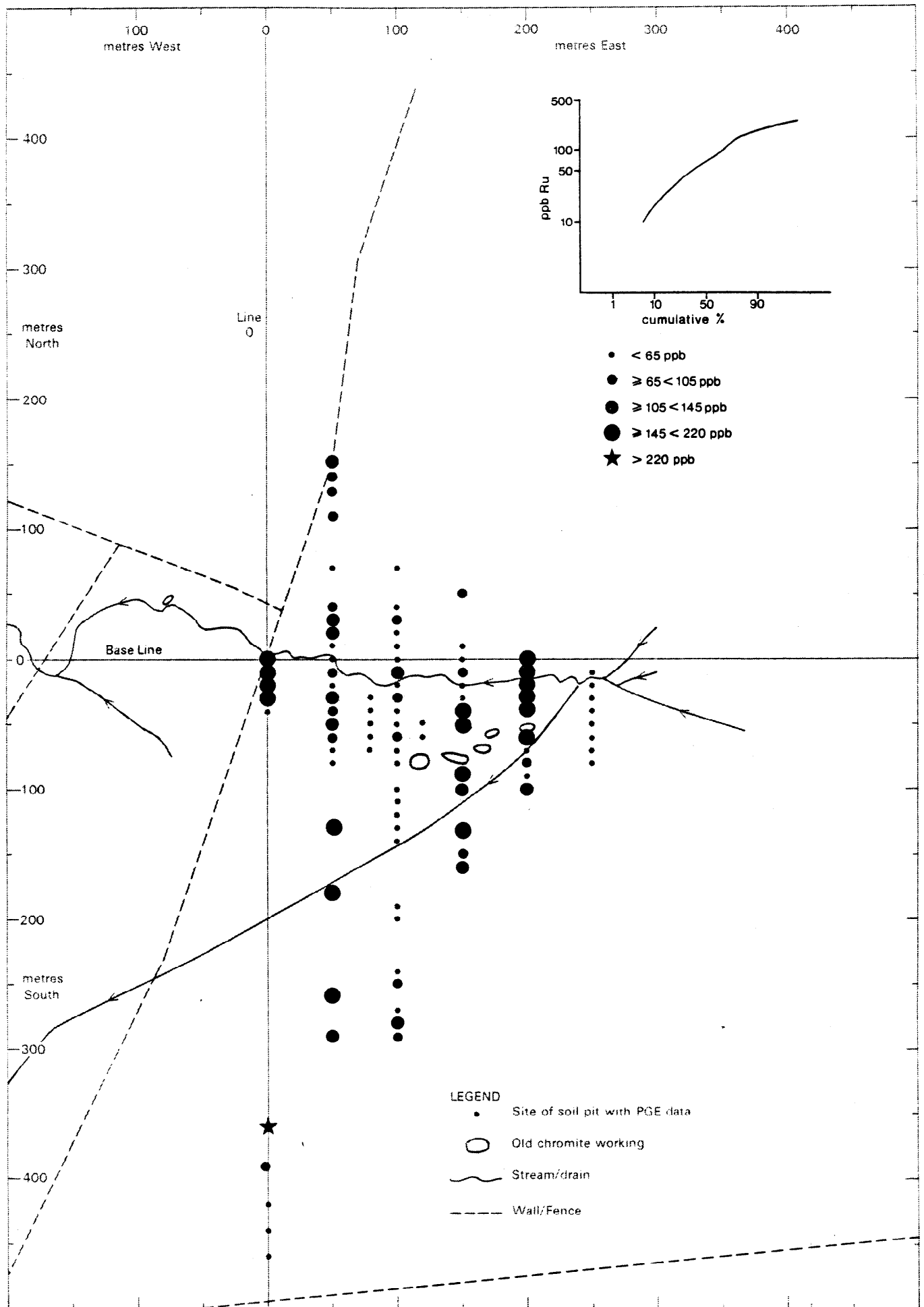
Fig. 27 Ru in panned overburden samples from Cliff area
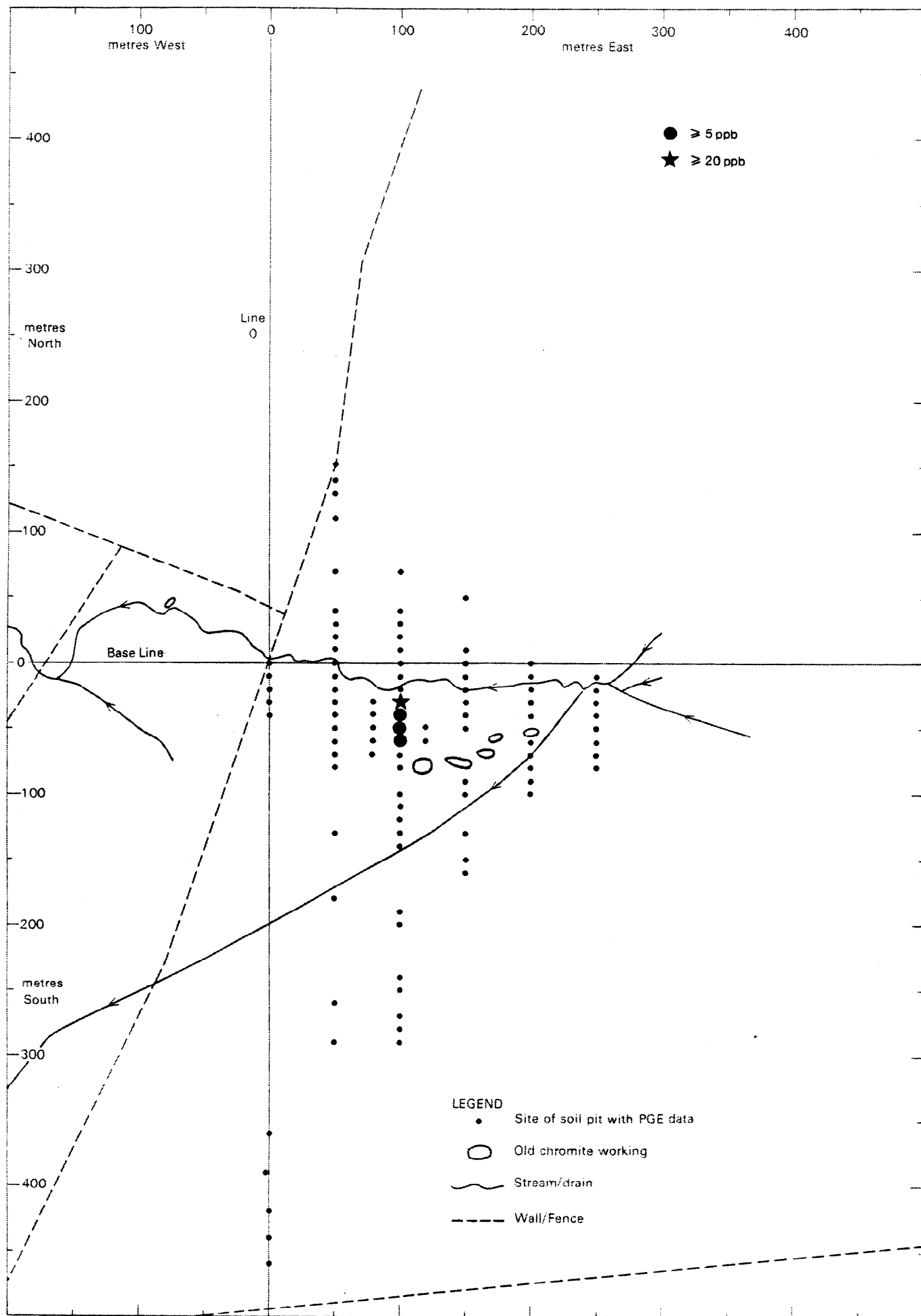
Fig. 28   Rh in panned overburden samples from Cliff area
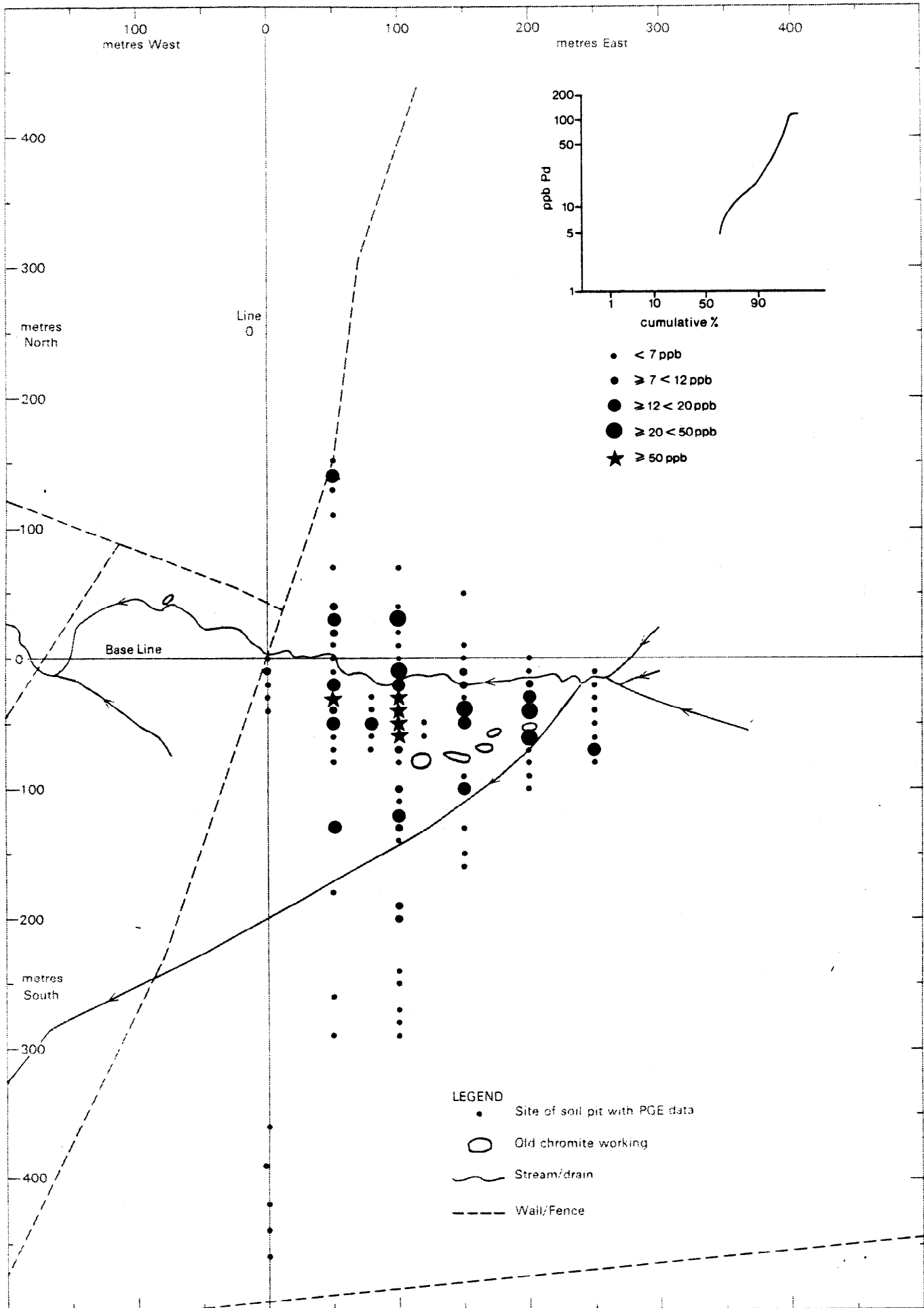
Fig. 29   Pd in panned overburden samples from Cliff area
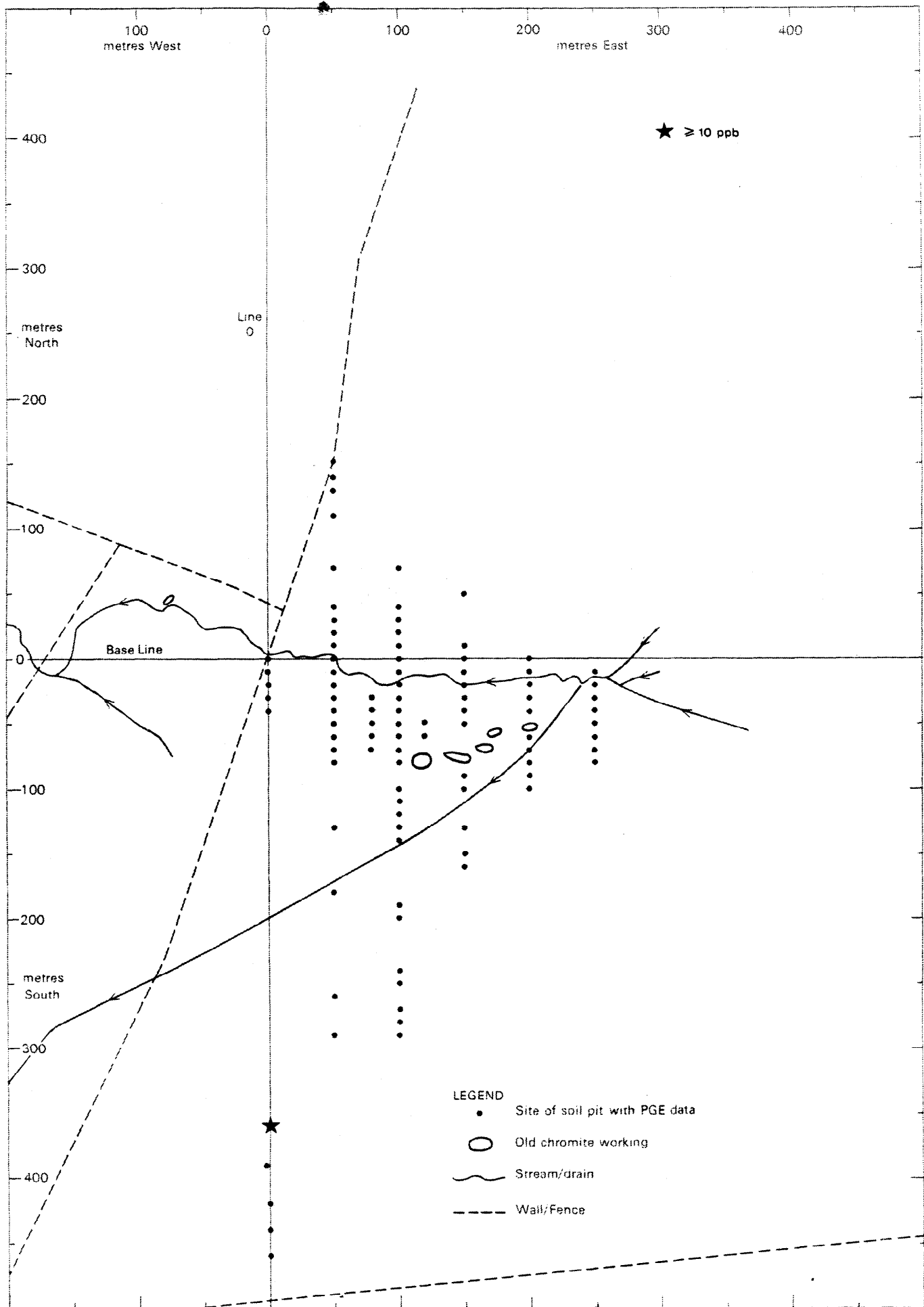
Fig. 30 Ir in panned overburden samples from Cliff area
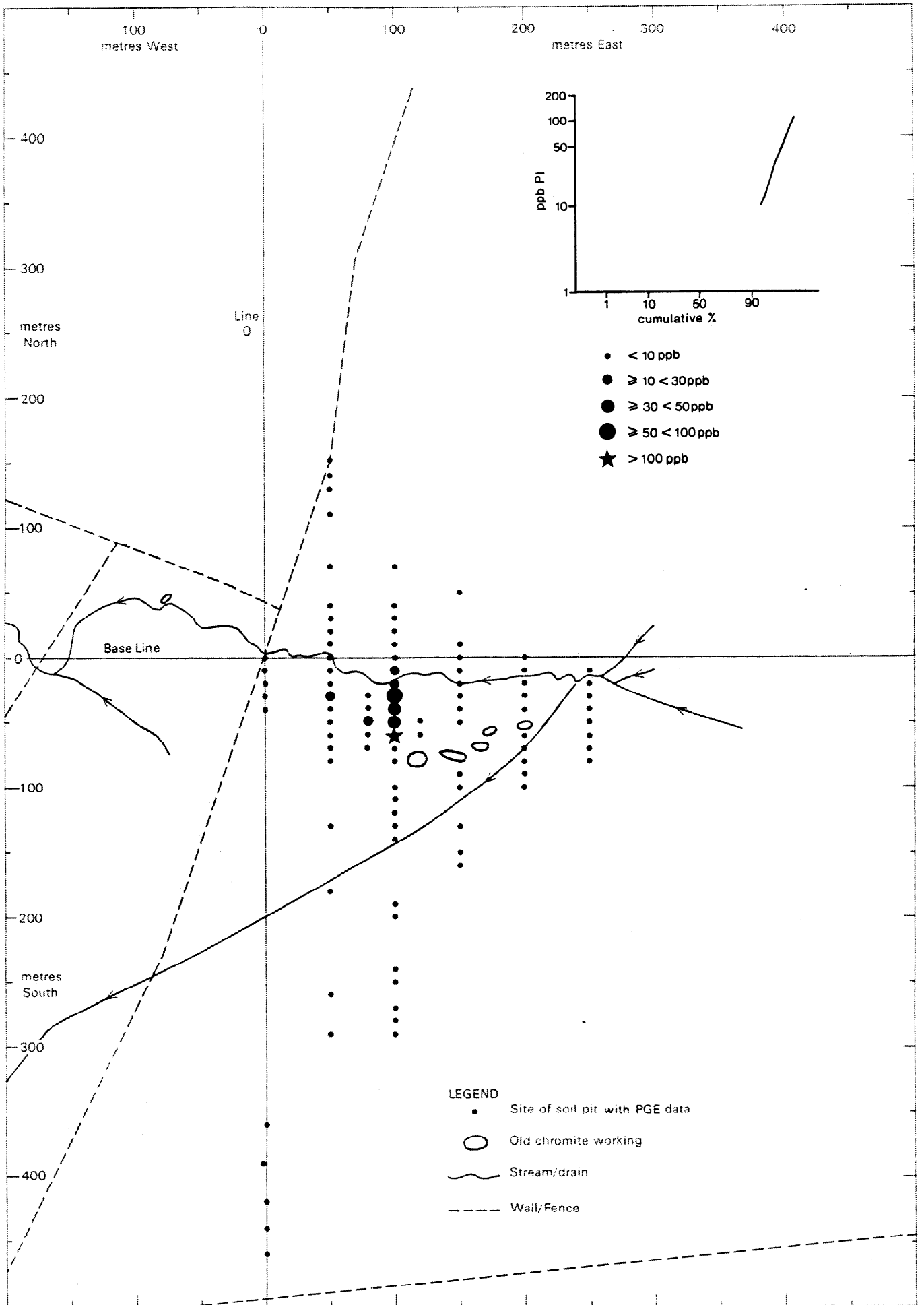
Fig. 31   **Pt in panned overburden samples from Cliff area**
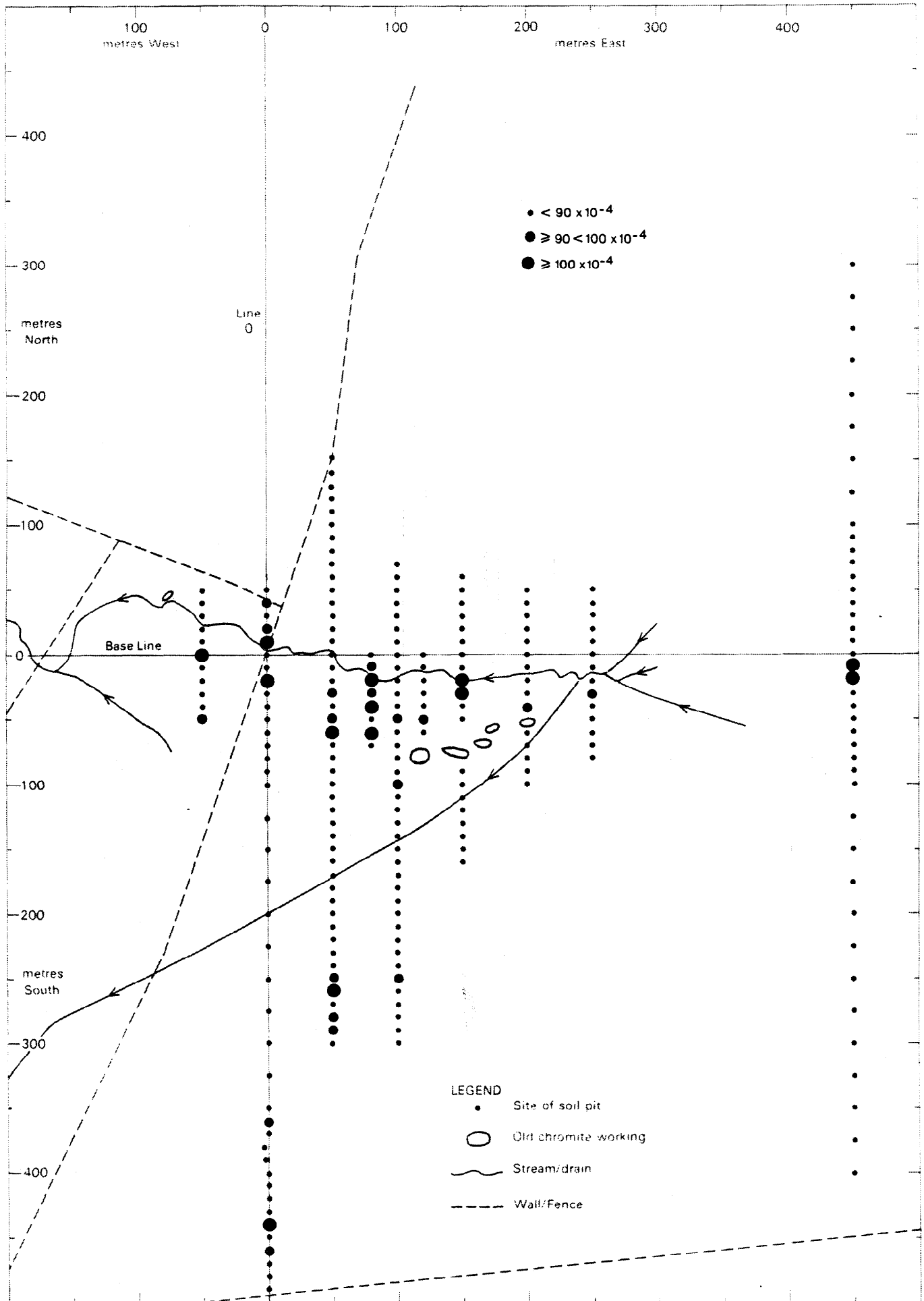
Fig. 32　　　Ni/MgO in panned overburden samples from Cliff area

Several regular distribution patterns emerge from consideration of the maps. The clearest pattern is shown by Cr (Figure 19) with relatively high levels confined to a zone trending roughly east-west. The chromite workings appear to be on the edge of this zone without an obvious halo of anomalous samples around them. The distributions of Co and Zn-rich samples (Figures 21 and 23 respectively) closely follow the pattern of Cr anomalies and these are also marked by samples with relatively low levels of Mg and Si (Figures 16 and 17). The two areas mentioned above in which chromite float was most common are both within zones of generally low Cr levels. There is some but slight enrichment in Cr above surrounding samples in the vicinity of the most concentration of chromite fragments. The distribution of Fe-rich samples (Figure 20) shows some correlation with the Cr anomaly pattern but there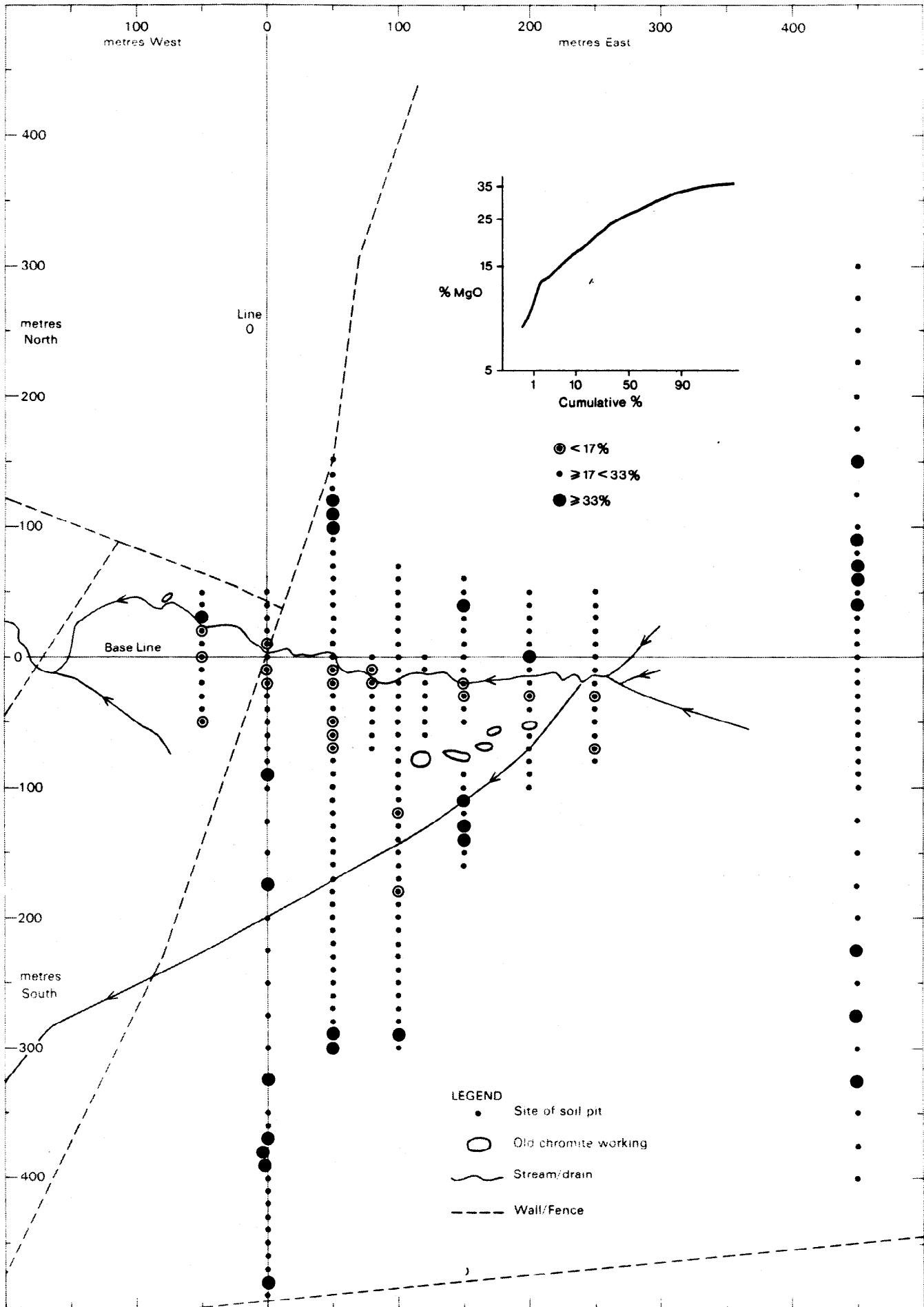 are also some samples containing relatively high levels of Fe without a corresponding similar enrichment in Cr. Ni levels (figure 22) are generally low in the Cr-rich samples and high in the Mg-rich samples but this relationship is not universal. The distribution of Ca (Figure 18) is markedly different from other elements with low Ca samples clustered in the extreme south of the area and also in the east. As these areas are also sites of widespread development of the pink coloured talc-carbonate rock float it is likely that Ca levels in general reflect differing degrees of alteration. The samples most rich in Si are also from areas with the maximum development of the talc-carbonate alteration. There is a concentration of samples with high levels of As (Figure 24) in the south of the area but the distribution patterns of Sb, Te and Bi (Figures 25 and 26) are much less clear.

The samples selected for PGE element analysis were based on grouping of the samples in terms of the other elements and on those with high levels of elements which could be potential pathfinders like Co, Ni, As, Sb, Te and Bi. Ru appeared (Figure 27) to be the most abundant PGE overall and was detectable in the majority of the samples. There is no clear indication of a correlation between Ru and Cr levels. The highest level of 500 ppb occurred in a sample from the south of the area which was also rich in As, Co and Fe relative to Cr. Ir was detected only in this same Ru-rich sample (Figure 30). Pd is the next most common PGE in the panned overburden samples and the distribution of anomalous samples (Figure 29) shows a general correlation with the east-west Cr-rich zone. In detail however there is no clear correlation between Pd and Cr levels in the overburden samples. The highest levels are not associated with the edge or strike extension of the line of old chromite workings but occur further to the NW. The relative scarcity of anomalous Pd in samples from the two short intermediate lines (80E and 120E) is puzzling, though Pd was uniformly low relative to Pt in the whole analytical batch of which those samples were part. There is a close correlation between the samples with detectable levels of both Pt and Rh (Figures 31 and 28) and those with the highest Pd levels. The distribution pattern shown by these three PGE is therefore completely different from that shown by Ru and Ir suggesting that two different types of PGE enrichment exist in the area. Consideration of levels of other elements in the most Pd rich samples, also illustrated by a profile diagram in figure 33, does not show any clear indication of an element with which the PGE are associated and could represent a pathfinder. Ni when expressed as the ratio Ni/MgO (Figure 32) appears to show the closest correlation with Pd but this is not very well defined. Ni is accommodated in olivine and serpentine as a minor component and therefore variations in amounts of these silicates is the major factor influencing the distribution of absolute levels of Ni (Figure 22). Plotting of Ni/MgO therefore allows samples with another phase containing a small but significant amount of Ni to be detected or samples with anomalous amounts of Ni in the silicate minerals. There is an indication of a correlation of Fe with some of the samples with high Ni/MgO as in the case of some of the drainage

samples. Levels of S in the overburden samples are low though Ni-Fe sulphides are commonly found in small amounts in fresh rock, probably reflecting oxidation in the near surface secondary environment.

Overburden sampling in other parts of harzburgite unit

Reconnaissance lines were sampled in other parts of the harzburgite unit but coverage has been too sparse to give an adequate picture of the distribution of mineralisation present and its possible controls. Nevertheless the data obtained suggests that further chromite mineralisation and areas of PGE enrichment exist and a more detailed and systematic coverage of the area would be worthwhile. Two short lines were sampled to the west of the Quoys chromite working (Figure 34) in undisturbed ground to see if either PGE or chromite mineralisation existed along strike from the pit. A chromium anomaly occurs in the easternmost line at a point equivalent to the strike extension of the workings but it is very subdued further along strike in the western line. Associated with the high Cr levels on the eastern line are relatively elevated contents of Fe, Co and especially Zn and low levels of Si and Mg as in the Cliff area. The most conspicuous feature of the line is the two samples with high Co and As levels and slight Ni enrichment to the south of the Cr anomaly. This probably reflects some enrichment in sulphide/arsenide mineralisation in the area, perhaps similar to the cause of the Co, As and Ru anomaly in the southern part of the Cliff area. Ru is relatively enriched in one of these samples but Pd levels are relatively low. The same As-rich feature is apparent on the western line but with lower amplitude and without clearly associated Co. No PGE determinations have been made on the western line.

A further reconnaissance line was sampled towards the upper part of Mill Burn, as shown on Figure 34, because of the high levels of Cr in the drainage samples from the area. The profile of this line (Quoys West) is shown in Figure 35. The most obvious features are the two anomalies of Cr, Fe, Co, Zn and Ni/MgO which appear to be similar to those derived from the east-west anomalous zone at Cliff. To the south of this zone there are several boulders and smaller fragments of massive chromitite which must be locally derived , a further parallel with the Cliff area. Insufficient samples from the line have been analysed for PGE for the presence of mineralisation to be established, but it is significant that a composite sample of chromite float from the area contained anomalous levels of Pd and Pt at 115 and 90 ppb respectively. One of the overburden samples analysed contains relatively high levels of Ru and Ir but there is no associated As anomaly as in the Cliff area and the significance of this remains unclear.

Four lines were sampled in the vicinity of the small chromite working near Harold's Grave (Figure 3). The distribution of the sample sites along these lines is illustrated in Figure 36. Analyses of rock and chromite samples from dumps had previously established an enrichment in Ru, Ir, Rh and to some extent Pt in this area. Plots of the distribution of MgO and CaO, Fe and Cr, Co and As, Ni and Ni/MgO and Ru and Pd along these lines are shown in figures 37 to 41. These indicate that a zone of high Cr, and to some extent high Co, and corresponding low MgO and Ni is traceable with a WNW trend through the old pit. Some samples with relatively high Ni/MgO ratios also occur within the zone. Only limited associated enrichment in Ru was detected and there is only one sample with relatively anomalous levels of Pd, Rh and Pt. This site is located on the edge of the zone and is not associated with either Ru or Cr enrichment. These data suggest that the Ru-rich material in the old pit is of very limited extent. The most Ru-rich samples occur well to the east of this zone (Figure 41), in
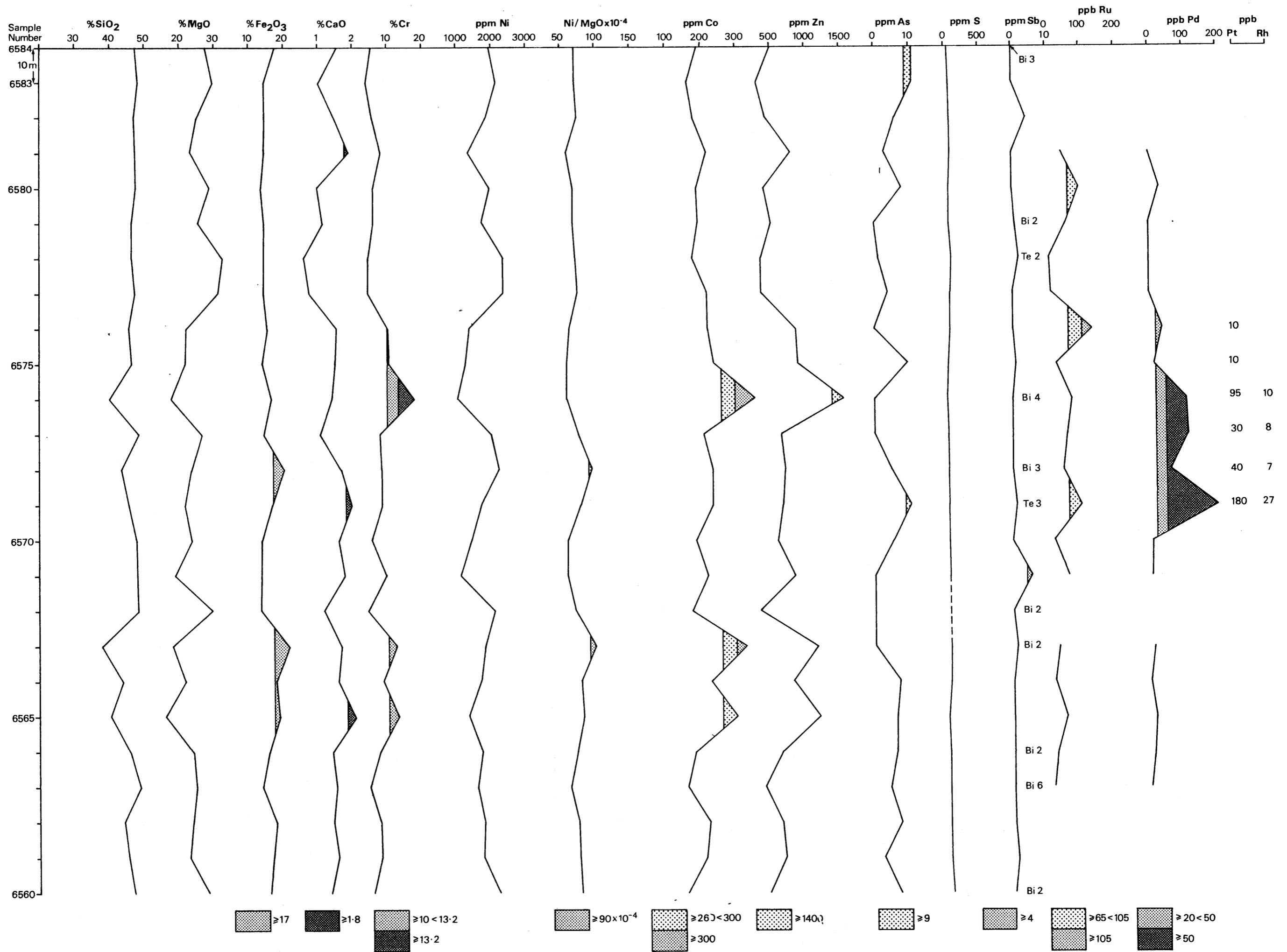
Fig. 33   Element distribution in panned overburden samples from line 100 E at Cliff

57
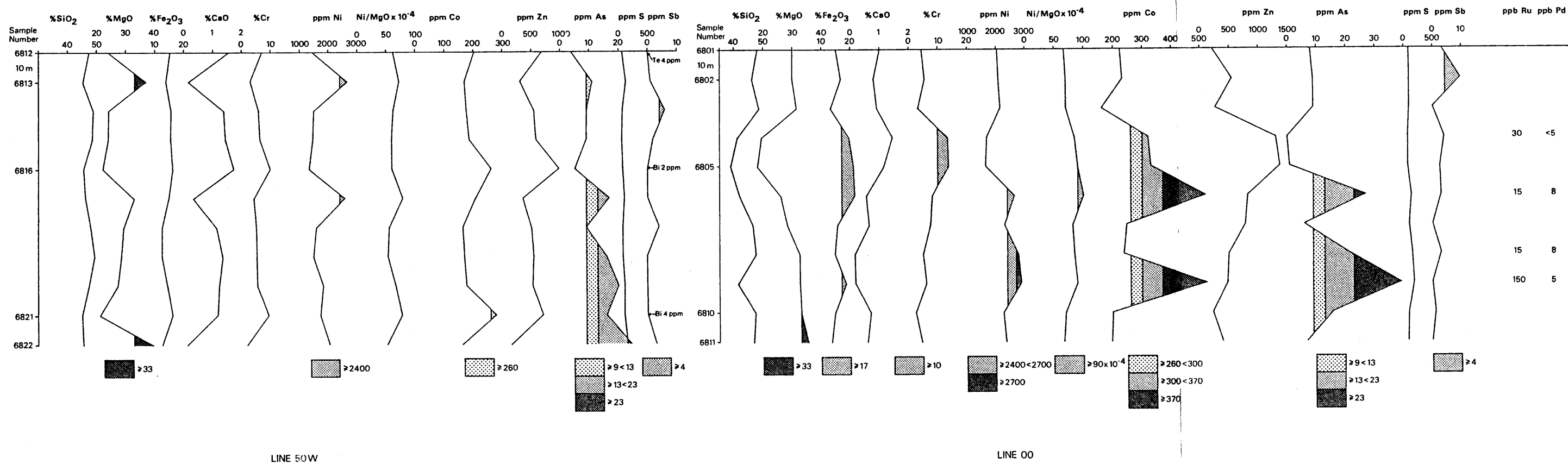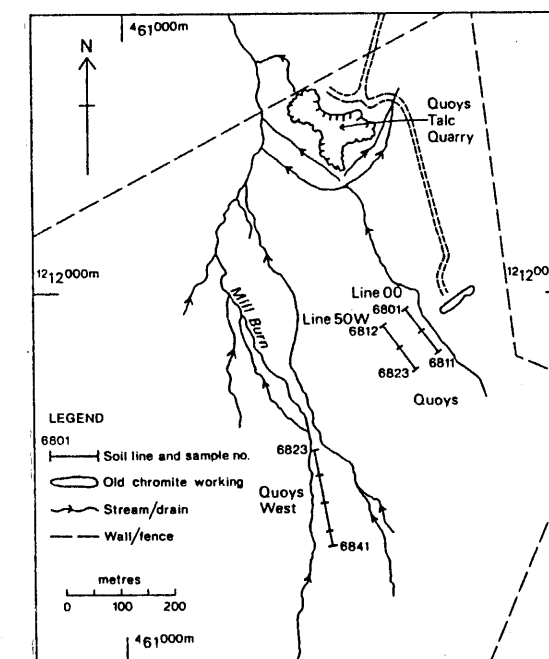
Fig. 34

Element distribution in panned overburden samples from Quoys area
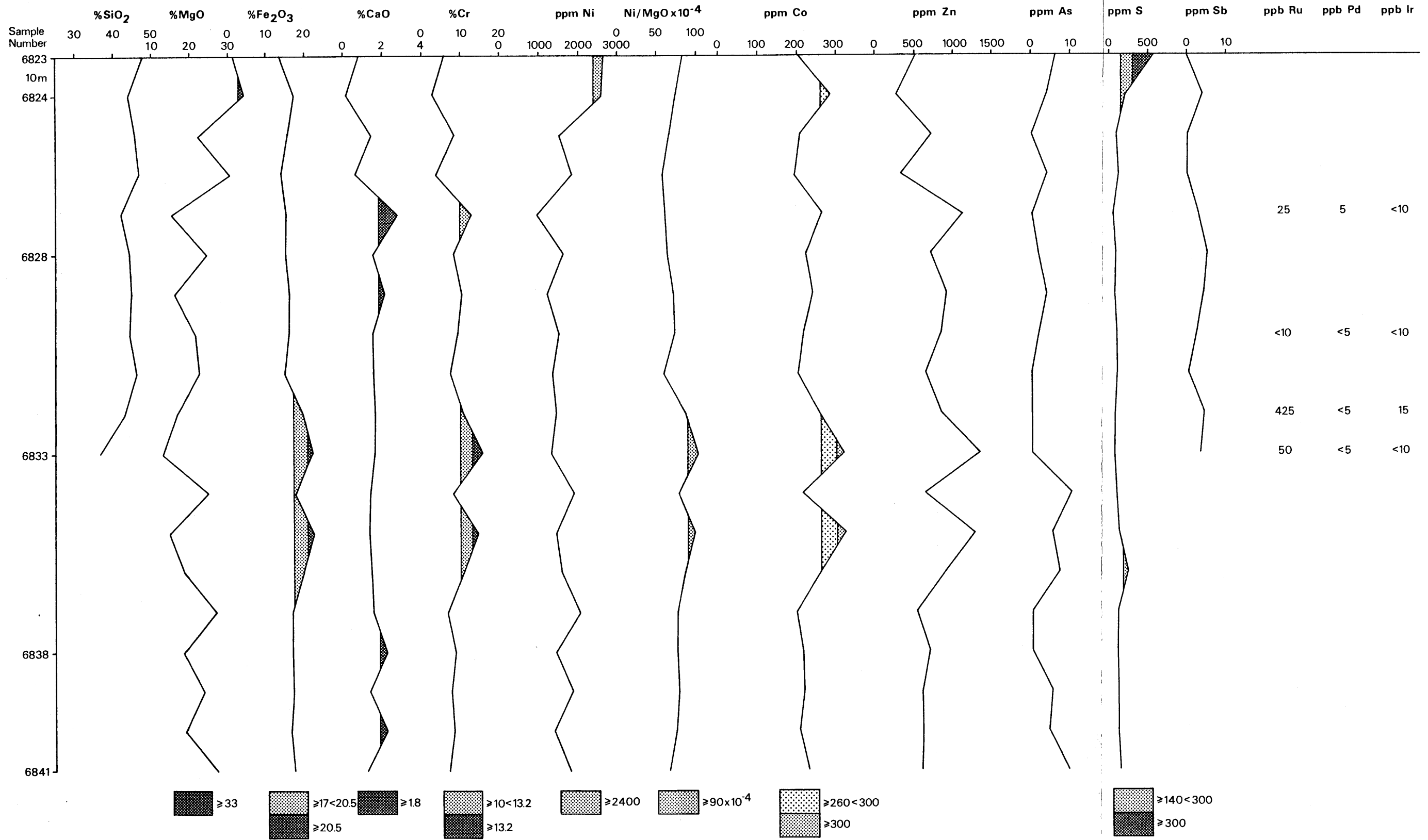
Fig. 35   Element distribution in panned overburden samples from Quoys West area

Fig. 36

The distribution of overburden sample sites
in the Harold's Quarry area

LEGEND

6923●   Site of soil pit and sample no.

◯   Old chromite working

〜   Stream

— —   Wall/Fence

N

Harold's Grave
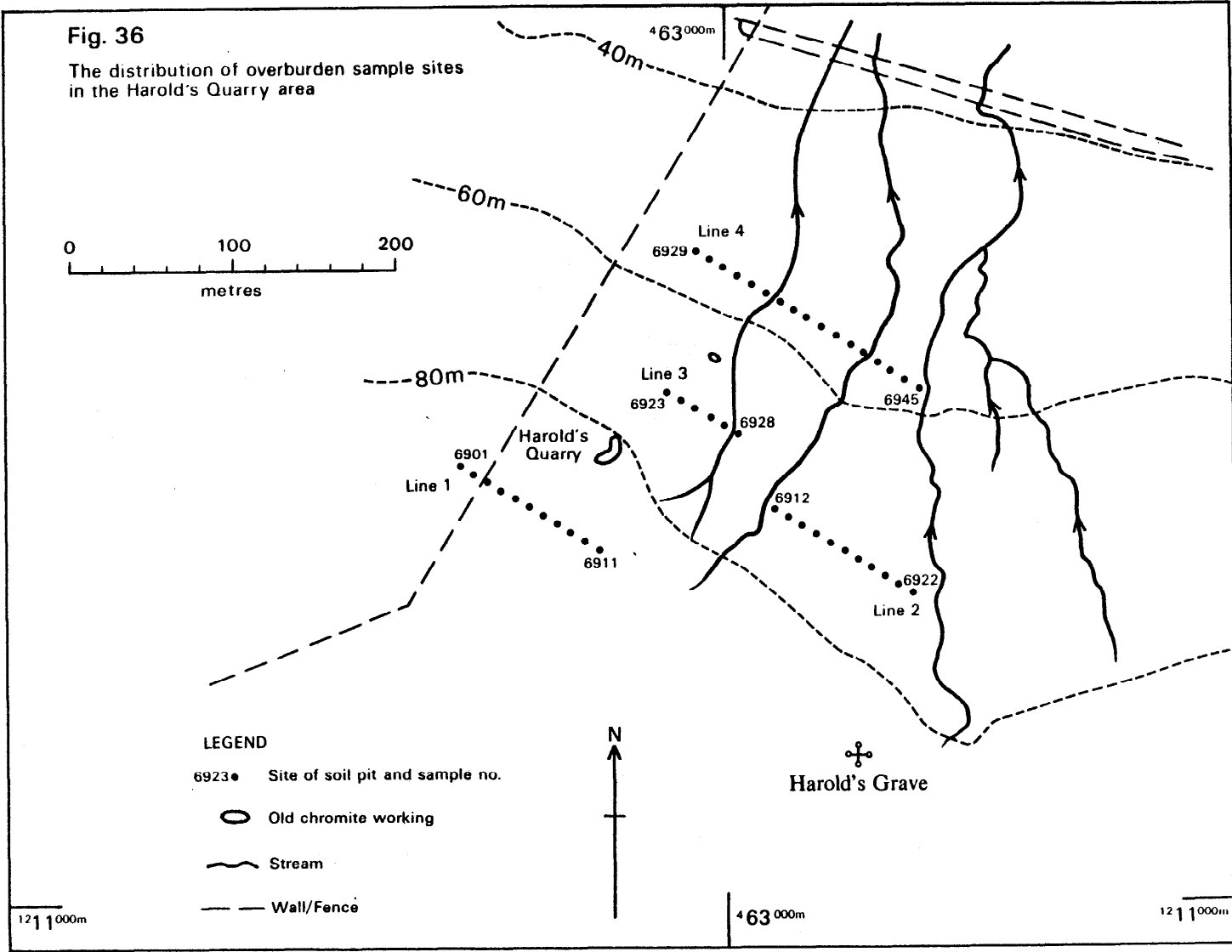
Fig. 37
CaO in panned overburden samples from Harold's Quarry area

- ● < 0.62 %
- • ≥ 0.62 < 1.8 %
- ★ ≥ 1.8 %

Harold's
Quarry

LEGEND

- • Site of soil pit
- ⬭ Old chromite working
- ∿ Stream
- – – Wall/Fence

N

Harold's Grave
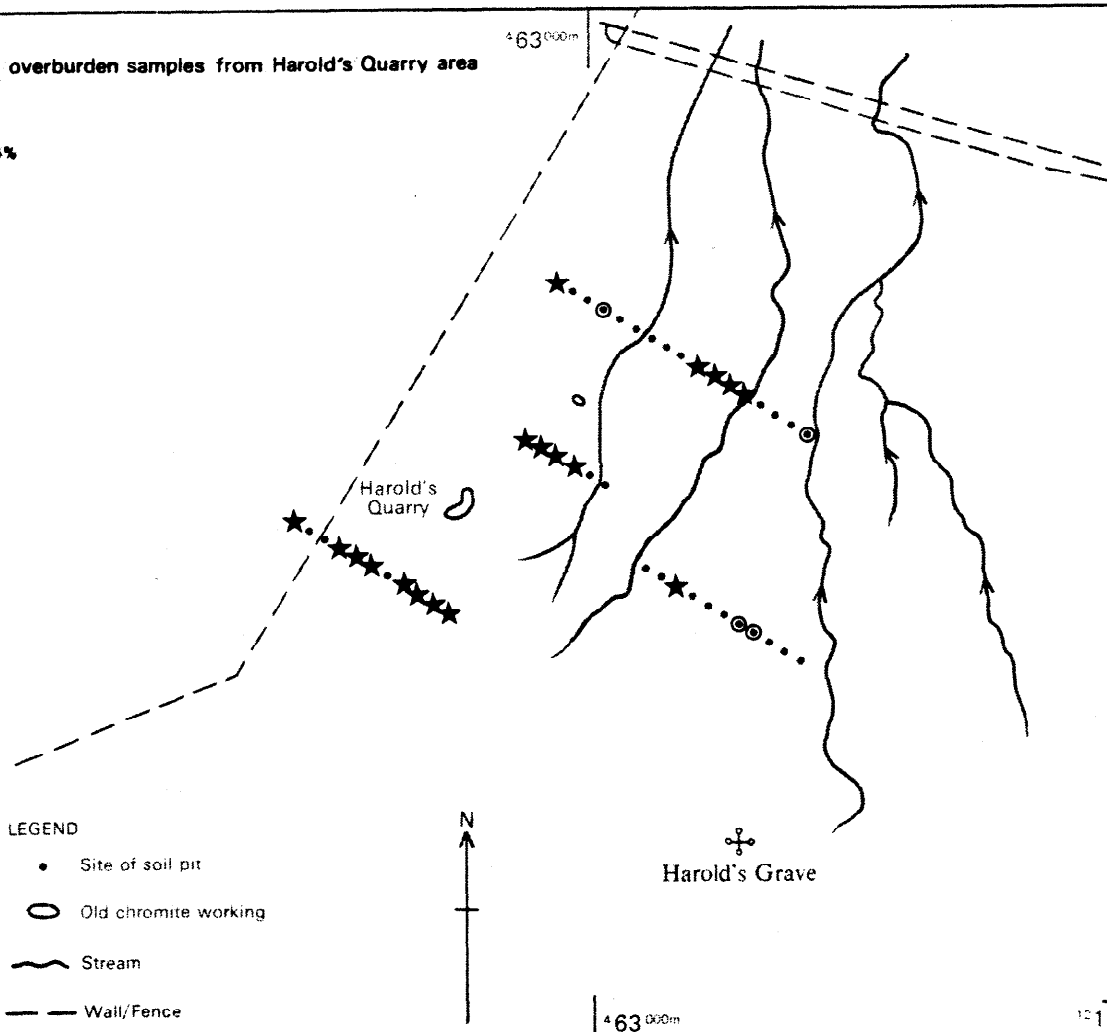
MgO in panned overburden samples from Harold's Quarry area

- ● < 17.0 %
- • ≥ 17.0 < 33.0 %
- ★ ≥ 33.0 %

Harold's
Quarry

LEGEND

- • Site of soil pit
- ⬭ Old chromite working
- ∿ Stream
- – – Wall/Fence

N

Harold's Grave
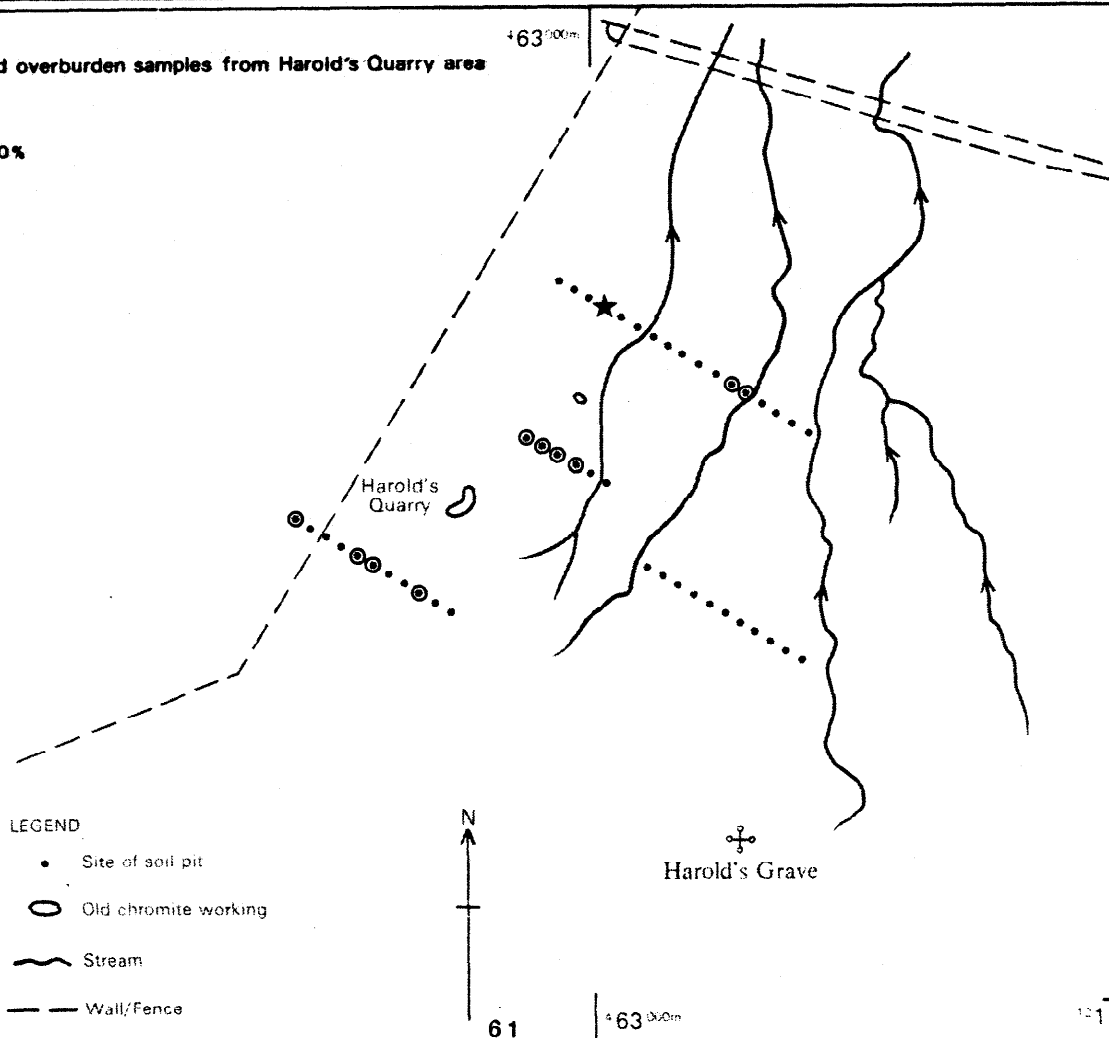
Fig. 38
Total Fe as Fe_2O_3 in panned overburden samples from Harold's Quarry area

- ● <13.0 %
- • ≥13.0 <17.0 %
- ● ≥17.0 <20.5 %
- ★ ≥20.5 %

Harold's
Quarry

LEGEND

- • Site of soil pit
- ⬭ Old chromite working
- ∿ Stream
- – – – Wall/Fence

N

Harold's Grave
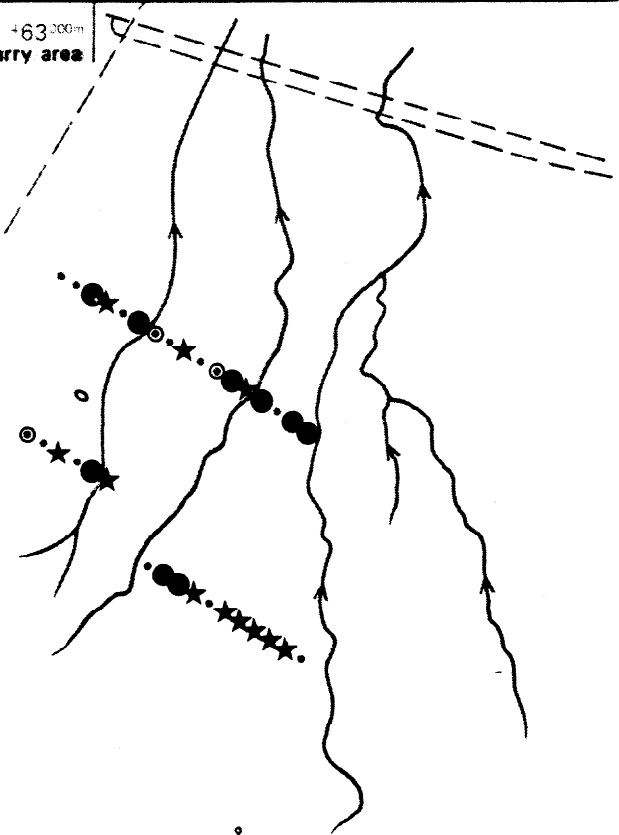
Cr in panned overburden samples from Harold's Quarry area

- • <10.0 %
- ● ≥10.0 <13.2 %
- ★ ≥13.2 %

Harold's
Quarry

LEGEND

- • Site of soil pit
- ⬭ Old chromite working
- ∿ Stream
- – – – Wall/Fence

N

Harold's Grave
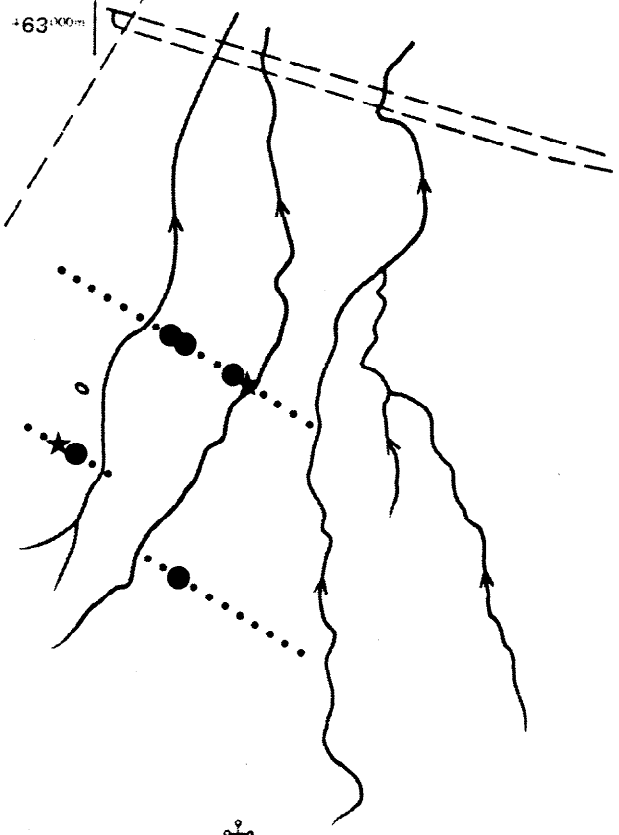
Fig. 39

As in panned overburden samples from Harold's Quarry area

- • < 9 ppm
- ● ≥ 9 ppm

LEGEND

- • Site of soil pit
- ⬭ Old chromite working
- ∿ Stream
- – – Wall/Fence

Harold's Quarry

Harold's Grave

N
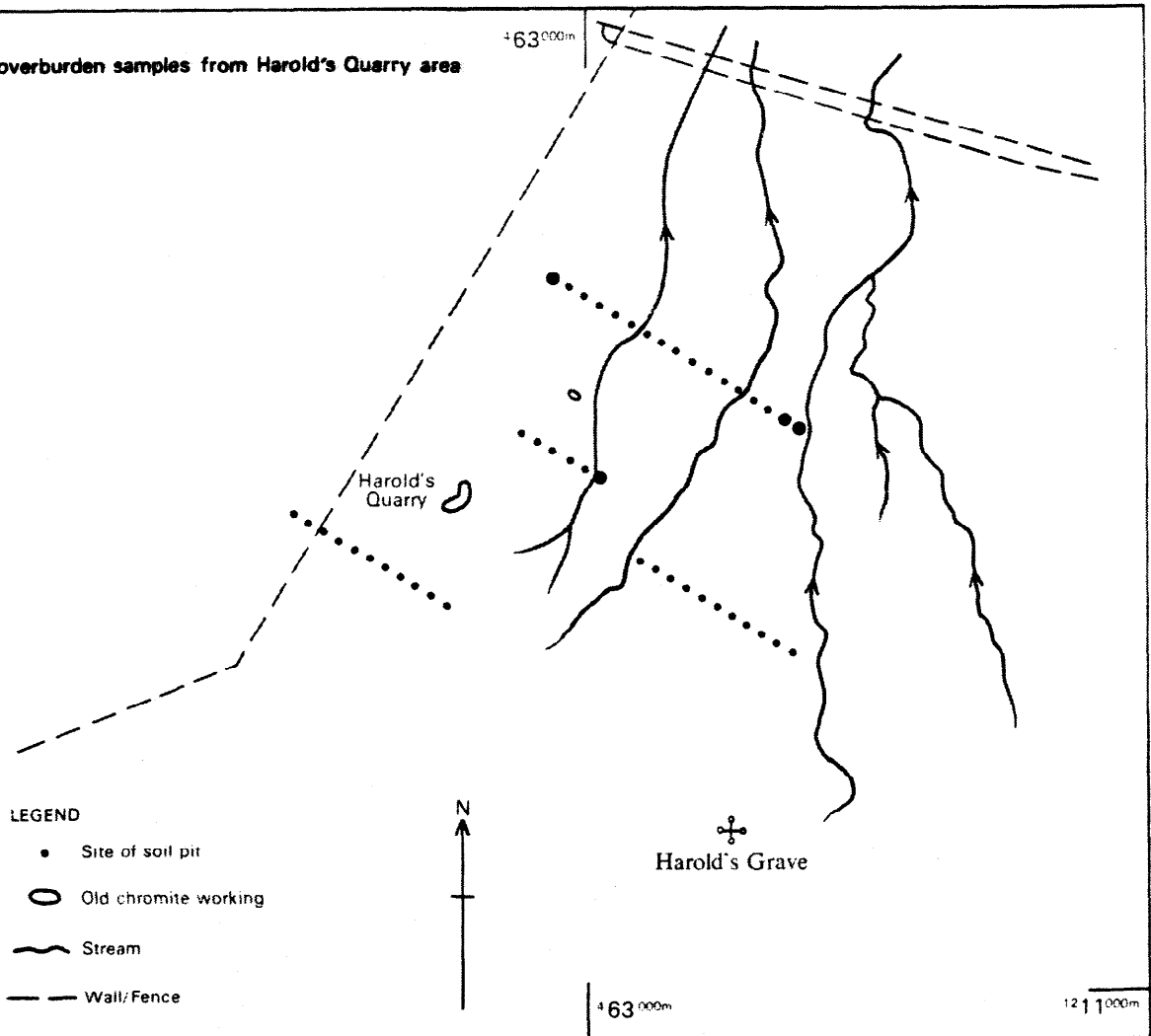
Co in panned overburden samples from Harold's Quarry area

- • < 260 ppm
- ● ≥ 260 < 300 ppm
- ● ≥ 300 < 370 ppm
- ● ≥ 370 ppm

LEGEND

- • Site of soil pit
- ⬭ Old chromite working
- ∿ Stream
- – – Wall/Fence

Harold's Quarry

Harold's Grave

N

63
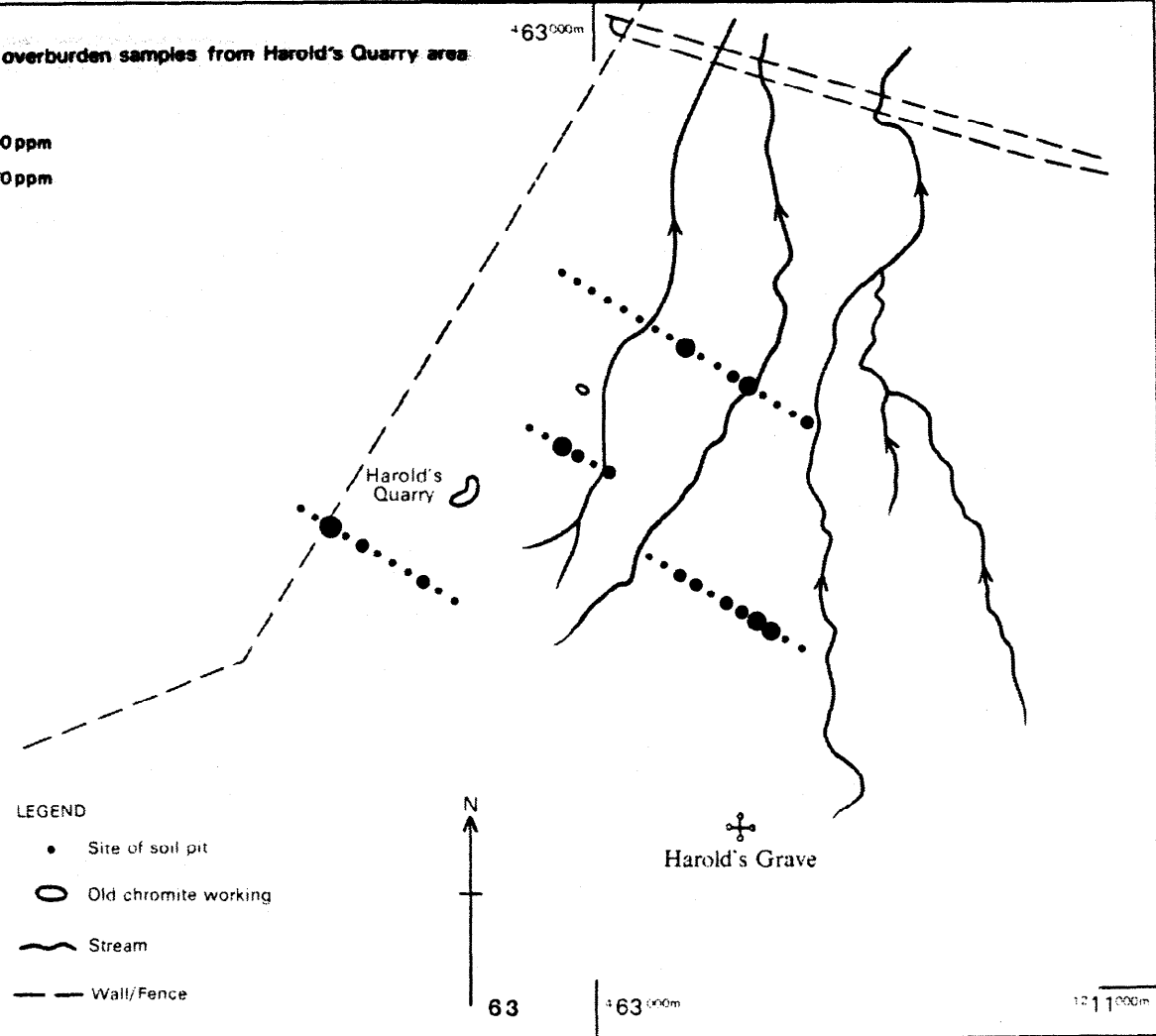
Fig. 40
Ni in panned overburden samples from Harold's Quarry area

- ⦿ <1300 ppm
- • ≥1300 <2400 ppm
- ⬤ ≥2400 ppm

LEGEND

- • Site of soil pit
- ⬭ Old chromite working
- 〜 Stream
- --- Wall/Fence

Harold's Quarry

Harold's Grave

Ni/MgO in panned overburden samples from Harold's Quarry area

- • <90 x 10⁻⁴
- ⬤ ≥90 <100 x 10⁻⁴
- ★ ≥100 x 10⁻⁴

LEGEND

- • Site of soil pit
- ⬭ Old chromite working
- 〜 Stream
- --- Wall/Fence

Harold's Quarry

Harold's Grave

Fig. 41
Ru in panned overburden samples from Harold's Quarry area

- • < 65 ppb
- ● ≥ 65 < 105 ppb
- ● ≥ 105 < 145 ppb
- ● ≥ 145 ppb

Harold's
Quarry

LEGEND

- • Site of soil pit with PGE data
- ⬭ Old chromite working
- ∿ Stream
- -- Wall/Fence

N

Harold's Grave
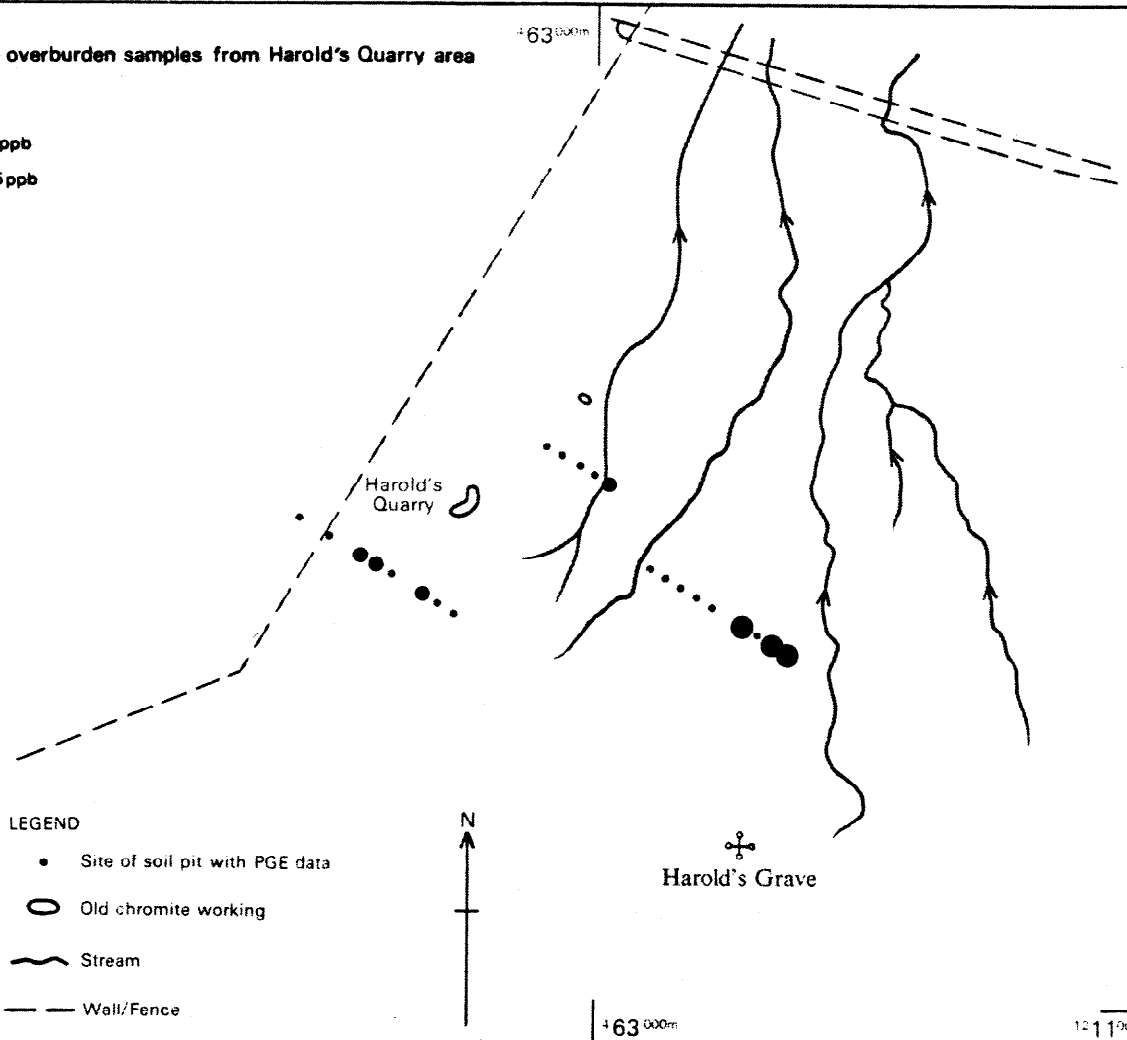
Pd in panned overburden samples from Harold's Quarry area

- • < 7 ppb
- ● ≥ 20 < 35 ppb

Rh 5
Pt 10

Harold's
Quarry

LEGEND

- • Site of soil pit with PGE data
- ⬭ Old chromite working
- ∿ Stream
- -- Wall/Fence

N

Harold's Grave

65
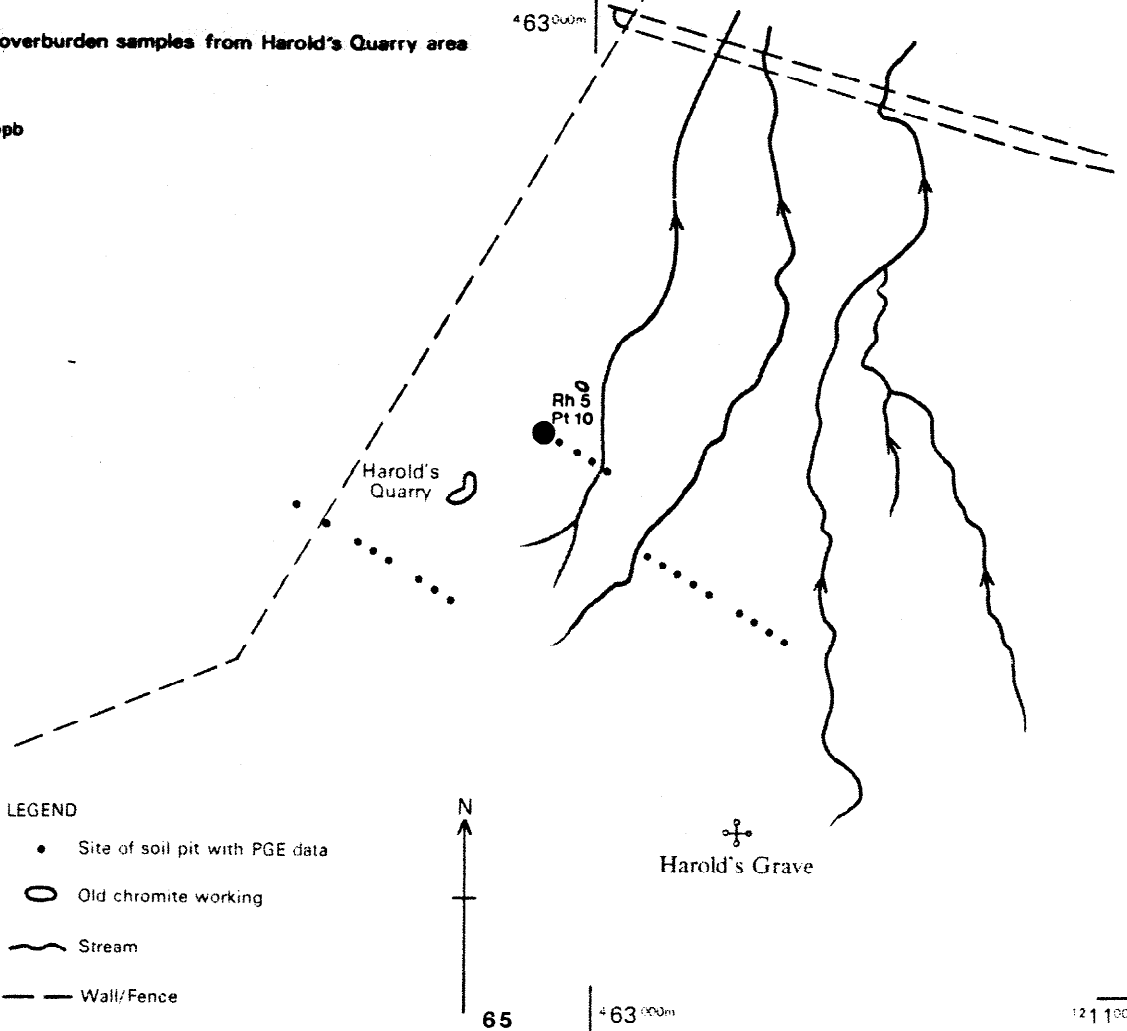
association with relatively high levels of Fe (without Cr) and some Co and Ni. The Ru levels however are not as high as the most anomalous samples from Cliff and Quoys. Ca levels are relatively low in some samples from this eastern sector suggesting that hydrothermal alteration may be relatively important there.

Overburden sampling in the dunite and wehrlite/pyroxenite units

A series of short lines were sampled to the south of Muckle Heog (Figure 42) because a sample with anomalous levels of PGE had been obtained from a nearby dump and because Brzozowski (1977) had reported sulphide concentrations in the area and overburden Ni anomalies. Table 8 shows that in general the samples derived from the dunite unit are richer in Cr, Fe, Co and particularly Cu compared with those from the harzburgite unit as a whole which is in accord with both the data from rock samples and drainage. On the other hand the levels of Zn and Ca present are only slightly higher and on average Mg and Ni contents lower.

Table 8 Comparison of overburden sample data sets

	Harzburgite unit			Dunite unit			Gerdie/Heliers Water		
	Mean	S. D.	Range	Mean	S. D.	Range	Mean	S. D.	Range
MgO%	25.00	6.20	7.80-39.08	18.72	4.08	10.34-26.65	13.13	3.25	8.10-21.71
CaO%	1.23	0.51	0.08- 2.79	1.53	0.64	0.63- 2.87	6.40	2.11	3.60-13.94
Sppm	90	40	41- 547	114	64	66- 414	107	81	47- 341
Cr%	7.26	3.69	0.80-20.39	11.54	3.05	7.90-18.57	7.87	2.83	3.37-13.58
Fe$_2$O$_3$%	15.88	2.81	8.38-27.91	20.66	2.69	14.36-25.93	20.48	4.56	11.48-30.31
Coppm	219	60	123- 527	266	41	178- 359	282	69	123- 410
Nippm	1864	502	533- 3535	1777	352	1286- 2601	1515	571	562- 2791
Cuppm	22	4	11- 36	66	21	44- 129	53	16	29- 90
Znppm	658	337	58- 1959	809	207	511- 1345	799	260	230- 1253
Asppm	5	5	<1- 39	2	2	<1- 7	6	5	<1- 18
Ruppb	78	74	<10- 500	78	21	55- 100	-	-	-
Rhppb			<5- 27			<5			<5
Pdppb	10	18	<5- 200	14	12	5- 40	13	17	<5- 55
Ptppb	8	23	<10- 180	13	9	<10- 30	10	8	<10- 30
No. samples	326, 126(PGE)			32, 11Pt, 6Pd, 4Ru			40, 11Pt, 9Pd		

Broad Cr peaks are evident on the southern part of the western line, one of which may also be traceable on the other line. Associated with the Cr peaks are elevated values of Ni/MgO with a backgound also significantly higher than typical for samples derived from the harzburgite unit. Maximum Cu levels do not correspond with Cr or relative Ni enrichment. The samples chosen for PGE analysis comprise those relatively rich in Cr and Ni/MgO and also Cu anomalies. Most were analysed only for Pd and Pt but Ru levels from the samples analysed more fully appear to be similar to background levels found in samples derived from the harzburgite unit. There is clearly a discrepancy between the Pd data from the Pb collection data and the full PGE determinations using nickel sulphide collection. It appears as though Pd has been significantly underestimated in the samples analysed after nickel sulphide collection in this analytical batch. Taking Pt data as more consistent it appears that some Cr and Ni/MgO enrichments and some Cu anomalies are associated with an enrichment in PGE. Enrichment in PGE has been confirmed at the site of 6406 (Figure 42) in a bedrock sample obtained by shallow drilling.

Lines were sampled at Gerdie and near Helliers Water to investigate the source of drainage anomalies in the Burn of Voesgarth in an area of very poor exposure (Figure 43). The Gerdie traverse, oriented roughly at right angles to the presumed strike of the rocks, provides important evidence of the geology in this little known sector of the island. The chemical data are plotted in Figure 44. The most striking feature of the profile is the progressive increase in Ca levels along the line. This suggests that a regular increase in the overall abundance of clinopyroxene occurs from north to south which would be consistent with a cumulate origin of the rocks. Furthermore the Ca levels of the northernmost sample of this traverse are significantly higher than levels found in samples from the Muckle Heog area. The contrast between the two areas is also reflected in the average CaO figures shown in table 8. Cr levels are lower than in the Muckle Heog samples and uniform throughout the traverse except at the extreme south where there is a marked increase in concentration. Since the same point on the traverse is marked by a sharp decrease in Ca and changes in other elements it is probable that a fault boundary is crossed at that point with dunite to the south. There are no clearly defined anomalies of Ni or Cu on the line and the few samples analysed for PGE contain background levels.

The Helliers Water traverse is oriented roughly at right angles to the Gerdie traverse and perpendicular to the broad depression which marks the trace of the important north-south lineament with which several drainage anomalies are associated (Figure 43). A profile plot of the chemical analyses of samples is shown in figure 45 with west at the top. Several significant features are displayed by this traverse. The distribution of Ca shows a flat profile in the western half followed by a sharp change to progressively increasing levels as in the Gerdie traverse. This can be interpreted as dunite in the west in faulted contact with the Gerdie type cumulate rocks to the east. Cr levels are very constant throughout the traverse, suggesting an absence of concentrations of the mineral but Ni expressed as Ni/MgO shows high levels compared with all other areas and a broad peak reaching a maximum value at around the position of the deduced fault. Co levels generally vary in accord with the Ni/MgO profile but there are no corresponding Cu or As peaks. PGE were determined in 6 samples from the line, all but one by the lead fire assay method. The data show low levels associated with the cumulate rocks but relatively high levels around the position of the fault and the Ni/MgO peak. The PGE anomalies in this traverse are of particular significance because they demonstrate that PGE can be enriched without the presence of chromite concentrations in a part of the complex remote from the Cliff area both spatially and in terms of the ophiolitic lithostratigraphy. Furthermore they suggest an association between PGE enrichment and a major discordant structure which according to the drainage data seems to be the site of significant hydrothermal activity.

A short line was also sampled inland from shore exposures at Ordale (Figure 43) where low amplitude enrichment in PGE had been found in several rock samples. The results are plotted in profile form in figure 46. The average composition of samples from this line is compared with the corresponding data from the Gerdie and Helliers Water lines in table 9.
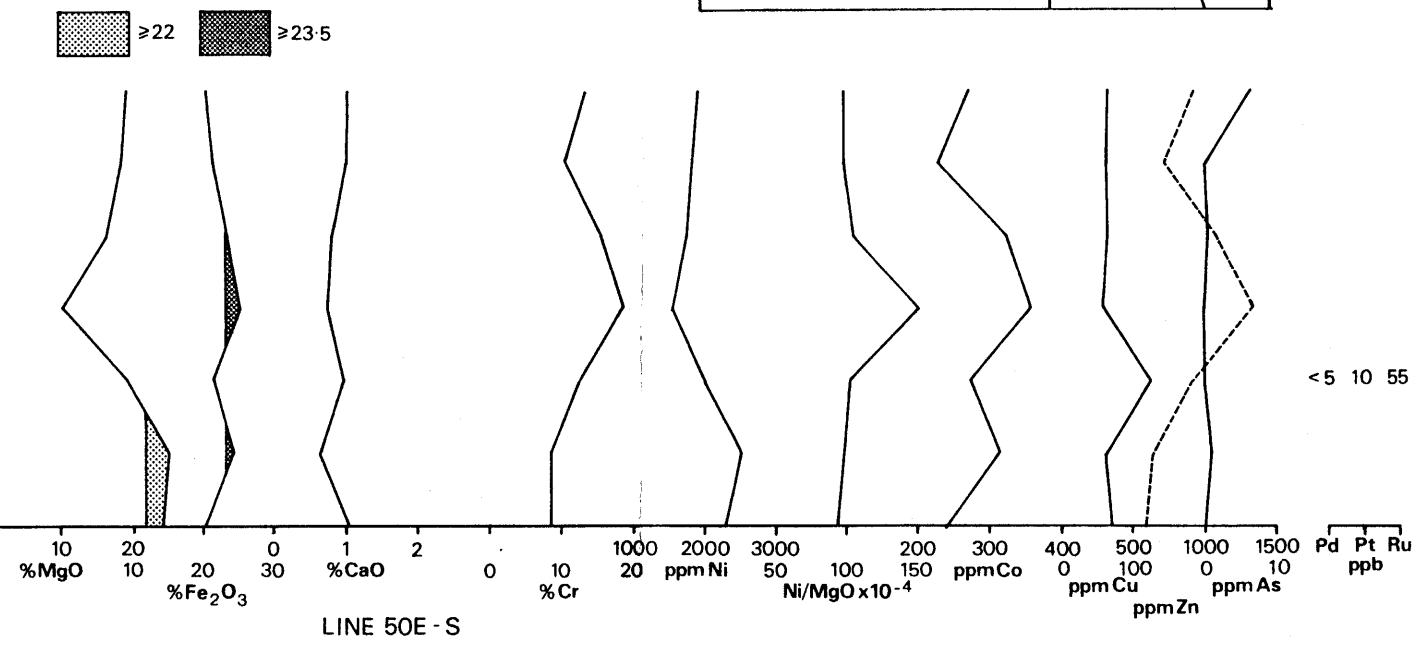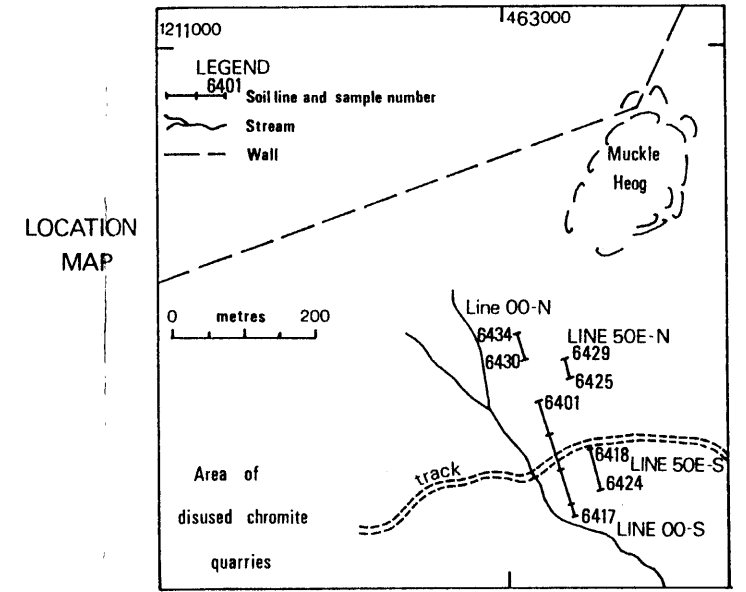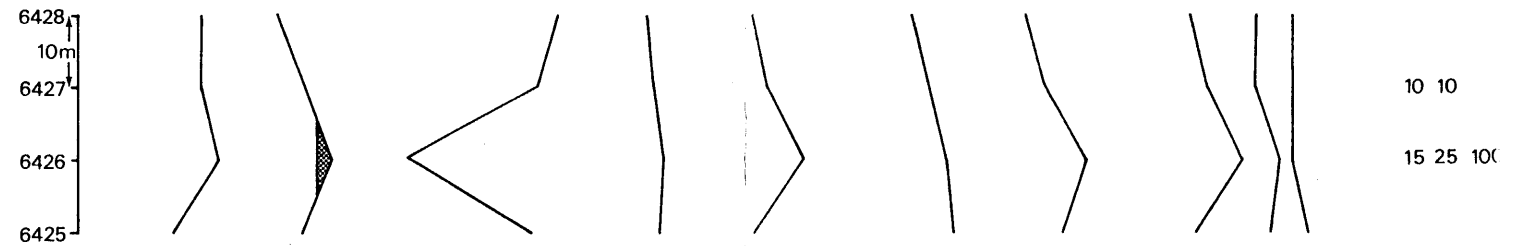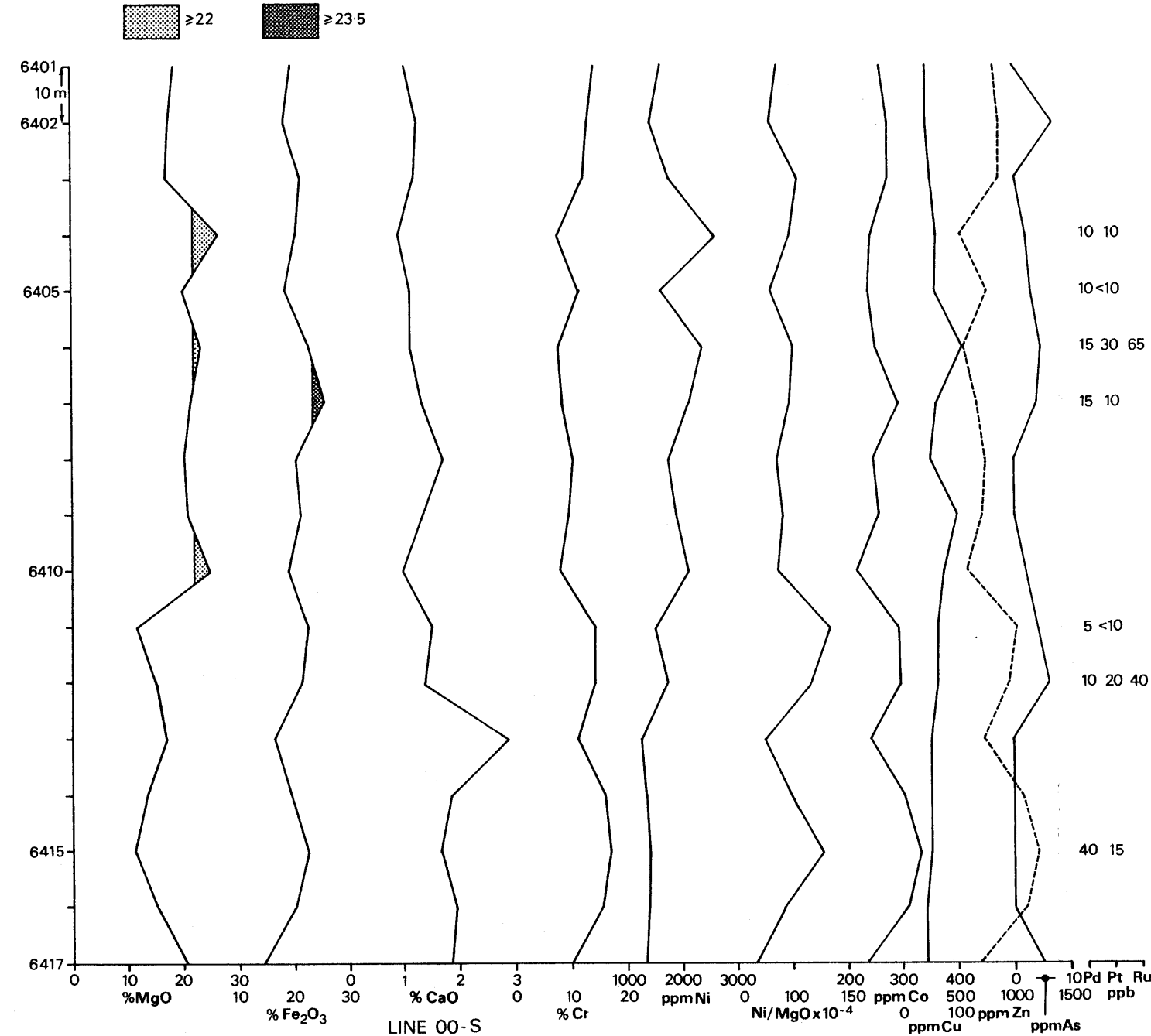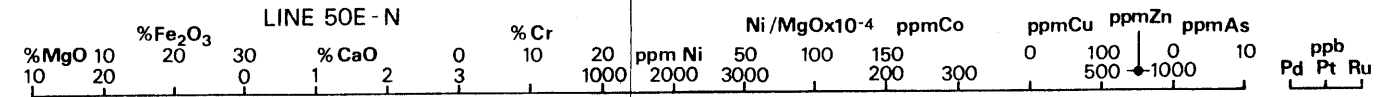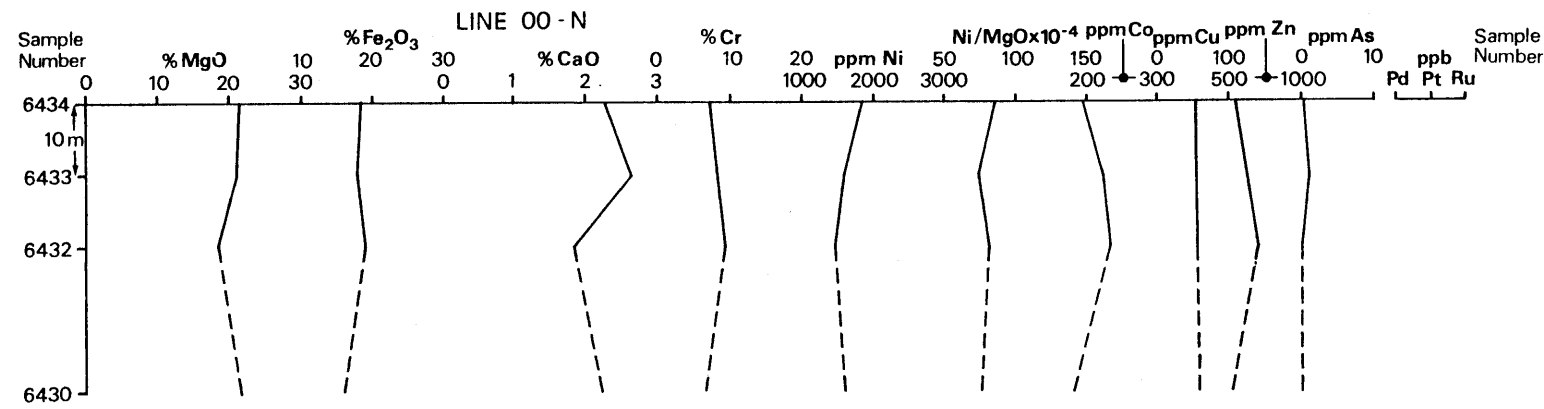
Fig. 42 Element distribution in panned overburden samples from the lower dunite, SW of Muckle Heog
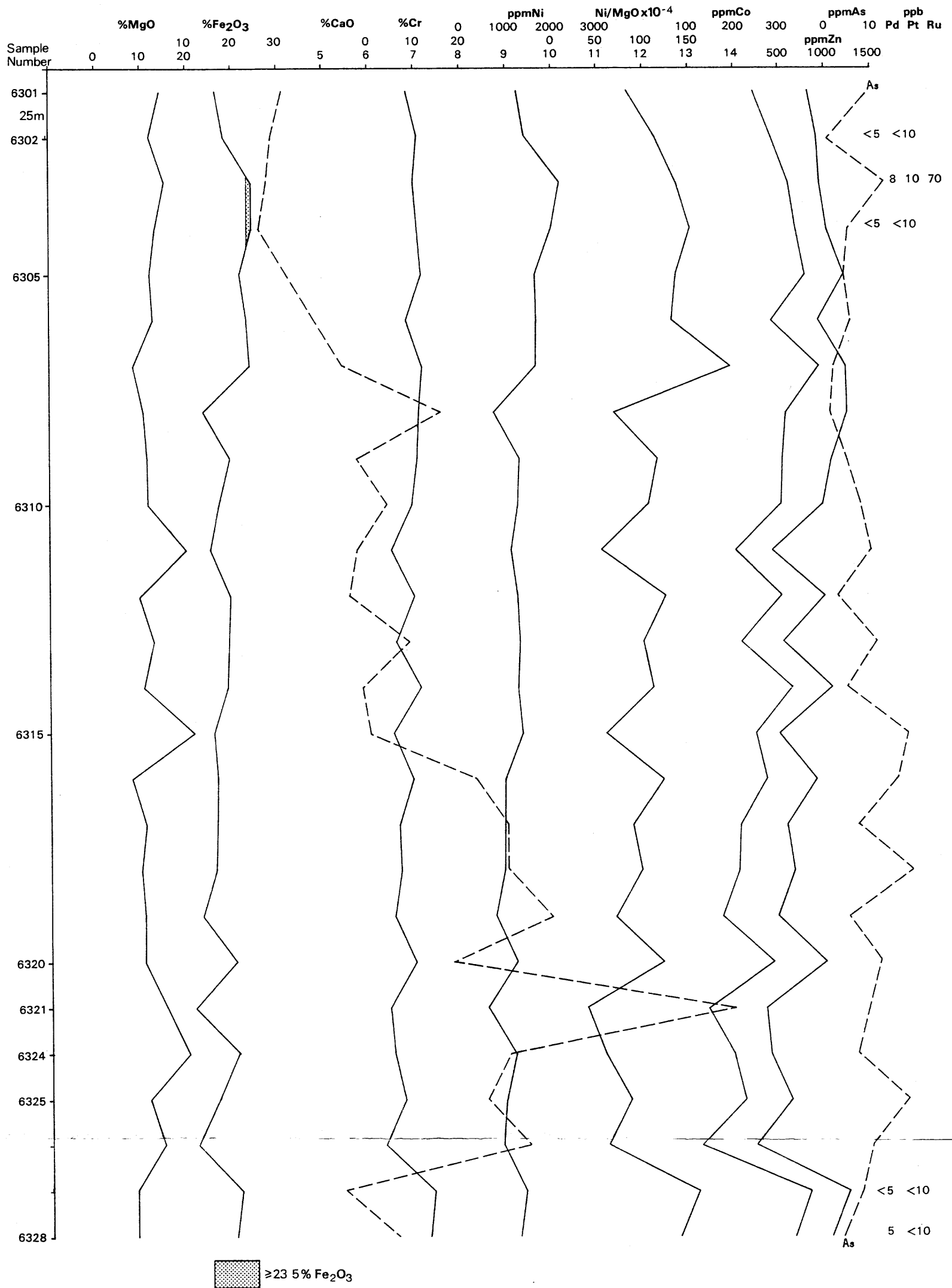
Fig. 44   Element distribution in panned overburden samples from Gerdie traverse.

Fig. 43 Location of traverses in the dunite and cumulate units south of Balta Sound

Fig. 45   Element distribution in panned overburden samples
from Helliers Water traverse

Table 9 Comparison of overburden samples from cumulate units

	Gerdie/Helliers Water			Ordale		
	Mean	S. D.	Range	Mean	S. D.	Range
MgO%	13.13	3.25	8.10-21.71	14.99	3.56	9.19-20.69
Cao%	6.40	2.11	3.60-13.94	7.10	1.46	4.47- 9.19
Sppm	107	81	47- 341	1177	340	548- 1712
Cr%	7.87	2.83	3.37-13.58	11.04	3.05	6.60-16.09
Fe$_2$O$_3$	20.48	4.56	11.48-30.31	14.55	4.00	11.32-17.74
Coppm	282	69	123- 410	315	66	225- 460
Nippm	1515	571	562- 2791	891	237	493- 1223
Cuppm	53	16	29- 90	47	8	33- 61
Znppm	799	260	230- 1253	819	223	470- 1221
Asppm	6	5	<1- 18	8	6	<1- 17
No. samples	40			11		

The general pattern of variation of Ca in the traverse is very similar to that shown by the Gerdie traverse though the trend of increasing Ca levels is in the opposite direction. There is more variation in Cr, Co and Zn in the samples from Ordale than from Gerdie and there are several overall chemical features which differ between the two areas. The Ordale samples are significantly richer in Cr but poorer in Fe than those from Gerdie and the ratios Fe/Cr and Zn/Cr are distincly different. Ni and Ni/MgO levels are much lower in the Ordale samples while amounts of S are very much higher. Variation in S contents may be influenced by the fact that the land at Ordale has been improved for pasture but it is unlikely that this would have made any significant difference to levels of elements like Fe and Cr in material immediately above bedrock. The chemical differences are sufficient to indicate that the rocks from the two areas represent different groups of cumulates. The relationship between the areas is unclear from the limited data available though structural interpretation suggests that the Ordale rocks are probably discordant to the Gerdie sequence. On the Ordale traverse the peaks for Ni/MgO are relatively subdued and the samples analysed for PGE have background levels. One sample however may be slightly enriched given the analytical problems with the Pd data set for that batch of samples analysed with nickel sulphide fire assay as described above.

Rock sampling

Cliff area

A suite of samples of chromitite and serpentinised dunite host rock was collected from all dumps in the Cliff area. This was augmented by samples from outcrop in the area and a few short drill holes to bedrock. The general compositional relationships between the various rock types and alteration assemblages have already been discussed above. Analyses of chromitite and chromite-rich dunite samples from the various dumps are shown in table 10. Most of these samples were composites of the textural varieties typical of a given dump. As it was not possible to deduce the source of some of the small dumps around pits D and E (Figure 13) the two have been combined in table 10.

Fig. 46   Element distribution in panned overburden samples from Ordale traverse.

Table 10. Composition of chromitites and chromite-rich dunites Cliff area

	F	A	B(1)	B(2)	C(1)	C(2)	D+E(1)	D+E(2)	Cr.	S.
MgO%	27.37	27.75	33.83	22.62	24.32	39.72	26.28	40.75	27.99	28.19
Al₂O₃%	7.89	7.04	4.79	8.10	6.72	2.56	7.46	1.10	9.16	8.76
SiO₂%	26.79	23.77	31.66	14.53	19.98	39.26	22.41	38.02	25.11	25.54
Sppm	73	110	304	126	116	312	81	238	59	51
CaO%	0.12	0.34	0.24	0.33	0.10	0.14	0.19	0.12	0.07	0.12
TiO₂%	0.06	0.08	0.08	0.14	0.15	0.04	0.09	0.01	0.06	0.09
Vppm	267	211	77	238	188	<1	269	<1	459	198
Cr₂O₃%	27.11	24.97	17.45	36.38	33.32	8.83	31.32	5.48	26.36	26.83
MnO%	0.21	0.22	0.13	0.20	0.19	0.11	0.11	<0.01	0.14	<0.01
Fe₂O₃%	11.66	16.99	12.76	18.81	16.13	9.57	13.29	10.00	11.75	11.48
Coppm	174	252	192	238	224	144	194	139	183	161
Nippm	2439	2540	7204	3432	2201	4961	3541	7453	2371	3048
Cuppm	21	40	293	148	26	145	57	305	23	54
Znppm	262	379	201	338	317	115	269	76	308	192
Asppm	129	19	276	70	8	56	16	30	12	29
Sbppm	<1	<1	15	7	13	10	1	<1	1	6
Teppm	<1	<1	12	6	<1	6	2	3	<1	<1
Bippm	<1	<1	3	<1	5	3	4	<1	<1	2
Ruppb	<10	15	5733	600	10	1600	317	800	<10	<10
Rhppb	6	12	1300	60	<5	540	99	250	<5	<5
Pdppb	15	57	46000	5000	110	13500	2104	7500	9	5
Irppb	<10	<10	3167	55	<10	400	65	210	<10	<10
Ptppb	<10	13	25667	3000	60	7000	948	3500	<10	<10
Ni/MgO	89	92	213	152	91	125	135	183	85	108
No. samples	1	2	3	1	1	1	5	1	1	1

Samples A to F from pits (Figure 14): Cr.- float from Crussa Field old trenches 15m E of site 450E,300S: S.- float from area around site 00,450S.

Apart from the very high level of PGE present in some samples the most significant feature of these and the other rock data is the high degree of positive correlation between the PGE. A plot of Pd against Pt in all analysed rock samples (Figure 47) shows a very strong positive correlation between the two in all rock types over a very wide range of concentrations. The samples from near Harold's Grave are an exception to this general pattern and are discussed below. In addition the most anomalous overburden samples (figure 47) also show a positive correlation between Pt and Pd and Pt/Pd ratios similar to the rock data. Figure 48 shows that a similar relationship exists between Rh and Pd with the same high degree of positive correlation. It is also apparent from figures 47 and 48 and table 10 that, while the most PGE-rich samples from the Cliff area are chromitites and chromite-rich dunites there are also similar samples from the same area with very low levels of PGE.

Table 11 compares the chemistry of chromitites and chromite-rich dunites with corresponding samples of serpentinised dunite collected from the old workings in the Cliff area.
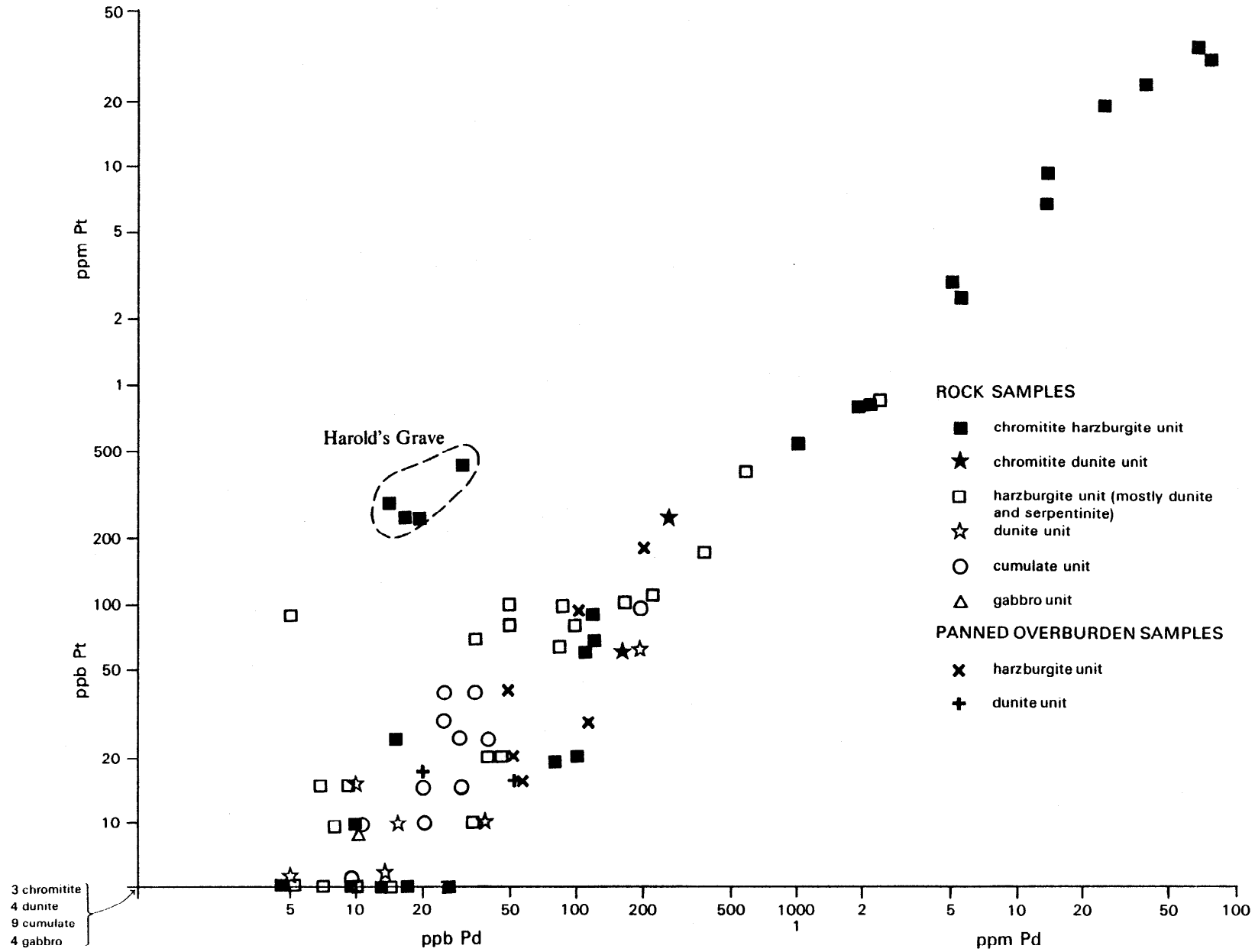
Fig. 47   Relationship between Pt and Pd in rock and panned overburden samples
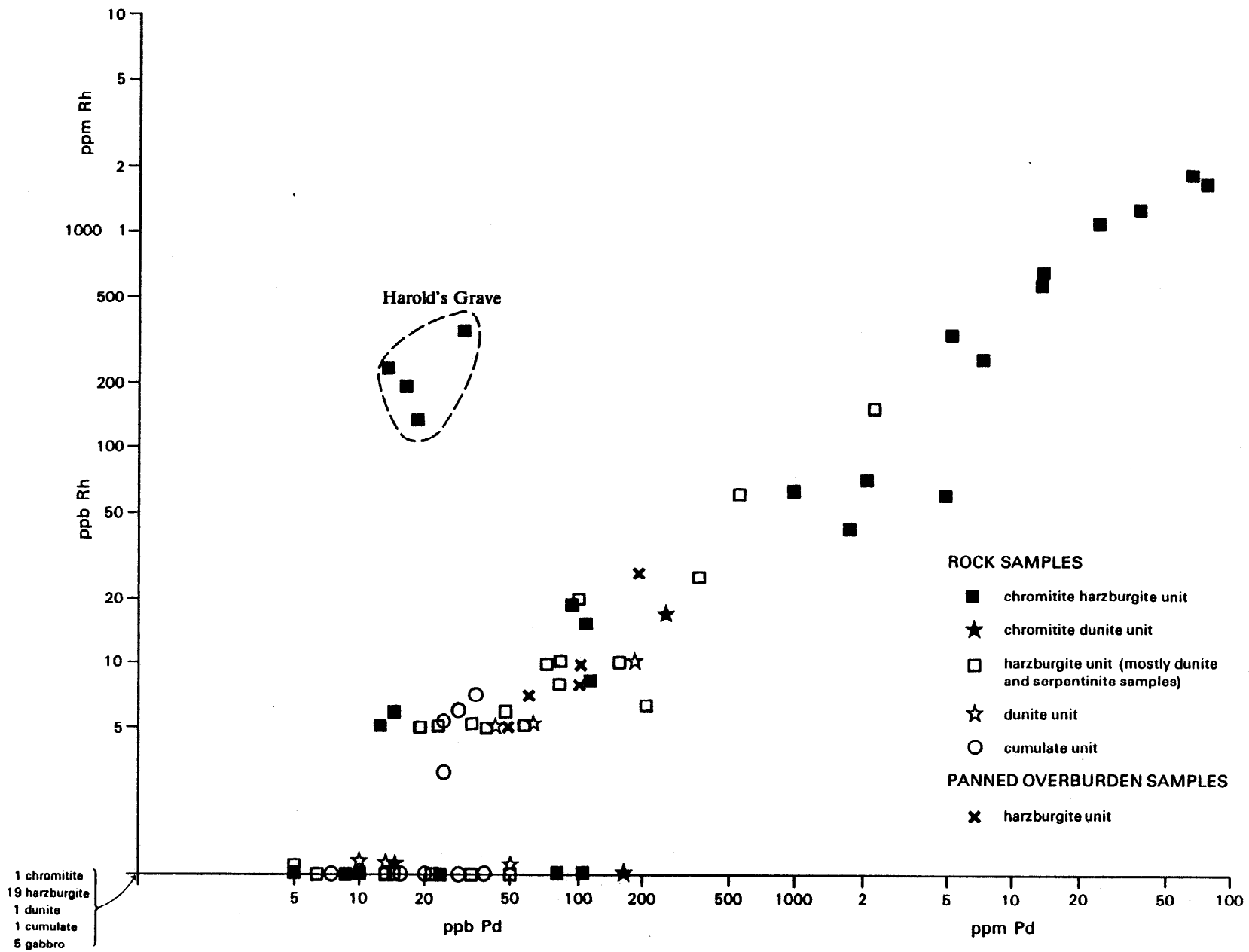
Fig. 48   Relationship between Rh and Pd in rocks and panned overburden samples

	F		A		B		B		C		D+E		D		E	
	Cr.	D.	Cr.	D.	Cr.	D.	Cr.	D.	Cr.	D.	Cr.	D.	Cr.	D.	Cr.	D.
MgO%	27.37	37.54	27.43	44.94	33.87	44.89	35.06	46.55	24.32	46.44	26.87	39.40	25.79	45.63	25.30	46.44
S ppm	73	206	66	87	283	334	388	436	116	181	88	165	63	123	63	231
Cr₂O₃%	27.11	0.67	27.14	0.34	17.72	0.32	15.12	0.91	33.32	0.25	29.30	0.26	31.79	0.26	33.62	0.19
Fe₂O₃%	11.66	9.88	17.06	8.62	13.43	9.77	12.23	8.65	16.13	8.62	12.39	9.32	14.53	9.60	14.27	8.26
Cu ppm	174	96	247	92	201	112	204	224	101	170	96	289	190	123		
Ni ppm	2439	2317	2551	2596	6292	3996	8044	2809	2201	2237	3847	3676	3243	5443		
Co ppm	21	17	39	35	267	162	284	120	<1	18	17	112	104	61		467
As ppm	129	13	17	19	284	57	361	196	26	8	7	20	9	8		45
Sb ppm	<1	1	<1	3	12	2	26	2	13	7	1	4	5			
Te ppm	<1	2	<1	<1	2	2	4	<1	2	2	4	1	1	4		5
Bi ppm	<1	1	1	2	6	2	15	2	5	<1	1	1	<1	3		
Ru ppb	<10	15	25	25	3000	80	9000	50	10	16	800	50	<10	110	200	160
Rh ppb	6	5	18	18	1100	25	1600	10	<5	<5	320	6	7	60	40	150
Pd ppb	15	45	100	100	25000	360	75000	160	110	50	5500	215	120	575	1800	2300
Ir ppb	<10	<10	<10	<10	1500	10	5000	<10	<10	<10	210	<10	<10	20	40	150
Pt ppb	<10	20	80	80	20000	170	32000	100	60	80	2500	70	410	800	850	
Ni/MgO	89	62	93	58	186	89	229	60	91	48	143	143	64	66	128	117

Cr. chromitite: D. dunite or serpentinite: A-F pit locality

The data in table 11 demonstrate that where the chromitites have the highest PGE concentrations the the corresponding dunites also show some enrichment in these elements. In pit B, from which the highest grades of PGE have been obtained, the dunites are much less enriched than the chromite-rich samples, but from some parts of pit D the reverse pattern is observed. These observations have important implications for exploration as they suggest that haloes of PGE enrichment may exist around the richest ore. Such haloes would present larger exploration targets which would therefore be easier to detect, especially when secondary environment samples are being used. Furthermore the presence of PGE enrichments in dunite of the same order of magnitude as in chromite suggests that the association of PGE with chromite enrichment is not primary.

A plot of Ru against Pd (Figure 49) also shows a very good positive correlation between the two elements for rock samples irrespective of type. There are however a few rock samples and most of the overburden samples which show relative enrichment in Ru relative to Pd. This indicates the presence of two types of PGE enrichment. One exhibits close correlation of all PGE but is Pd dominant and the other is relatively rich in Ru with little or no associated Pd. By virtue of the relatively large number of overburden samples showing this relative Ru enrichment it can be regarded as a background population which locally is more enriched. Ir also shows a good positive correlation with Pd but only for relatively high Pd levels (Figure 50). There is also a good correlation between Ru and Ir (Figure 51), also observed in the overburden samples, which suggests a close association of these two elements in both types of PGE enrichment.
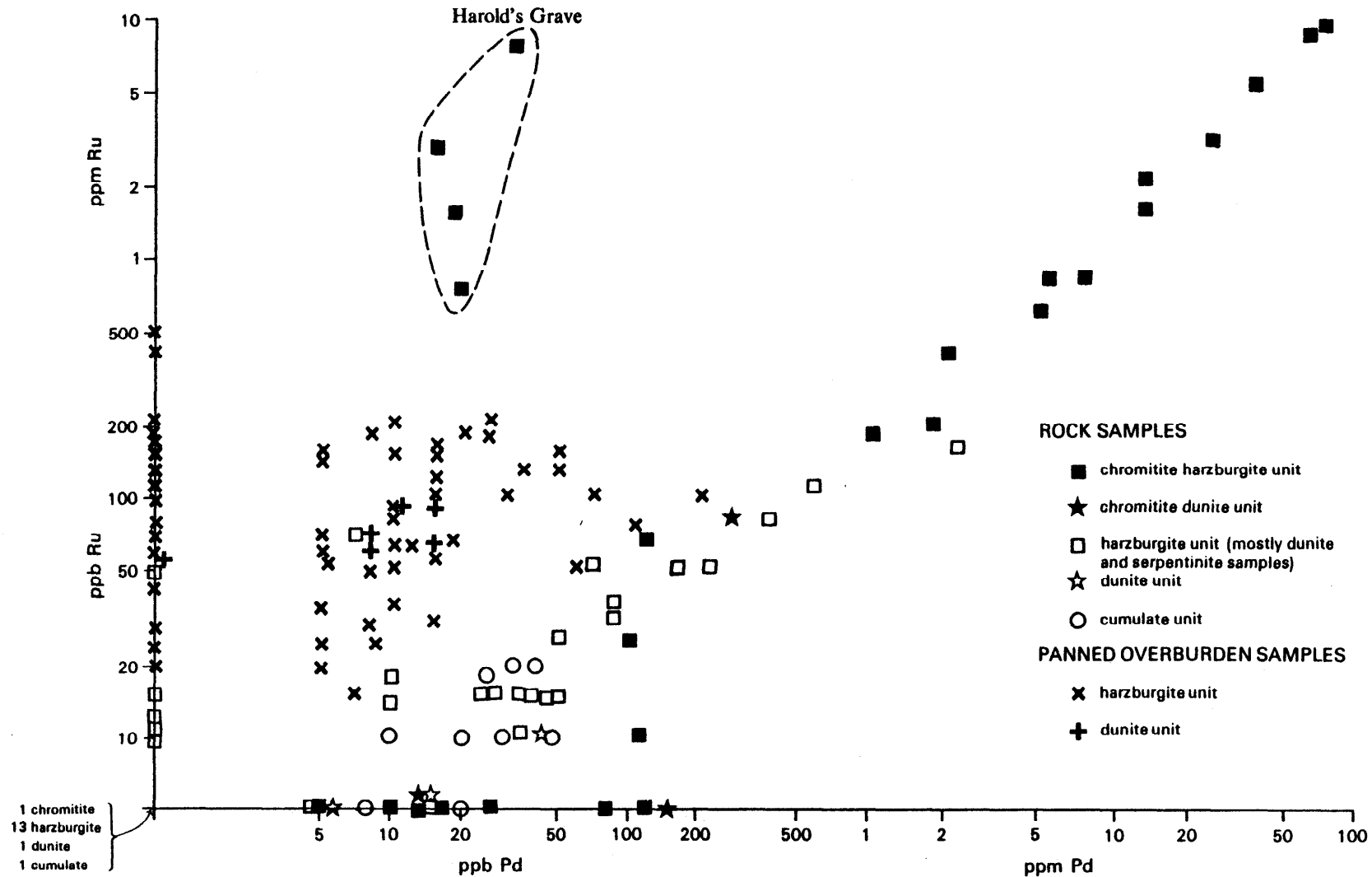
Fig. 49   Relationship between Ru and Pd in rock and panned overburden samples
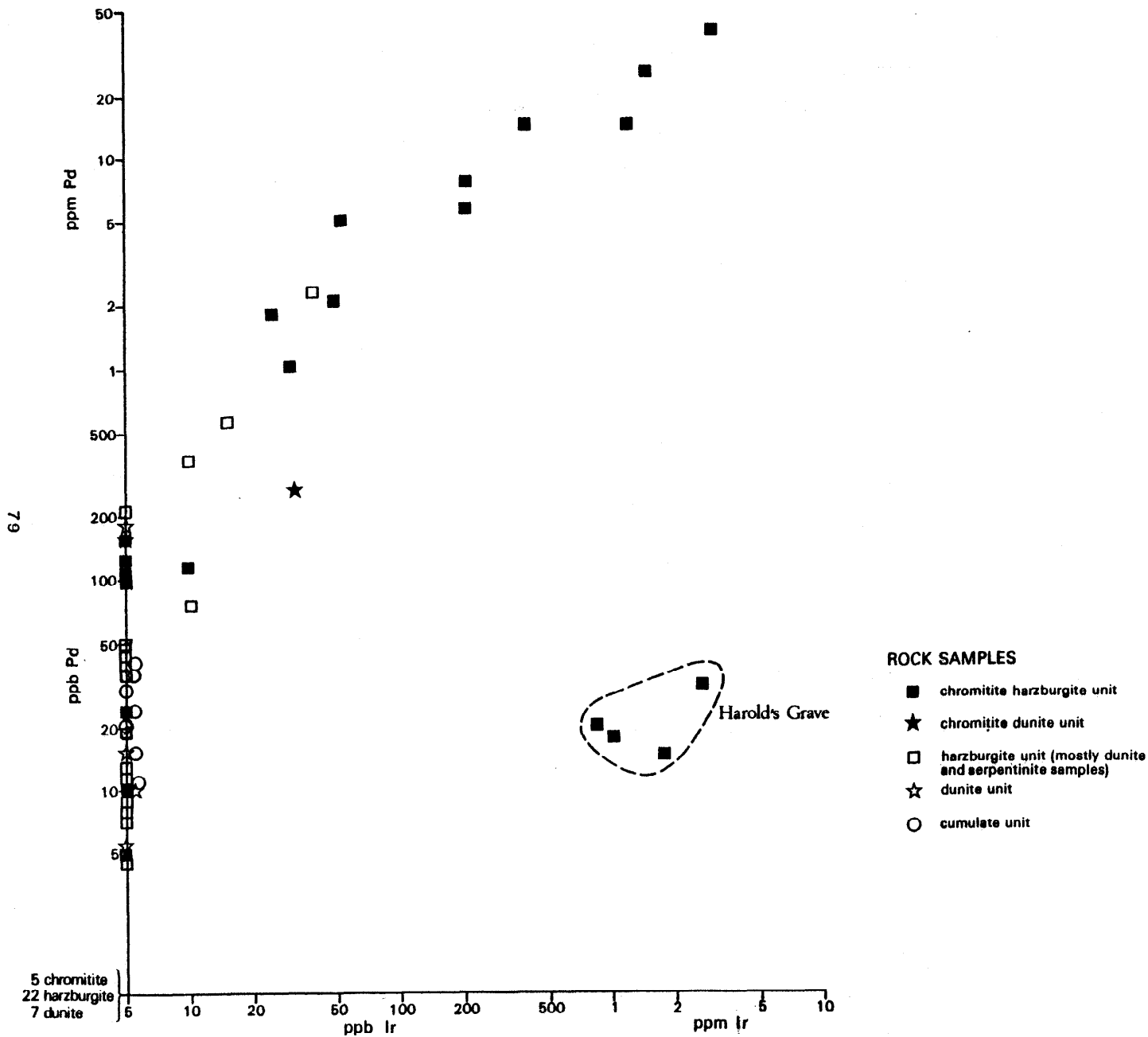
Fig. 50   Relationship between Pd and Ir in rock samples

ROCK SAMPLES

■ chromitite harzburgite unit

★ chromitite dunite unit

□ harzburgite unit (mostly dunite and serpentinite samples)

☆ dunite unit

○ cumulate unit

Harold's Grave

ppm Pd
ppb Pd

ppb Ir   ppm Ir

5 chromitite
22 harzburgite
7 dunite

79

Other parts of harzburgite unit

A few rock samples were collected from other occurrences of chromite within the harzburgite unit and chemical analyses of these are shown in table 12 below.

Table 12   Composition of chromitite and associated rocks from harzburgite unit

| | Quoys West | | Quoys main | | | Quoys South | | Harold's Grave | | | |
	Cr	D.	Cr.	Cr.	D.	Cr.	D.	Cr.	Cl.	D.	Cr.
MgO%	23.87	37.26	18.45	28.93	45.57	27.15	40.36	15.64	42.91	44.54	13.74
Al2O3%	-	0.40	10.20	6.15	0.81	12.50	0.57	10.49	8.94	0.67	14.20
SiO2%	-	45.39	10.29	25.58	45.01	16.35	46.79	9.69	39.19	43.47	4.00
Sppm	203	91	101	129	168	69	45	42	227	246	16
CaO%	0.26	0.35	0.20	1.39	0.61	0.38	0.33	0.64	0.30	0.22	0.06
TiO2%	-	0.00	0.09	0.07	0.00	0.09	0.00	0.17	0.01	0.00	0.30
Vppm	-	21	442	45	26	411	29	954	68	25	1087
Cr2O3%	35.31	0.25	39.50	26.26	0.32	25.09	0.44	38.45	0.53	0.33	41.84
MnO%	-	0.13	0.21	0.24	0.05	0.16	0.06	0.26	0.00	0.13	0.21
Fe2O3%	14.88	9.67	16.17	12.61	4.56	15.72	9.69	23.62	5.78	9.75	23.30
Coppm	170	89	162	196	48	187	100	234	52	96	168
Nippm	3771	1898	1212	2202	2133	2359	2083	940	2475	2315	778
Cuppm	52	1	33	23	6	22	5	37	914	5	32
Znppm	237	23	267	283	<1	289	31	637	6	10	499
Asppm	49	5	74	90	33	20	14	<1	2	<1	6
Sbppm	-	2	2	1	2	3	<1	1	4	3	10
Teppm	-	<1	2	1	3	<1	<1	1	<1	<1	2
Bippm	-	<1	1	3	<1	2	<1	2	1	<1	<1
Ruppb	65	<10	116	<10	<10	<10	<10	4014	<10	<10	740
Rhppb	15	<5	6	<5	<5	<5	<5	249	<5	<5	129
Pdppb	115	<5	15	8	4	<5	<5	20	<5	<5	19
Irppb	10	<10	24	<10	8	<10	<10	1803	<10	<10	831
Ptppb	90	<10	-	8	<10	<10	<10	325	<10	<10	250
Ni/MgO	105	51	66	76	47	87	52	60	58	52	57
No. samp.	1	1	2	2	1	1	1	3	1	1	1

Cr. chromitite: D. dunite or serpentinised dunite: Cl. chloritic rock
Qouys South small pit ca 100m SW of main pit.

The samples generally contain low background levels of PGE with the exception of the chromitites from the Harold's Grave area which are highly enriched in all PGE except Pd. A consequence of this is that in graphs of Pd against other PGE the Harold's Grave samples plot in a separate field to the samples from the Cliff and other areas (Figures 47, 48, 49 and 50) and in the Ru-Pd-Pt triangular diagram shown in figure 52. On the other hand the same samples show a similar ratio between Ru and Ir to all the others as shown in figure 51. The Harold's Grave mineralisation is therefore compositionally entirely different from that at Cliff. It is classified as a different type, compositionally related to the background concentrations of PGE typical of the harzburgite unit in general as revealed from the chemistry of the many overburden samples shown in figure 49. The composite sample of chromite float from Quoys West with mildly anomalous levels of PGE is, in contrast, very similar in its proportions of PGE to the PGE-rich samples from Cliff. There are some other significant differences in chemistry between the Harold's Grave chromitites and the other samples of chromitite particularly in V, Ti and Fe the significance of which will be discussed below.
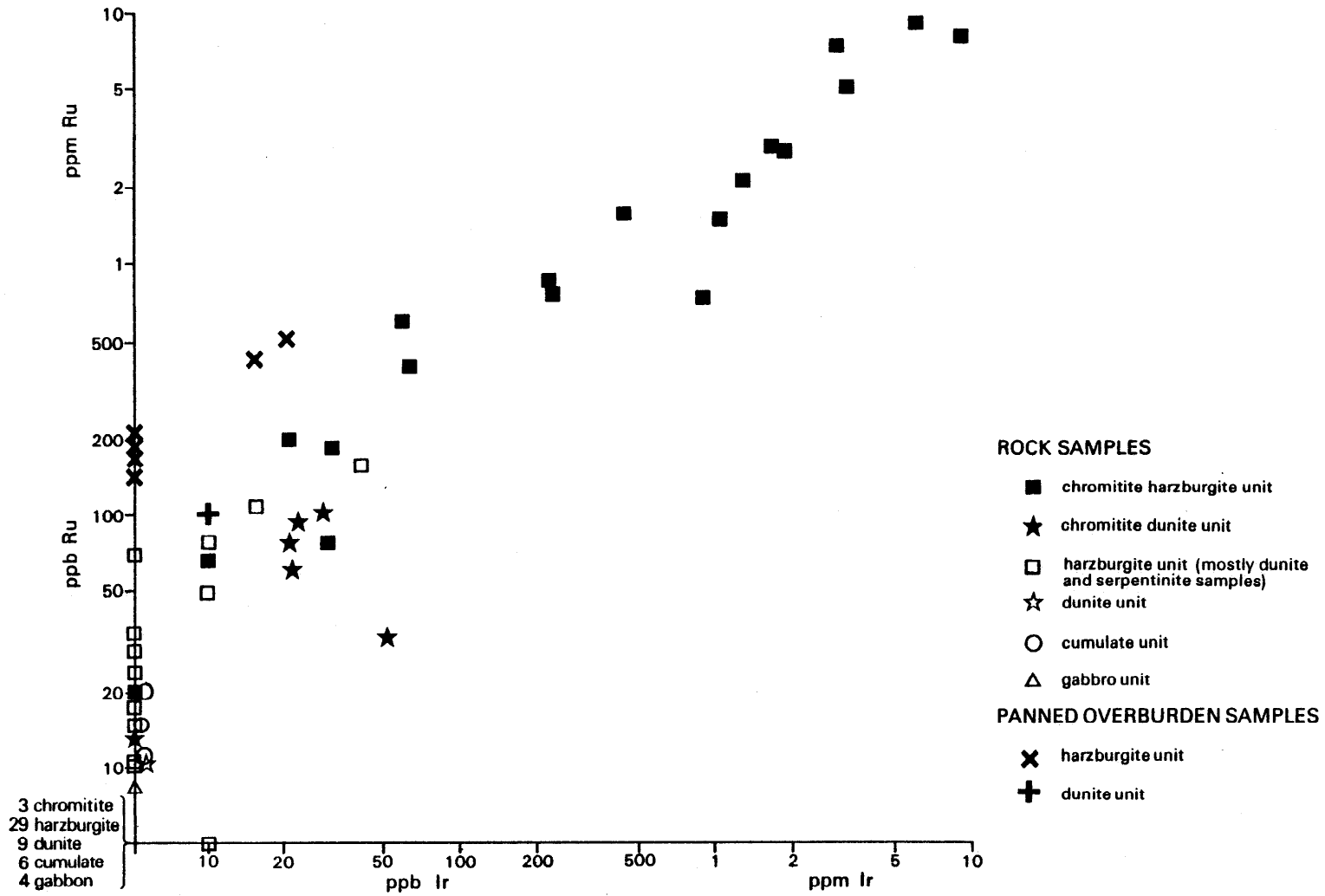
Fig. 51 Relationship between Ru and Ir in rock and panned overburden samples

ROCK SAMPLES

■ chromitite harzburgite unit

★ chromitite dunite unit

□ harzburgite unit (mostly dunite and serpentinite samples)

☆ dunite unit

○ cumulate unit

△ gabbro unit

PANNED OVERBURDEN SAMPLES

✗ harzburgite unit

✚ dunite unit

3 chromitite
29 harzburgite
9 dunite
6 cumulate
4 gabbon

ppm Ru

ppb Ru

ppb Ir

ppm Ir

Ru

× chromitite in harzburgite
+ chromitite in dunite
• serpentinite
▲ dunite
▼ cumulate
⬭ field of compositions from Harold's Quarry

Harold's Quarry

Pd

Pt

Fig. 52

Variation of Pd-Ru-Pt in rock samples

82

Dunite unit

Samples of chromitite and adjacent rocks have been analysed from a number of widely scattered localities in the dunite unit. Chemical analyses of these samples are shown in table 13.

Table 13 Chromitites and associated rocks from dunite unit + its lower contact

| | Nikkavord | | | Muckle Heog | | | M. G. | Hag. | Wat. | Sobul |
	Cr-m	Cr-1	Cr.	Cl/D.	D.	D.	Cr.	Cr.	Cr	Cr.
MgO%	20.22	26.26	21.03	41.99	42.30	41.26	25.43	25.97	19.59	19.96
Al₂O₃%	12.91	10.40	21.38	1.99	0.39	-	10.94	-	8.69	6.60
SiO₂%	11.90	19.77	8.73	42.52	39.30	-	17.27	-	13.30	12.34
Sppm	40	142	1381	353	555	654	138	1290	147	215
CaO%	0.08	0.22	0.06	0.10	0.10	0.07	0.11	0.14	0.19	0.15
TiO₂%	0.12	0.11	0.15	0.00	0.00	-	0.14	-	0.16	0.09
Vppm	529	326	569	20	16	-	386	-	424	380
Cr₂O₃%	35.34	22.42	29.26	0.53	0.40	0.26	23.51	32.36	31.12	37.04
MnO%	0.20	0.18	0.18	0.10	0.15	-	0.20	-	0.28	0.26
Fe₂O₃%	15.45	12.71	14.09	7.81	11.45	11.47	14.46	14.41	22.38	18.92
Coppm	168	162	190	44	111	134	120	215	231	217
Nippm	1377	1870	3780	1467	2385	3104	1717	4718	1427	1186
Cuppm	30	35	765	155	66	183	42	723	36	64
Znppm	335	166	245	9	22	26	194	256	333	367
Asppm	3	1	<1	2	<1	7	<1	<1	8	125
Sbppm	2	1	2	<1	3	-	2	-	<1	2
Teppm	1	<1	<1	<1	<1	-	<1	-	<1	<1
Bippm	1	<1	<1	<1	<1	-	-	-	<1	2
Ruppb	62	16	81	<10	<10	<10	48	<10	14	72
Rhppb	6	1	16	<5	<5	9	6	<5	4	9
Pdppb	-	-	260	15	10	180	-	160	-	-
Irppb	19	7	31	<10	<10	<10	-	<10	6	39
Ptppb	-	<10	250	10	15	60	<10	65	<6	-
Ni/MgO	68	71	180	35	56	75	68	182	73	60

Locations :- M. G. Mid Garth, Hag. Hagdale, Wat. Burn of Watlee.
Samples from Nikka Vord in gradational contact zone between dunite and harzburgite.
Cr. chromitite: D. dunite/serpentinite: Cl/D. Chloritic serpentinite:
Cr-m massive chromite: Cr-l layered chromite.

Anomalous amounts of PGE in similar proportions to the rich samples from Cliff occur in two samples of chromitite and one of dunite from the dunite unit. These data indicate that the Cliff type PGE enrichment is of widespread extent throughout the ultramafic part of the Unst ophiolitic complex, not necessarily in association with chromite concentrations.

Relationships between PGE and other elements

The chemical analyses of rock and chromitite samples do not reveal any general correlation between levels of Cr and PGE. In fact the samples most rich in PGE tend to be slightly depleted in Cr compared with other chromitite samples as shown in Figure 53. In all units and rock types including chromitites there is a complete spectrum of PGE contents. This suggests that controls other than those related to the formation of chromitites were important in locating the Cliff

type PGE mineralisation.

Figure 53 shows that there is an absence of correlation between Pd and S levels
except perhaps within the samples from the dunite unit. The corresponding plot of
As against Pd in figure 54 shows evidence of a significant positive correlation
between the two elements above the 2 ppm Pd level but an absence of correlation
at lower concentrations. Furthermore there are several samples containing
relatively high levels of As with background levels of Pd. This limits the
potential use of As as a simple pathfinder. The levels of As in samples derived
from the dunite unit are low compared with those from other units (table 13,
figure 54), although one sample from Sobul for which an AAS Pd determination is
not available contains 227ppm As. The relationship between Sb and Pd resembles
the behaviour of As, with enrichment to a maximum of 28ppm in one of the most
PGE-rich samples and general correlation between the two elements above the 2ppm
Pd level. There are also samples with up to 13 ppm Sb associated with only mild
enrichment in PGE, and up to 8ppm Sb with background PGE concentrations. Te
behaves in a similar way to Sb with a maximum level of 15 ppm in the most
PGE-rich sample and a correlation between Pd and Te at high levels of PGE.
Levels of up to 5ppm Te are also present in samples with background PGE. The
chemical data therefore indicates some genetic association in the Cliff area
between the PGE and As, Sb and Te but not S. In contrast the PGE-rich samples
from the Harold's Grave area have associated very low levels of S, As ,Sb and Te
except for one sample which contains 10ppm Sb without enrichment in the other
elements.

The plot of Cu against Pd in Figure 55 demonstrates a general positive
correlation between the two elements but with a considerable scatter. It is also
clear that samples from the dunitic unit are on average richer in Cu than those
from the harzburgite unit, a feature also indicated by the drainage data set
(table 4) and the overburden data set (table 8). Ni is also enriched to a
considerable degree in the samples most rich in PGE, reaching a maximum of
8044ppm. Alhough a correlation between Ni and Pd is evident at Pd levels above
about 5ppm Pd, as shown in figure 56, below that level the correlation is
absent. Since Ni is a minor component of silicate minerals like olivine and
serpentine which are common in the ultramafic rocks and since the abundance of
these minerals is inversely proportional to the amount of chromite a better way
of demonstrating a correlation between Ni and PGE is to plot Pd against Ni/MgO
as in figure 57. This plot shows that the correlation between PGE and Ni extends
to lower levels of PGE, with separate lines for chromitites and the silicate
rocks. However a relatively large scatter still remains. The chromitites from
the dunite unit are richer in Ni than samples from the harzburgite with similar
PGE levels. In contrast to Cu and Ni, Co does not show a correlation with PGE.
The PGE-rich samples from the Harold's Grave area do not show any enrichment in
Cu or Ni of the type shown by the Cliff samples where a genetic association
between PGE and Cu and Ni is indicated.

The associations between PGE and other trace elements in the rock data set
suggest that some elements could be of value as pathfinders. Sb and Te are not
likely to be useful since their levels are lower than PGE in the most
mineralised samples. The elements As, Cu and especially Ni are of some value
since their concentrations exceed those of the PGE. Ni has the most potential as
a pathfinder when allowance is made for variation in the background due to
varying the common rock-forming silicates by use of the ratio Ni/MgO.
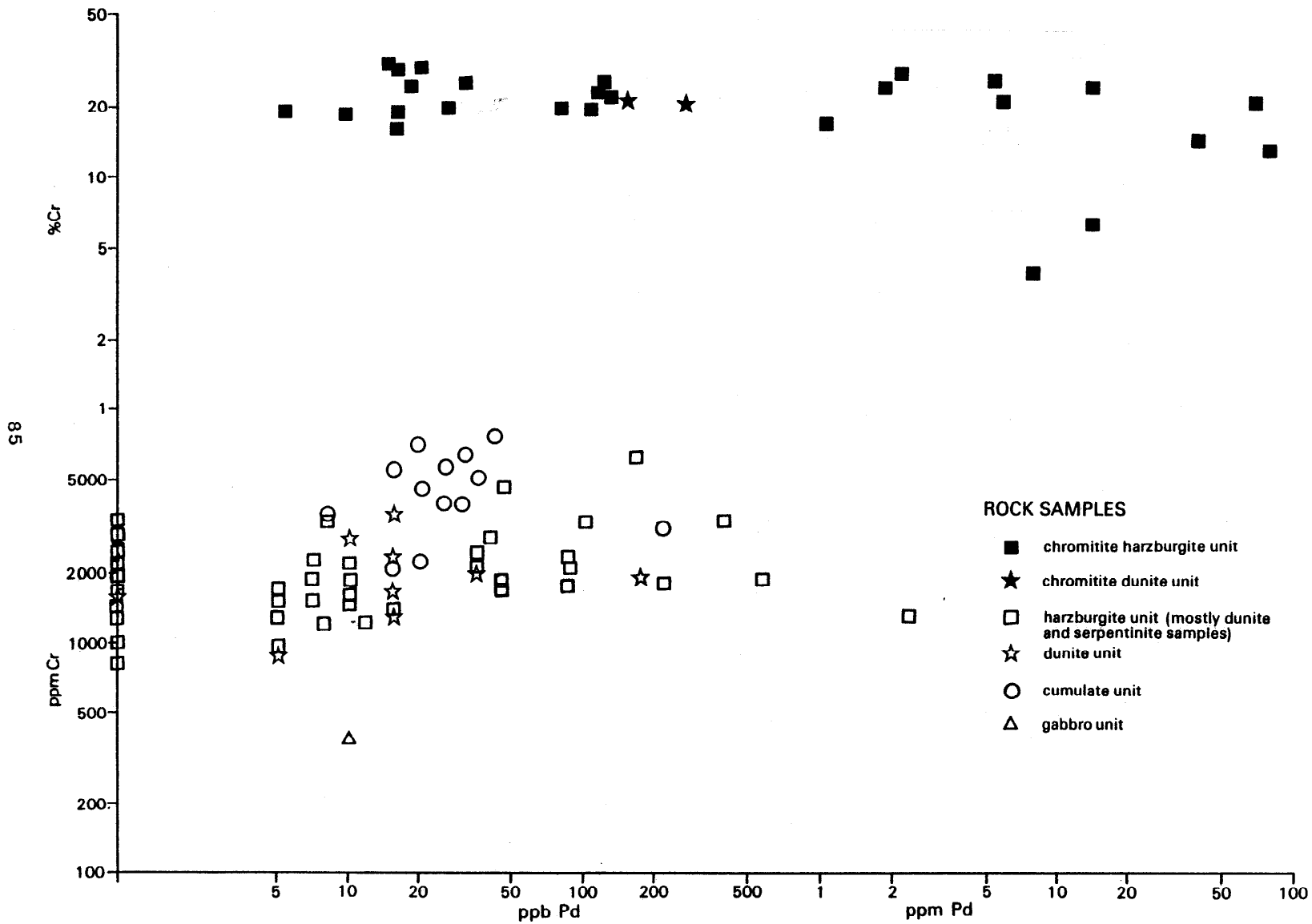
Fig. 53   Relationship between Cr and Pd in rock samples
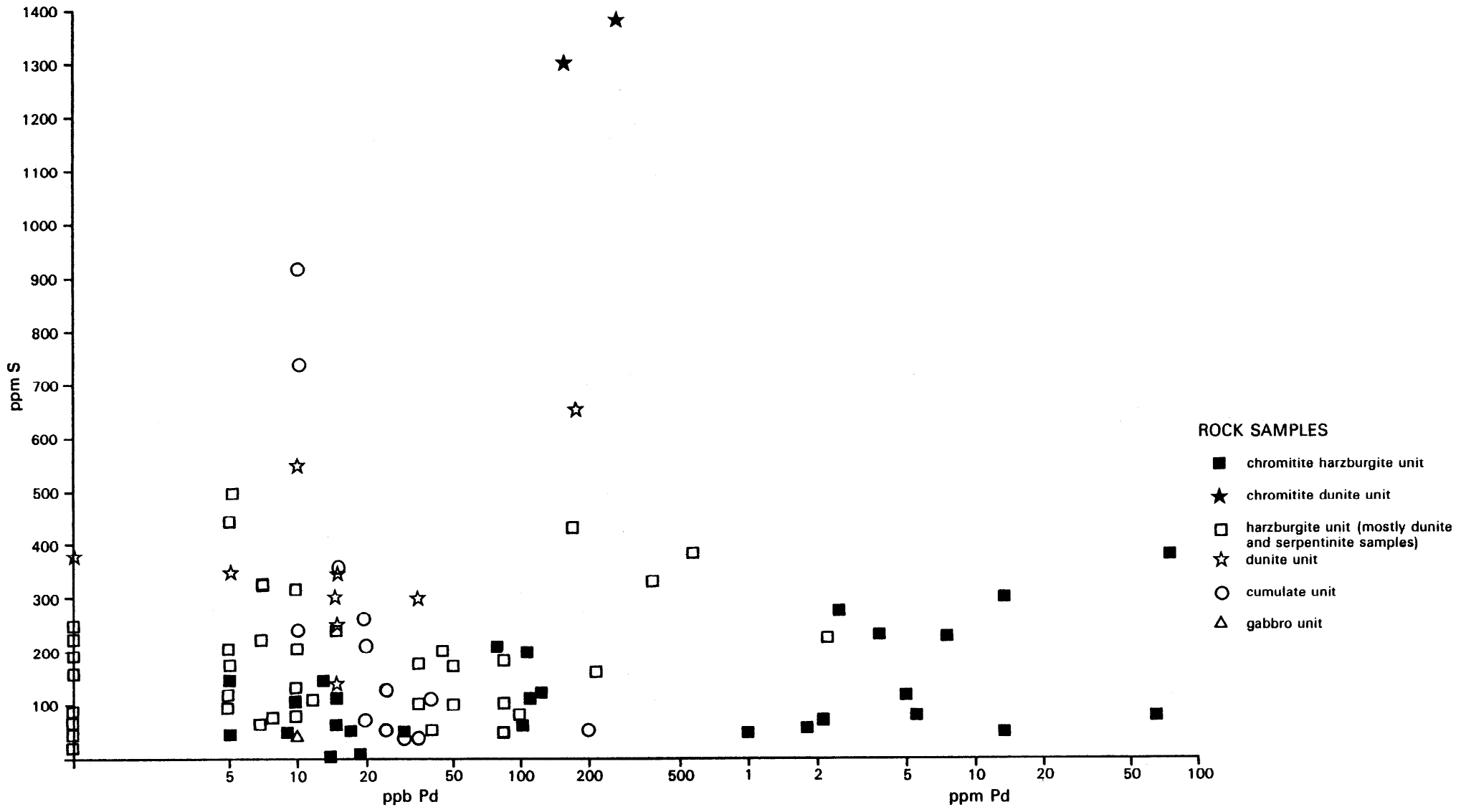
Fig. 54   Relationship between Pd and S in rock samples
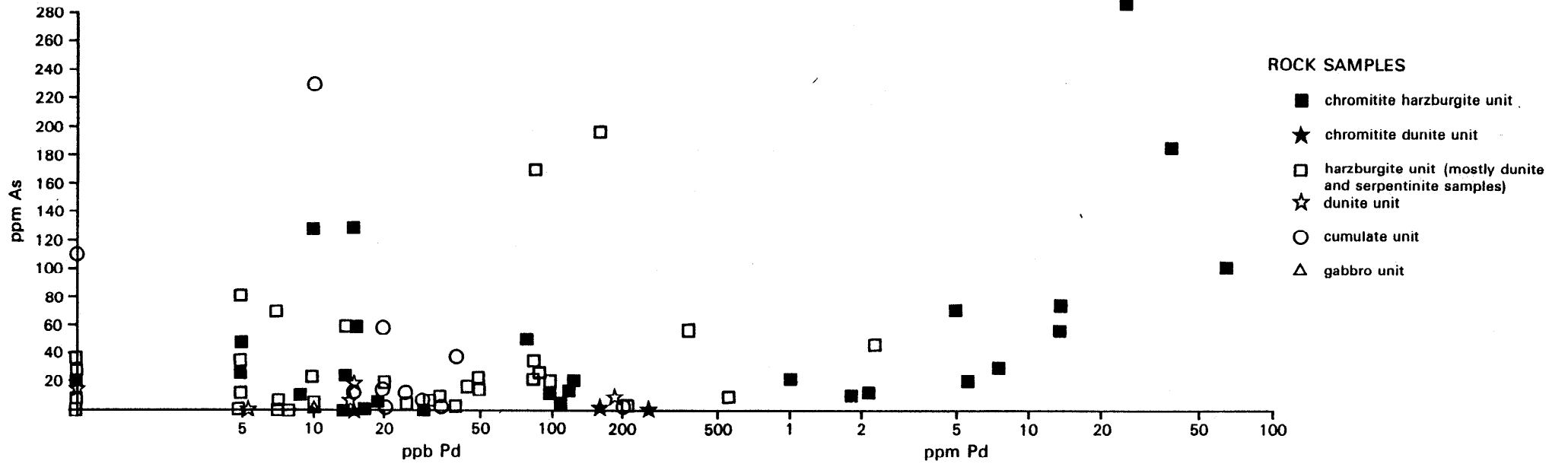
Fig. 55   Relationship between Pd and As in rock samples
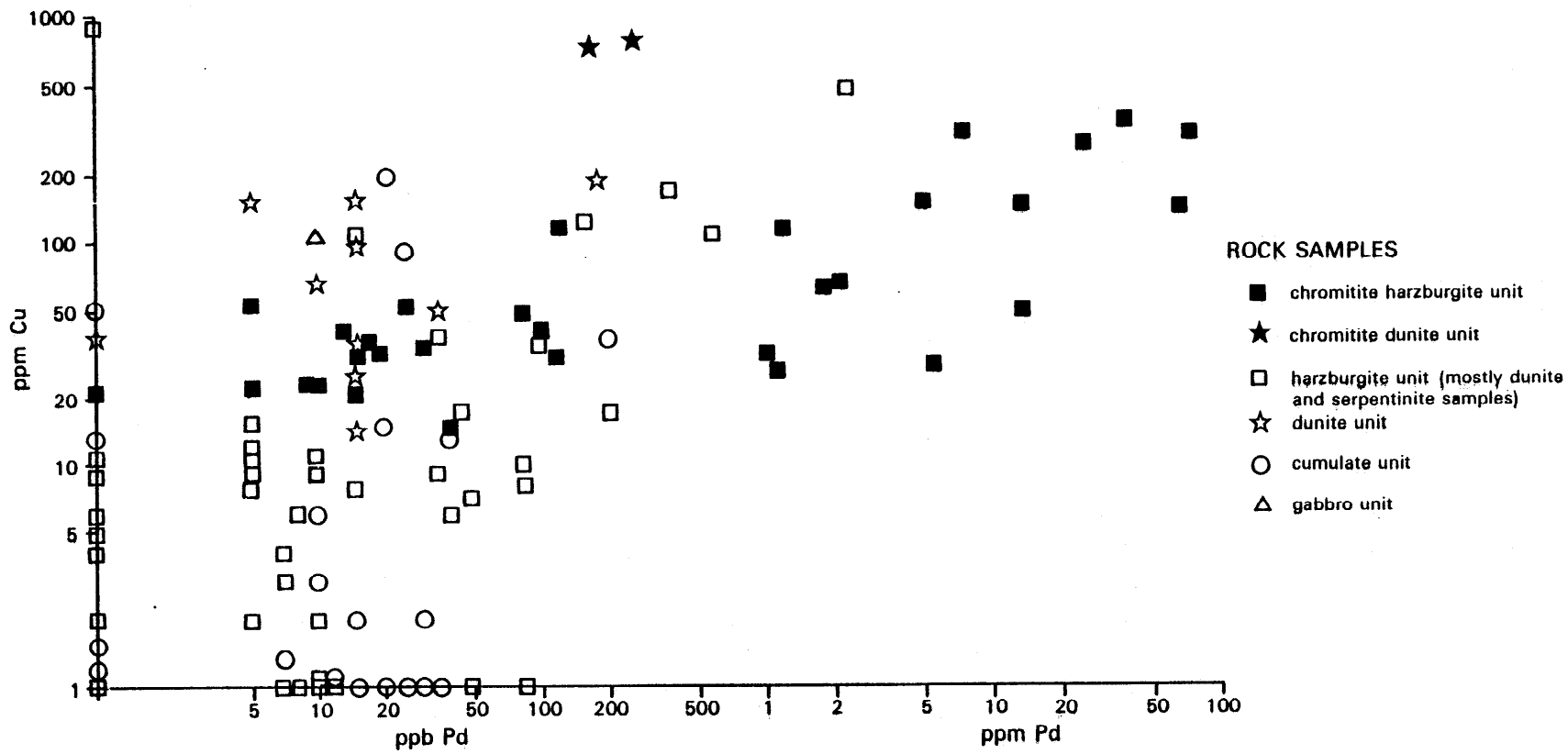
Fig. 56   Relationship between Pd and Cu in rock samples
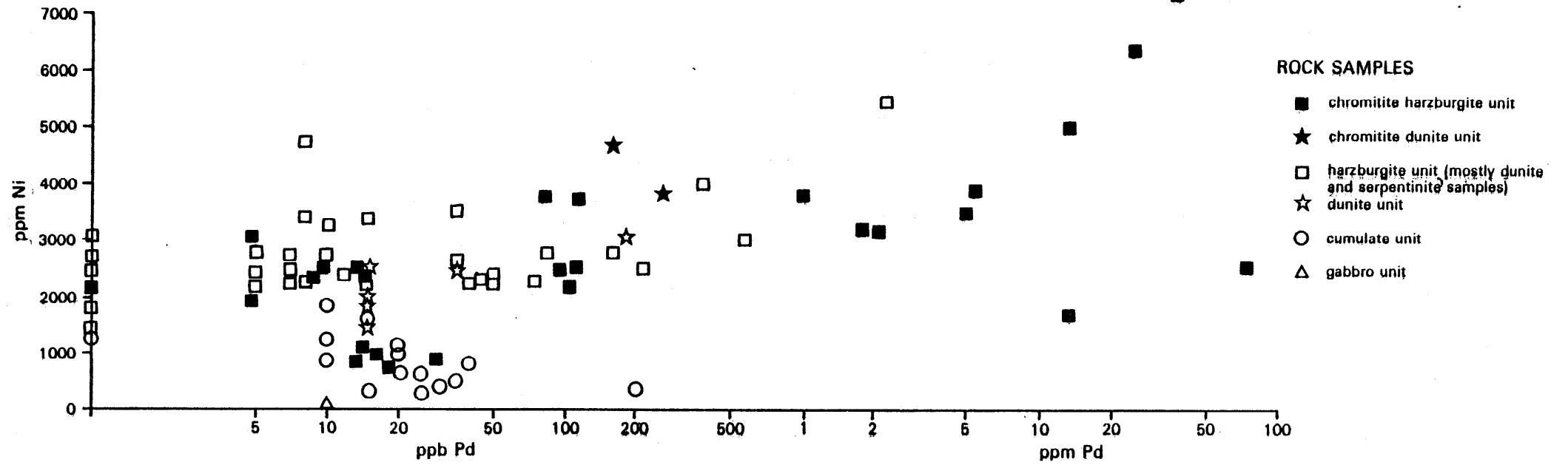
Fig. 57   Relationship between Pd and Ni in rock samples

ROCK SAMPLES

- ■ chromitite harzburgite unit
- ★ chromitite dunite unit
- □ harzburgite unit (mostly dunite and serpentinite samples)
- ☆ dunite unit
- ○ cumulate unit
- △ gabbro unit

Fig. 58   Relationship between Pd and Ni/MgO in rock samples

Cumulate rocks

PGE levels are relatively enriched in several analysed samples of cumulate rocks (table 2) reaching a maximum of 200ppb Pd and 100ppb Pt in a sample of pyroxenite from near Sobul. The proportions of the PGE are very similar to those typical of the Cliff type of mineralisation but their behaviour in these rocks appears different from that in the harzburgite and dunite units. In the cumulate rocks there is no indication of a correlation of PGE with As or Ni and only a slight indication of a correlation with Cu. On the other hand there may be some correlation of PGE with Cr, at least in the Ordale area from where all but one of the samples were obtained (Figure 52).

MINERALOGICAL STUDIES

In order to facilitate the interpretation of the controls of PGE mineralisation the mineralogy of a series of samples, mainly from the Cliff area, was examined in detail with the aid of an electron microprobe.

Analytical method

Chemical analyses of minerals were carried out using a Cambridge Instruments Geoscan electron probe X-ray microanalyser fitted with a Link Systems energy-dispersive X-ray spectrometer (EDS). The electron beam was focused to a diameter of between 5 and 10 microns and an accelerating voltage of 15kV and a specimen current of around 5×10^{-9} amps were used throughout.

The EDS analyser system can detect all elements of atomic number 11 (Na) and greater, but the detection limits depend on whether K, L or M lines are used and on any spectral interference that may exist. All analyses were made within the energy window 0-10KeV, hence K lines were used for atomic numbers 11-30, L lines for atomic numbers 31-70 and M lines for atomic numbers greater than 70. Detection limits for K lines vary from 0.1% up to 0.3% where there are interferences and for L and M lines from 0.3 to 0.5% and 0.6% to 1.0% respectively. The precision of analyses is largely a function of the counting statistics and hence varies with the concentration of an element. Thus for elements with concentration ranges above 5-10% it is better than 2%, for concentrations down to 2% better than 5% and increasing, as the detection limit is approached, to greater than 10%.

The quality of the results was affected by some additional factors which are difficult to quantify. The analytical work was carried out shortly after the instrument had been moved from London to Keyworth and some calibration problems were encountered due to instrument instability and changes in the laboratory environment. The general effect of this was to cause small systematic errors for some elements or groups of elements. A small calibration problem exists for the use of M lines and there is a slight tendency to overestimate Pt, Ir and Os in the analyses quoted. Nevertheless it is considered that the relative error never exceeds 10% and generally is much lower.

Platinum Group minerals (PGM)

PGM have been located, identified and analysed in 6 polished sections from rock samples with significant PGE contents. Other sections from rocks with similar PGE contents contained no visible PGM, probably a reflection of the heterogeneity of distribution of the minerals. Probe analyses of the PGM are

given in appendices 1, 2 and 3. The occurrences of PGM in these six samples are described below.

1. PGR 6007 (pit B). This sample of a chromite-rich dunite contains ca. 35% chromite, surrounded by chlorite alteration haloes, and interstitial serpentine. There are also late cross-cutting carbonate and serpentine veins. The PGM generally occur as clusters of small grains generally 5-10 microns in size in the chlorite haloes and to a lesser extent in the blackened altered rims of the chromite (plate 1). They comprise in rough order of abundance sperrylite ($PtAs_2$), stibiopalladinite (Pd_3Sb), hollingworthite (RhAsS) and two mixed Ir, Rh, Ru, S, As phases (appendix 3). In some places they occur intergrown with pentlandite ($(Ni, Fe)_9S_8$) and orcellite (Ni_2As) and in one place with a Ni-rich carbonate.

2. PGR 6012 (pit B). This sample is of chromite-rich dunite with about 40% chromite, surrounded by chlorite and with interstitial serpentine intergrown with reevsite (Ni-Fe hydrated carbonate). The PGM comprise mostly grains of stibiopalladinite and sperrylite up to 20 microns in diameter disseminated in the chlorite haloes often close to pentlandite and orcellite grains.

3. PGR 6027 (pits D/E). This chromitite sample with about 90% chromite and interstitial chlorite is veined by magnesite, chlorite and magnetite and also by separate veins of zaratite (hydrous nickel carbonate). All the PGM occur as small grains up to 10 microns in diameter close to the chlorite-carbonate-magnetite veins, within magnetite rims on altered chromite and in the chlorite haloes surrounding the chromite The minerals comprise two different Pd, Sb, Te phases, sperrylite, laurite (RuS_2) and an Ir, Rh, Pt, Ru, As, S phase.

4. PGR 6029 (pit D). This sample is of partially serpentinised dunite containing 1-2% chromite as scattered grains. The rock is made up mostly of type 1 serpentine with cross-cutting veins and fracture zones with coarser serpentine, carbonate, pentlandite, orcellite and native copper. Close to these veins some chromites are partly replaced by pentlandite. The PGM generally occur with orcellite and pentlandite in altered chlorite haloes around chromites close to the veins. Sperrylite is the most conspicuous PGM and it contains inclusions of native Cu and orcellite.

5. PGR 6033B (pits D/E). This sample of extremely recrystallised serpentinite with 1-2% chromite contains abundant thin magnetite veins. The PGM in this specimen comprise stibiopalladinite, sperrylite, hollingworthite and laurite, with sperrylite grains up to 100 microns in size, in the chlorite halo of a chromite included in a magnetite vein (plate 1) and also in finer grains (up to 10 microns) in magnetite veins not adjacent to chromite.

6. PGR 6035 (pits D/E). This sample consists of coarse-grained recrystallised serpentinite containing around 1% chromite cut by numerous veins of magnesite, magnetite, serpentine and chlorite. Chromite shows some replacement by pentlandite in the veins. The PGM occur both in clusters of fine grains associated with pentlandite close to altered chromites and as fine grains in the carbonate veins away from the chromite.

Compositions of PGM

Sperrylite appears to be the most abundant PGM, but this is probably partly due to its occurrence in larger grains, often 10-20 microns and up to 100 microns, than other PGM. Compositions of sperrylite from all 6 of the above samples are

PLATE 1

Photo 1: PGR 6033B.

Large sperrylite grains in magnetite vein cutting chlorite halo around chromite grain in dunite.

Sp = Sperrylite; Mt = Magnetite; Chl = Chlorite; Serp = Serpentine; Or = Orcellite: Cr = Chromite.

Scale bar = 100 microns.

Photo 2: PGR 6033B.

Close up of sperrylite grain showing alteration along cleavage planes.

Scale bar = 50 microns.

Photo 3: PGR 6007.

Pentlandite, sperrylite and other PGM in chlorite surrounding chromite in chromite-rich dunite.

Pe = Pentlandite.

Scale bar = 50 microns

Photo 4: PGR 6007.

Close up showing fine grained PGM in chlorite.

St = Stibiopalladinite; La = Laurite; Ho = Hollingworthite.

Scale bar = 20 microns

PLATE 1

1

2

3
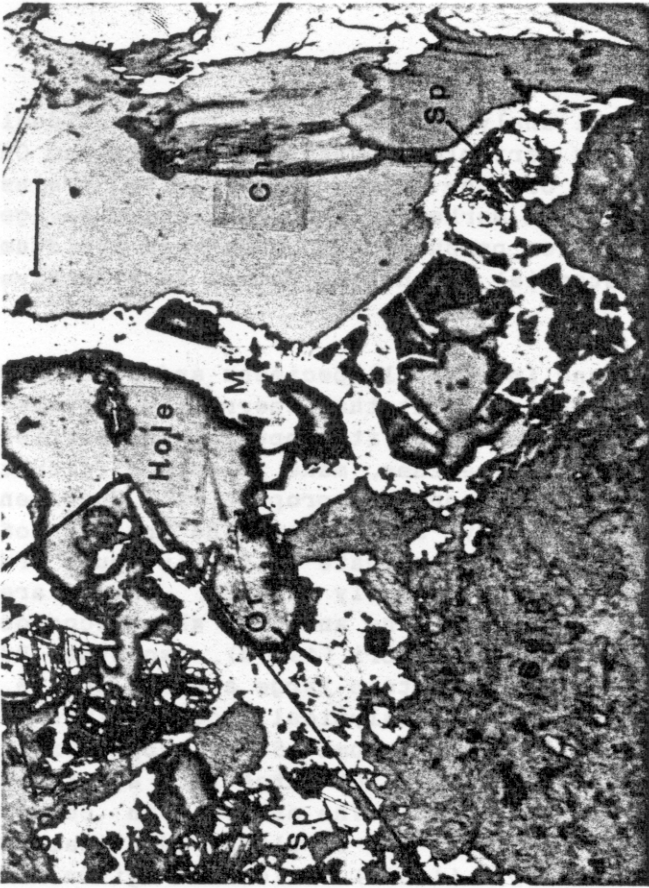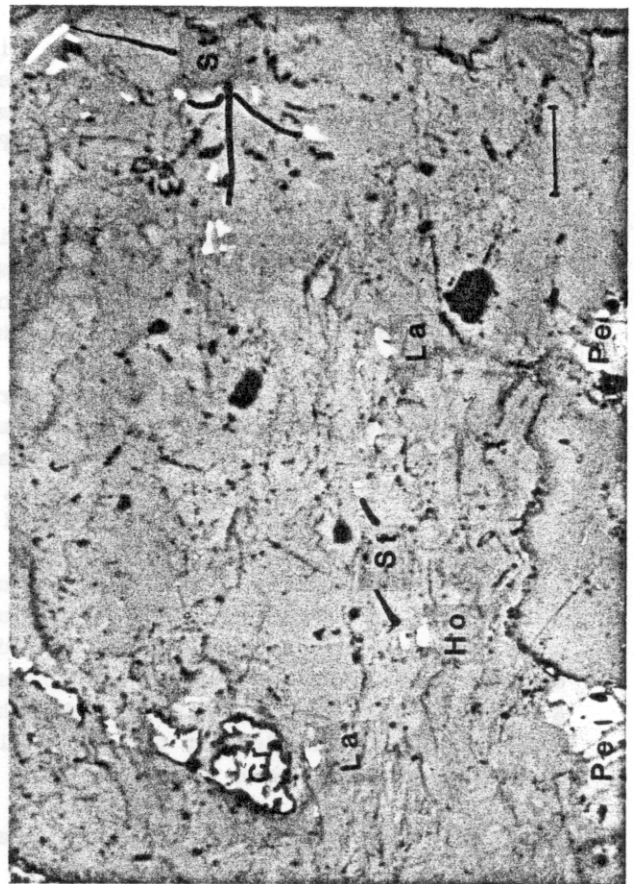
4

given in appendix 1. It is apparent that all analyses are close to the ideal formula composition ($PtAs_2$) with small but variable amounts of Ir, Rh, Fe and Cu replacing Pt and S and Sb replacing As. Some of the larger sperrylite grains have a well developed cleavage, sometimes with marked alteration along cleavage planes (plate 1). In some grains the alteration produces a very Pt-rich residuum by removal of As, while in others substantial amounts of Fe and less Cu have been added.

Stibiopalladinite ($Pd_{3+x}Sb_{2-x}$) has been found in several specimens and according to the bulk chemical analyses should be more abundant than sperrylite. However its smaller size, generally less than 10 microns, and its optical properties which are very similar to those of the nickel arsenides, make it more difficult to recognise than other PGM which have distinctive optical properties. Specimen PGR 6012 contains stibiopalladinaite rimmed by sperrylite. The analyses of stibiopalladinite given in appendix 2 (columns 1-4) indicate a fairly pure Pd and Sb mineral but with consistently approximately 4% Cu. There are substantially greater than 5 cations per 2 As+Sb+S in the analyses which accords with the analyses and formula $Pd_{3+x}Sb_{2-x}$ given by Cabri (1981a). Two other Pd minerals have been found in specimen PGR 6027 that contain large amounts of Te. Because of inadequate standardisation for Te the analytical figures given in appendix 2 are by difference. The analysis forming column 5 of appendix 2 corresponds to a formula of Pd_8NiTe_3Sb which does not match with any known mineral but may be related to telluropalladinite Pd_9Te_4. The analysis in column 6 of appendix 2 corresponds to a formula of Pd_2SbTe and is almost identical to the unnamed mineral from China UN 1974-6 of Cabri (1981b) which is given in column 7 of appendix 2 for comparison.

Laurite is thought to be widely present but always occurs in small grains typically less than 5 microns which is smaller than the beam of the electron microprobe. Consequently analyses often contain some elements present in the matrix eg Si and Mg. Analyses are given in appendix 3, columns 1 and 2. The analysis in column 2 has had elements from the matrix removed and has been recalculated to 100%. Compositions are close to the ideal formula RuS_2 with small but varying amounts of other PGE present.

Hollingworthite has been found in several specimens but always as very small grains. Analyses corrected for the matrix component and normalised are given in appendix 3, columns 3 to 5. The compositions are close to the ideal formula of RhAsS with only small amounts of other PGE and base metals.

Two analyses were obtained that correspond to the general formula (Rh,Ir)AsS but with varying ratios of Rh/Ir (appendix 3, columns 6 and 7). These grains could be intergrowths of hollingworthite and irarsite (IrAsS), a mineral reported from Unst by Prichard et al. (1985), but examination by optical microscopy and back-scattered electron microscopy (resolution 1 micron) did not detect evidence of any intergrowth. The mineral is therfore thought to be a single phase intermediate member of the hollingworthite-irarsite series, similar to those described by Stumpfl (1972). The analysis in appendix 3 column 8 gives an even more complex composition which could be interpreted as an intergrowth of laurite either with the (Rh,Ir)AsS phase or with hollingworth and irarsite or alternatively as a complex single phase. The latter possibility is perhaps the least likely considering the general tendency for Ru and Rh to occur in separate minerals in the other samples.

A conspicuous feature of the PGM are their generally simple pure compositions,

usually containing only PGE in abundance. This indicates relatively low temperatures of equilibration although the PGE could have originally been contained in more complex higher temperature phases, of which (Rh, Ir) AsS might be an example. Stability fields of the various PGM are poorly known so that the physico-chemical conditions of their deposition must be deduced from coexisting mineral assemblages.

Ni-Fe sulphides and arsenides

(Ni, Fe) sulphides, Ni sulphides and Ni arsenides occur widely in small amounts in rocks with or without PGM. Pentlandite (Ni, Fe)$_9$S$_8$ is the predominant mineral, occurring in grains usually hundreds of microns, and up to 1 mm, in size. In dunites and serpentinites it generally occurs in veins and fractures in association with various combinations of coarse serpentine, chlorite, carbonate and magnetite. In chromitites it occurs most commonly in the chlorite haloes or in the Fe-rich rims of altered chromite grains but there is still a general spatial association with veining. It also occurs in fractures within chromite and as scattered grains in interstitial serpentine. In a few samples textures suggest that pentlandite is replacing chromite.

The Ni sulphides and arsenides tend to occur as smaller grains up to a few tens of microns in size. They occur as scattered grains in the serpentine in dunites or serpentinites, in chlorite haloes in chromitite and in association with pentlandite either close to, in contact with or included within the latter. There is no distinct lamellar form or prefered orientation of the included blebs within pentlandite which would suggest an exsolution relationship between the minerals. The mode of occurrence of these minerals is generally similar to the PGM which are often found close to and in some places intergrown with the sulphides and arsenides suggesting that they are products of the same phase of mineralisation.

Compositions of Ni minerals

A selection of analyses of (Ni, Fe) sulphides which are found in many samples is given in appendix 4. The analyses correspond fairly closely to the ideal pentlandite formula of (Ni, Fe)$_9$S$_8$, with a Co content of around 1% and in one case (column 4) a significant Cu content. No correlation between pentlandite composition and either chromite or PGE content of the sample is evident.

Two varieties of Ni sulphide have been found and analyses of these are given in appendix 5. The analyses in columns 1 and 2 correspond with the formula of godlevskite (Ni$_7$S$_6$) and contain small amounts of Fe. The analyses in columns 3 to 5 correspond with the composition of heazelwoodite (Ni$_3$S$_2$). These also contain small amounts of Fe and in two cases As in addition. A few sulphide grains have been found to contain large amounts of Co (column 6), the analysis of which would correspond to a formula (Ni, Co)$_7$S$_6$, a cobaltian godlevskite.

Nickel arsenides are present in many of the samples and analyses are given in appendix 6. Most of the mineral grains correspond to compositions between Ni$_4$As$_2$ and Ni$_3$As$_2$ and represent orcellite. The general formula for orcellite is Ni$_{3-x}$As$_2$ but a recent study by Lorand and Pinet (1984) showed the mineral to have compositions ranging from Ni$_{4.2}$As$_2$ to Ni$_{3.5}$As$_2$. Some rocks also contain another nickel arsenide (column 7) with a composition which corresponds to maucherite (Ni$_3$As). All the analysed arsenides are relatively pure with only minor amounts of Fe, S and Sb.

The minerals orcellite, maucherite, heazelwoodite and godlevskite are typically if not exclusively associated with the serpentinisation of peridotites (Craig and Scott 1974) and therefore are formed at temperatures lower than the magmatic range. Pentlandite is thought to be stable up to 610°C (Kullerud 1963) and godlevskite and heazelwoodite are stable up to similar temperatures. Furthermore the association pentlandite-godlevskite-heazelwoodite was found to be stable only at temperatures below 476°C in experiments on the Ni-Fe-S system by Craig et al (1968). Lorand and Pinet (1984) concluded that orcellite is formed at temperatures in the range 400-450°C. This evidence therfore suggests that the sulphide/arsenide assemblages observed in this study formed at temperatures less than 500°C. The close association and textural relationships of PGM with the nickel sulphides/arsenides in the Cliff area indicate that the PGE mineralisation there was deposited at similar temperatures, well outside the range of magmatic conditions.

Chromite

The chemistry of chromite from Unst has been extensively studied by previous workers (Brzozowski 1977, Prichard 1982) especially in terms of variation with host rock type and textural type. In this study analyses were obtained to show chemical changes of chromite during alteration and the formation of the dark rims which are widely present. The chemical analyses in appendix 7 columns 1 to 4 show the differences in composition between the reddish brown centres of large grains and the black edges. Columns 5 and 6 in appendix 7 show the difference in composition between smaller fresh brown chromite grains and altered black grains in a harzburgite sample.

There are clearly large changes in chemistry associated with the partial or complete alteration of chromite during serpentinisation or hydrothermal alteration. In particular there is a marked tendency for Al and Mg to be removed from the margins of chromite grains with a corresponding increase in Fe, especially as Fe^{3+}. This leads to the formation of the ill-defined ferro, ferri or ferrit-chromite. In addition there are overgrowths of magnetite on some chromites which are particularly conspicuous in some PGE-rich samples.

Silicate minerals

A limited amount of work has been done on the chemistry of the silicate minerals associated with chromite and PGM but as variation appears very complex only general conclusions can be made.

The composition of chlorites forming haloes around chromite is generally similar except for Cr content which varies from < 0.2% to 6% Cr_2O_3 as shown in appendix 8. Little variation is apparent within a specimen and there is no correlation between chlorite composition and bulk Cr or PGE levels.

Serpentine minerals show a much greater complexity of variation in composition and further study is required to evaluate this satisfactorily. This is of importance as chemical reactions during the various phases of serpentinisation must play a part in the redistribution, transportation and deposition of the Ni with which the PGE mineralisation is associated. In general serpentines which crystallised as a result of the first phase of serpentinisation tend to have Ni contents very similar to the olivine from which it was formed ie 0.25-0.5% NiO and to be similar in various rock types as shown in appendix 9 columns 1 to 4. Serpentines originating in the second phase of serpentinisation are pale coloured with Ni contents below the detection limit of the analytical method

(0.2% NiO) as shown in appendix 9 column 5. In contrast some serpentines that are texturally similar to typical phase 1 serpentines are strongly coloured with anomalously high Ni contents of around 2% NiO (appendix 9 columns 6 and 7). One specimen (appendix 9 column 8) contains what appears to be an almost pure Ni serpentine. These Ni-rich serpentines are often associated with Ni-rich carbonates and may be due to a later phase of Ni enrichment that does not greatly affect the textural appearance of the serpentine. Some Ni-rich grains may represent a very fine-grained intergrowth of Ni carbonate and serpentine. In some rocks there is a close association between the Ni-rich serpentine or carbonate/serpentine and PGM and it is possible that some anomalous panned overburden samples may contain such grains which would account for the correlation between PGE and Ni/MgO in that data set.

Carbonates and other minerals

Carbonate minerals are found in most rocks but their abundance varies from < 1% in the freshest rocks to > 50% in the talc carbonate rocks. Magnesite is much the most common carbonate mineral in the talc carbonate rocks, replacing serpentine in chromite-rich rocks and in most of the veins. It contains small amounts of Ca, Fe and Mn in some specimens.

Several Ni-rich carbonate minerals have been found mostly in small amounts. In one PGE-rich sample the presence of a member of the pyroaurite group, probably reevesite ($Ni_{3.6}Fe_4(CO_3)_3.12H_2O$), has been confirmed by X-ray diffraction finely intergrown with serpentine (chrysotile). Other unidentified Ni-rich carbonate minerals have also been found. Zaratite ($Ni_3(CO_3)(OH)_4.4H_2O$) occurs as late cross-cutting veins.

Some grains of Ni arsenides show alteration to anabergite ($(Ni,Co)_3(AsO_4)_2.8H_2O$) and some pentlandites are altered to unidentified (Ni,Fe) sulphates. Alteration of magnetite to hematite and goethite is present in some specimens but it is not extensive. These minerals probably originated by weathering processes.

GENESIS OF PGE MINERALISATION

It is evident from analyses of drainage heavy mineral concentrates that, overall, there is an enrichment in Ir and other PGE in the basic-ultrabasic rocks of Unst relative to other areas of comparable geology which have been studied in Britain (Lizard, Girvan-Ballantrae, Aberdeenshire Younger Basics). The reason for such differences is not understood.

The first of the assemblages of PGE that have been recognised on Unst is characterised by a predominance of Ru, with subordinate Os and Ir, minor Rh and Pt but little or no Pd. This type occurs in some samples of background harzburgite and is represented by the majority of overburden samples from the harzburgite unit. Locally there are enrichments of PGM to produce mineralisation of the type found near Harold's Quarry. The relative proportions of the individual PGE within this type of mineralisation and also background samples of harzburgite normalised relative to the PGE proportions in chondrites are illustrated diagramatically in figure 59. These patterns are very similar to PGE distribution patterns of ophiolitic chromitites from Oman, Greece, Turkey, Northern California and New Caledonia (Page et al., 1982). Data from Oman are also plotted for comparison in figure 59. Prichard et al. (1985) reported the presence of sulphides and alloy minerals of Ru, Ir and Os within chromite grains, but not their silicate haloes, in chromitite samples from the Harold's Grave

Fig. 59   Chondrite - normalised PGE ratios in Unst rocks

Labels within figure: Unst background, Cliff type, Oman, Harold's Quarry type, Sudbury, Merensky Reef

Y-axis: PGE in rock / PGE in Chondrite

X-axis: Element (Os, Ir, Ru, Rh, Pt, Pd)
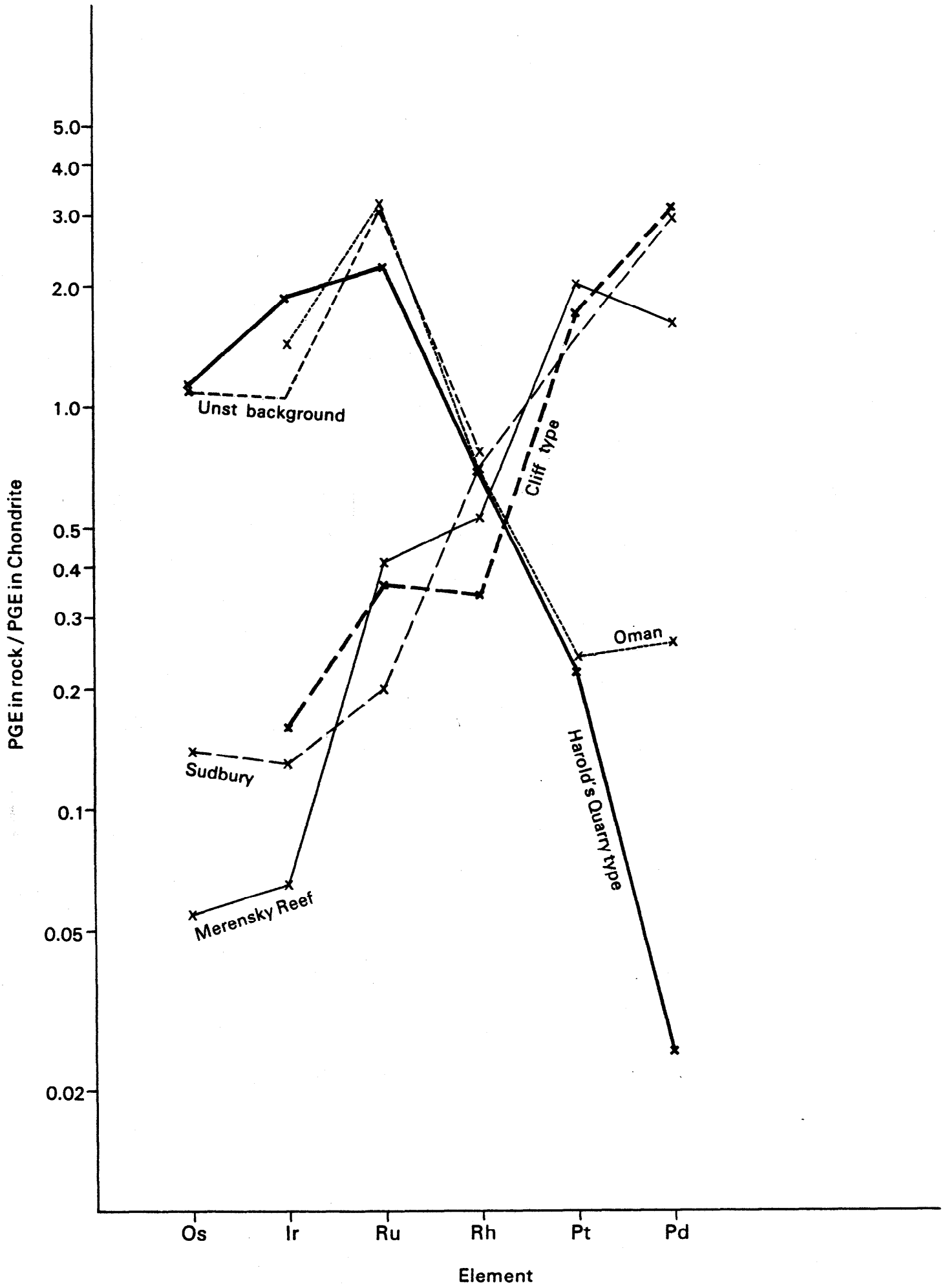
area. Such minerals have also been observed in other ophiolitic complexes eg Southwest Oregon (Stockman and Hlava, 1984), Troodos (Constantinides et al., 1979).

The second PGE assemblage, which is typical of mineralisation at Cliff but widely distributed throughout the complex, is dominanted by Pd and Pt with minor Rh, Ru, Ir and Os. A plot of the average PGE proportions of 16 mineralised samples from Cliff and elswhere relative to chrondrite PGE proportions gives a line with a steep positive slope in Figure 59, markedly different from the distribution pattern for the harzburgite background and Harold's Grave type mineralisation. The Cliff type PGE distribution pattern is very similar to those present in the Cu-Ni deposits of the Sudbury complex and the sulphide-rich rocks of the Merensky Reef in the Bushveld complex. The PGE proportions of mineralised layers within the Stillwater layered intrusion are also similar, though compared with the Merensky Reef they are richer in Pd. The compositonal field of Stillwater mineralisation (Lee, 1983) is shown in the Pd-Rh-Pt triangular diagram in figure 60 upon which the composition of all Unst samples with PGE levels significantly above detection limits are superimposed. The bulk of the Unst samples plot within the Stillwater field though they are relatively impoverished in Rh. In contrast the Harold's Grave mineralisation samples plot well away from the Stillwater field.

The close association of PGM in the Cliff mineralisation with Ni sulphides and arsenides which crystallised at temperatures of less than 500°C and the frequent association of PGM with veining indicate that this second type of mineralisation is hydrothermal in origin, most likely associated with the second stage of serpentinisation. In addition to PGE the hydrothermal solutions carried Ni, Cu, S, As. Sb and Te and there is also evidence of an association with carbon. The association with As, Sb , Te and carbon suggests similarity with the chemistry of Au transport and indeed Au is a minor component of the Cliff mineralisation reaching levels of 5ppm in some of the most richly mineralised samples. The physico-chemical controls of the solution and transport of the precious metals are as yet poorly understood.

There are very few documented occurrences of PGE mineralisation which have been ascribed to hydrothermal proccesses. The New Rambler deposit, located in the Medicine Bow mountains of Wyoming, comprising vein-type Cu sulphide rich in Pd and Pt, has been interpreted as the product of hydrothermal leaching of metagabbroic rocks and redeposition along shear zones (McCallum et al 1976). In this deposit thermochemical data on the sulphide assemblages present suggest temperatures of the mineralisation somewhat below 335°C. Similarly Pd-Pt enriched mineralisation has been described from a hydrothermal Cu deposit near Messina in South Africa (Mihalik et al., 1974). An association of the mineralisation with propylitic alteration of the country rocks is clear and the coexisting sulphide assemblage suggests deposition in the range 270-400°C. These and other occurrences demonstrate the operation of relatively low temperature transport and deposition of PGE. Stumpfl (1962) first drew attention to the possible role of late and post-magmatic fluids in this respect, a process increasingly recognised by several authors (eg Piispanen and Tarkian, 1985), though still imperfectly understood.

Many chromitite samples contain background levels of PGE but nearly all of the most PGE-rich samples are chromitite or chromite-rich dunite. There is also a close spatial association between PGM and the margins or haloes of chromite grains. This may be the result of steep chemical gradients which would exist at
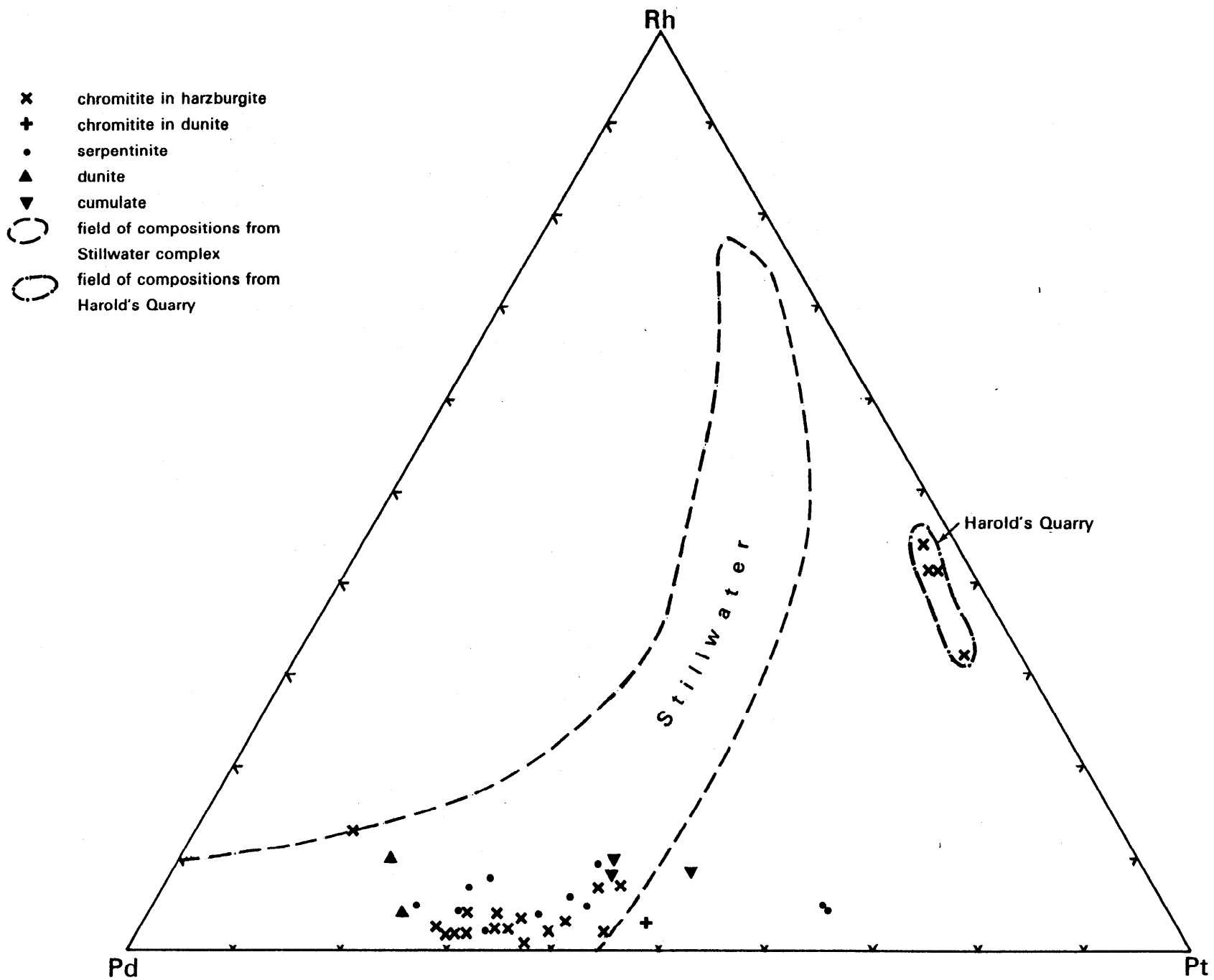
Fig. 60   Variation of Pd-Rh-Pt in rock samples

Legend:
- ✗ chromitite in harzburgite
- ✚ chromitite in dunite
- • serpentinite
- ▲ dunite
- ▼ cumulate
- ⌒ field of compositions from Stillwater complex
- ⌒ field of compositions from Harold's Quarry

Rh

Pd

Pt

Harold's Quarry

Stillwater

the sites of chromite alteration which in turn could lead to preferential deposition of PGM. This process would only occur where suitable passageways for fluid movement existed within close proximity to the chromite mineralisation.

On a larger scale steeply inclined faults appear to exert some control on the incidence of Ni, Cu, As and associated PGE mineralisation. The mineralised area at Cliff is the focus of several groups of faults and associated hyrothermal alteration. Evidence from the secondary environment samples suggests that the major N-S fault zone which is traceable for at least 7 km cutting across harzburgite, dunite and possibly cumulate units is an important locus of mineralisation.

The source of PGE enrichment in samples of cumulate rocks is more uncertain. The PGE proportions are very similar to those found at Cliff, and pentlandite, godlevskite, heazelwoodite and maucherite have been found in the interstitial serpentine in pyroxenite samples. This suggests the mineralisation in the cumulate rocks crystallised at the same time as the Cliff type mineralisation and that faulting may have exerted some control on the sites of mineral deposition. Richer grades of PGE mineralisation could therefore occur in fault zones, which, because of absence of exposure, were not sampled. Insufficient samples have been collected to establish whether there is any general PGE enrichment in the cumulate complex, but the limited data currently available are consistent with such a possibility. This enrichment could be of magmatic origin since a Pd-Pt enriched PGE distribution pattern has been observed in the mafic and ultramafic cumulate units of the Polar Urals ophiolite (Page et al 1983) and in the Thetford Mines ophiolite of Quebec (Oshin and Crockett 1982). Since Unst appears to be regionally enriched in PGE the possibility of a relatively large tonnage PGE concentration, analagous to those found in layered intrusive complexes, exists in the cumulate complex.

RECOMMENDATIONS FOR FUTURE WORK

Continuous sections through the PGE mineralised zone at Cliff and other localities from angled diamond drill holes would be of great benefit as in no area is there adequate exposure of the mineralisation. At present it is impossible to assess the form, thickness and length of mineralised material and therefore its economic significance.

The drainage and overburden sampling procedures utilised in this study have been effective in detecting indications of mineralisation concealed beneath overburden. The amount of ground covered in the reconnaissance overburden samples is very small and more sampling is needed to cover the complex, particularly where important fault lines or other zones with intense hydrothermal activity are suspected. Linear dunitic zones within the harzburgite unit are easily traced with overburden samples and where these are extensively faulted by subparallel faults, as in the Cliff area, they could represent important exploration targets. There is clear evidence for the occurrence of chromitite in the upper reaches of Mill Burn and further occurrences may be located by overburden sampling.

There is evidence from the rock, overburden and drainage sampling that pathfinders could be useful in the detection of PGE mineralisation. These are of two types, chemical and mineralogical. Consideration of the chemistry of the most mineralised rock samples indicates that PGE enrichment of the Cliff type is accompanied by elevation of Ni, Cu and As. A triangular plot of As-Cu-Ni/10 in

102
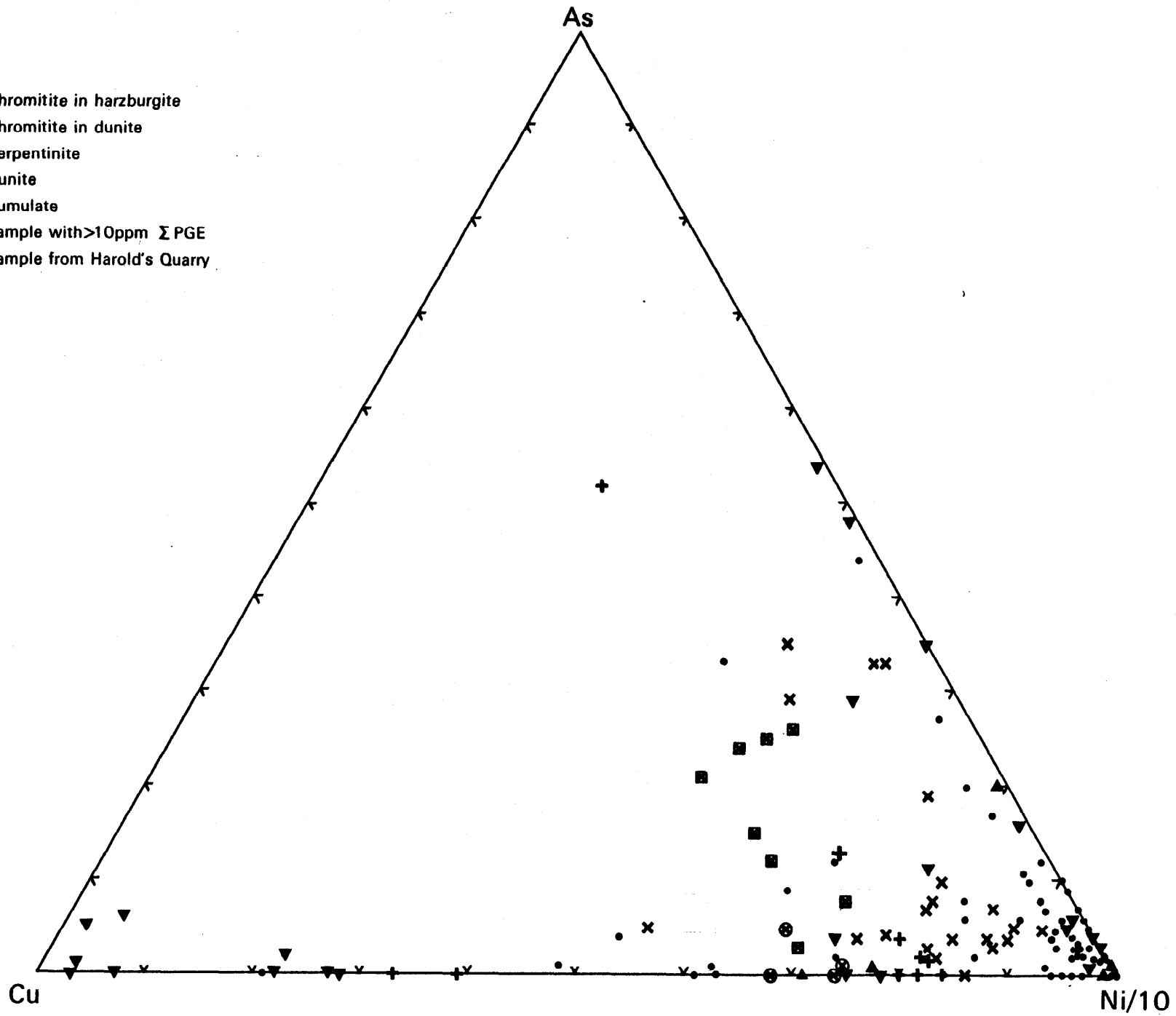
Fig. 61   Variation of Cu-As-Ni in rock samples

figure 61 shows the most PGE-rich samples to be also enriched about equally in Cu and As as well as Ni. Samples with relative enrichment only in either Cu or As are not as highly enriched in PGE. Overburden or drainage samples with relative enrichment in these three elements may therefore indicate anomalous PGE levels. This is confirmed in the existing secondary environment data as the highest PGE level in drainage is derived from the zone which also shows anomalous levels of Ni, As and Cu. In addition PGE enrichment in overburden samples show a clear correlation with relative Ni enhancement and with some Cu anomalies. Grains of the deep green Ni-rich serpentine or serpentine/carbonate are possible mineralogical pathfinders for PGM which could be readily identified by binocular microscopic examination of the panned overburden samples. The presence of coarse and composite chromite grains or the distinctive purple Cr-rich chlorite kammererite is also indicative of chromitite or chromite-rich dunite.

A detailed structural analysis of the complex is required to locate and categorise the main fault zones and areas of hyrothermal alteration. This can be carried out, as in the Cliff area, by a combination of photogeological interpretation, ground observation and overburden sampling.

Insufficient work has been done on the cumulate complex to establish if the observed PGE enrichments are more widespread and whether local concentrations of possible magmatic origin exist. In order to achieve this, systematic rock sampling together with a series of overburden traverses at right angles to the strike of layering will be required. Similar work should also be carried out in the gabbro unit as magmatic concentrations may occur higher up the sequence.

ACKNOWLEDGEMENTS

REFERENCES

Amin, M.S. 1954. Notes on the ultrabasic body of Unst, Shetland Islands. Geol. Mag., vol. 91, pp. 399-406.

Anonymous, 1972. Penrose field conference on ophiolites. Geotimes, vol 17, pp24-25.

Brzozowski, T.J. 1977. VLF elctromagnetic surveys and associated studies in North Dartmoor and Unst. Ph.D. Thesis, Chelsea College (Unpublished).

Cabri, L.J. 1981a. The platinum-group minerals. In Cabri, L.J. (ed.) Platinum-group elements: mineralogy, geology, recovery. CIM special volume 23, Can. Institute for Mining and Metallurgy.

Cabri, L.J. 1981b. Unnamed platinum-group minerals. In Cabri, L.J. (ed.) Platinum- group elements: mineralogy, geology, recovery. CIM special volume 23, Can. Institute for Mining and metallurgy.

Constantinides, C.C., Kingston, G.A. and Fisher, P.C. 1979. The occurrence of platinum group minerals in the chromitites of the Kokkinorotsos chrome mine, Cyprus. In Panayiotou (ed.), Ophiolites. Proc. Int. Ophiolite Symp. (1979). Cyprus Geol. Surv. Dep., Ministry of Agricultue and Natural Resources, Nicosia, Cyprus.

Craig, J.R., Naldrett, A.J. and Kullerud, G. 1968. The Fe-Ni-S system: $400°C$ isothermal diagram. Carnegie Inst. Wash. Year Book 66, pp440-441

Craig, J.R. and Scott, S.D. 1974. Sulphide phase equilibria. In Ribbe (ed.) Sulphide Mineralogy. Mineralogical Society of America Short Course Notes.

Flinn, D. 1958. On the nappe structure of north-east Shetland. Q. Jnl. Geol. Soc. vol. 114, pp107-136.

Flinn, D. 1970. Some aspects of the geochemistry of the metamorphic rocks of Unst and Fetlar, Shetland. Proc. Geol. Ass., vol. 81, pp509-527

Flinn, D., May, F., Roberts, J.L. and Treagus, J.E. 1972. A revision of the stratigraphic succession of the East Mainland of Shetland. Scott. J. Geol., vol. 4, pp335-343.

Flinn, D. and Pringle, I.R. 1976. Age of migmatisation in the Dalradian of Shetland. Nature Phs. Sci., vol. 259, pp299-300.

Garson, M. S. and Plant, J. 1973. Alpine type ultramafic rocks and episodic mountain building in the Scottish Highlands. Nature Phs. Sci., vol. 242, pp34-38.

Haines, J and Robert, R. V. D. 1982. The determination by atomic-absorption spectrophotometry using electrothermal atomisation of platinum, palladium, rhodium, ruthenium and iridium. Mintek report no. M34.

Heddle, M. F. 1879a. The geognosy and mineralogy of Scotland, Isle of Unst. Min. Mag., vol. 2, pp12-35.

Heddle, M. F. 1879b. A brief description of the maps of Shetland. Min. Mag., vol. 2, pp253-285.

Hitchen, C. S. 1929. Unst and its chromite deposits. Min. Mag., vol. 40, pp18-24.

Hoffman, E. L., Naldrett, A. J., Van Loon, J. C. and Hancock, R. G. V. 1978. The determination of all the platinum group elements in rocks and ore by neutron activation analysis after preconcentration by a nickel sulphide fire-assay technique on large samples. Analytica Chimica Acta, vol. 102, pp157-166.

Johnson, C. E., Smith, C. G. and Fortey, N. J. 1980. Geophysical investigations of chromite- bearing ultrabasic rocks in the Baltasound-Hagdale area, Unst, Shetland islands. Mineral Reconnaissance Programme Rep. Inst. Geol. Sci., No. 35.

Kullerud, G. 1963. The Fe-Ni-S system. Carnegie Inst. Wash. Year Book 62 pp175-189.

Leake, R. C. and Smith, R. T., 1975. A comparison of stream sediment sampling methods in parts of Great Britain. In Elliot I. L. and Fletcher, W. K. (Editors), Geochemical Exploration 1974, pp579-594. Elsevier, Amsterdam.

Lee, C. A., 1983. Trace and platinum-group element geochemistry and the development of the Merensky Unit of the Western Bushweld Complex. Mineraliun Deposita, Vol. 18, pp.173-190

Longlands, J. G. 1974. Geochemical and geological prospecting for Ni, Cu, Mo, Pb - Unst, Fetlar, North Roe. Unpublished report of Noranda Exploration (UK) Ltd.

Lorand, J. P. and Pinet, M. 1984. L'orcelite des peridotites de Beni Bousera (Maroc), Ronda (Espagne), Table Mountain et Blow-Me-Down Mountain (Terre-Neuve) et du Pinde Septentrional (Grece). Canadian Mineralogist. vol. 22, pp553-560.

McCallum, M.E., Loucks, R.R., Carlson, R.R., Cooley, E.F. and Doerge, T.A. 1976. Platinum metals associated with hyrothermal copper ores of the New Rambler Mine, Medicine Bow Mountains, Wyoming. Econ. Geol., vol.71, pp1429-1450.

Mihalik, P., Jacobsen, J.B.E. and Hiemstra, S.A. 1974. Platinum minerals from a hydrothermal environment. Econ. Geol., vol. 69, pp257-262.

Miller, J.A. and Flinn, D. 1966. A survey of age relations of Shetland rocks. Geol. J., vol. 5, pp95-116.

Oshin, I.O. and Crocket, J.H. 1982. Noble metals in Thetford mines ophiolites, Quebec, Canada. Part 1: Distribution of gold, iridium, platinum, palladium in the ultramafic and gabbroic rocks. Econ. Geol., vol. 77, pp1556-1570.

Page, N.J., Aruscavage, P.J. and Haffty, J. 1983. Platinum-group elements in rocks from the Voikar-Syninsky ophiolite complex, Polar Urals, U.S.S.R. Mineralium Deposita, vol. 18, pp 443-455.

Page, N.J., Cassard, D. and Haffty, J. 1982. Palladium, platinum, rhodium and iridium in chromitites from the Massif du Sud and Tiebaghi Massif, New Caledonia. Econ. Geol., vol.77, pp1571-1577.

Phillips, F.C. 1927. The serpentines and associated rocks and minerals of the Shetland Islands. Q. J. Geol. Soc., vol. 83, pp 622-651.

Piispanen, R. and Tarkian, M. 1984. Cu-Ni-PGE mineralisation at Rometolvas, Koillismaa layered igneous compplex, Finland. Mineralium Deposita, Vol. 19, pp 105-111.

Prichard, H.M. 1982. The chromite of the Shetland ophiolite: a re-appraisal in the light of new theory and techniques. A report for the Commission of European Communities. Unpublished.

Prichard, H.M., Potts, P.J. and Neary, C.R. 1981. Platinum group minerals in the Shetland ophiolite complex. Trans. Instn. Min. Metall., vol 90, ppB186-188.

Prichard, H.M., Neary, C.R. and Potts, P.J. 1985. Distribution and genesis of platinum group minerals in the Shetland ophiolite complex. Abstract of paper presented at conference" Metallogeny of Basic and Ultrabasic Rocks", Edinburgh April 1985.

Read, H.H. 1934. The metamorphic geology of Unst, in the Shetland Islands. Proc. Geol. Ass., vol. 47, pp283-293.

Rivington, J. B. 1953. Recent chromite exploration in Shetland. Min. Mag. Lond., vol 89, pp327-337.

Robert, R. V. D., Van Wyck, E., and Palmer, R. 1971. Concentration of the noble metals by a fire assay technique using nickel sulphide as the collector. National Institute for Metallurgy report no. 1371.

Robert, R. V. D., Van Wyck, E., and Ellis, P. J. 1977. An examination of fire-assay techniques as applied to chromite-bearing materials. National Institute for Metallurgy report no. 1905.

Stockman, H. W. and Hlava, P. F. 1984. Platinum-group minerals in alpine chromitites from southwestern Oregon. Econ Geol., vol. 79. pp 491-508.

Stumpfl, E. F. 1962. Some aspects of the genesis of platinum deposits. Econ. Geol., vol. 57, pp619-623.

Stumpfl, E. F. 1972. Compositional variations in the hollingworthite-irarsite group. Neues Jahrbuch Mineralogie. Monatshefte 9, pp406-415.

APPENDIX 1

Compositions of sperrylite.

	1	2	3	4	5	6
Ni	3.65	0.00	0.00	1.74	0.00	0.44
Fe	0.28	0.00	0.00	0.00	0.40	0.80
Cu	0.00	0.00	0.00	0.00	0.00	0.00
Pt	54.81	55.60	58.47	56.22	57.68	56.46
Ir	0.00	3.44	0.00	0.00	0.00	1.56
Os	0.00	0.00	0.00	0.00	0.00	0.00
Pd	0.00	0.00	0.00	0.00	0.00	0.00
Rh	0.00	0.74	0.00	0.00	0.00	1.28
Ru	0.00	0.00	0.00	0.54	0.00	0.00
S	0.88	0.80	0.55	0.43	0.00	0.92
As	39.32	37.32	37.70	37.41	36.09	38.27
Sb	0.00	2.09	1.59	3.13	1.54	0.65
Total	98.94	99.99	98.31	99.47	95.71	100.38

Number of atoms on the basis of 2 S+As+Sb

	1	2	3	4	5	6
Ni	0.23	0.00	0.00	0.11	0.00	0.03
Fe	0.02	0.00	0.00	0.00	0.03	0.05
Cu	0.00	0.00	0.00	0.00	0.00	0.00
Pt	1.02	1.06	1.12	1.07	1.20	1.06
Ir	0.00	0.07	0.00	0.00	0.00	0.00
Os	0.00	0.00	0.00	0.00	0.00	0.00
Pd	0.00	0.00	0.00	0.00	0.00	0.00
Rh	0.00	0.03	0.00	0.00	0.00	0.05
Ru	0.00	0.00	0.00	0.02	0.00	0.00
S	0.10	0.09	0.06	0.05	0.00	0.11
As	1.90	1.84	1.89	1.85	1.95	1.88
Sb	0.00	0.06	0.05	0.10	0.05	0.02

1. 6007
2. 6012
3. 6027
4. 6029
5. 6033B
6. 6035

Compositions of stibiopalladinite and Pd-Sb-Te phases

	1	2	3	4	5	6	7
Ni	0.00	0.00	0.00	0.27	4.14	2.76	1.10
Fe	1.40	0.36	0.00	0.56	0.65	0.00	0.00
Cu	4.33	4.03	3.47	4.50	0.00	0.00	0.00
Pt	0.00	0.00	0.00	0.00	0.00	0.00	0.00
Ir	0.00	0.00	0.00	0.00	0.00	0.94	0.00
Os	0.00	0.00	0.00	0.00	0.00	0.00	0.00
Pd	66.59	63.62	65.59	61.25	59.74	43.53	41.20
Rh	0.00	0.00	0.00	0.00	0.00	0.00	0.00
Ru	0.00	0.00	0.00	0.00	0.00	0.00	0.00
S	0.00	0.00	0.00	0.00	0.00	0.00	0.00
As	0.00	0.00	0.00	0.00	0.00	0.00	0.00
Sb	27.67	30.00	30.81	28.77	9.87	21.10	23.00
Te	0.00	0.00	0.00	0.00	25.60	31.67	30.60
Total	99.99	98.01	99.87	95.35	100.00	100.00	95.90

Number of atoms on the basis of 2 S+As+Sb

	1	2	3	4	5	6	7
Ni	0.00	0.00	0.00	0.04	0.51	0.22	0.09
Fe	0.22	0.05	0.00	0.08	0.08	0.00	0.00
Cu	0.60	0.52	0.43	0.60	0.00	0.00	0.00
Pt	0.00	0.00	0.00	0.00	0.00	0.00	0.00
Ir	0.00	0.00	0.00	0.00	0.00	0.02	0.00
Os	0.00	0.00	0.00	0.00	0.00	0.00	0.00
Pd	5.53	4.87	4.89	4.89	4.07	1.95	1.81
Rh	0.00	0.00	0.00	0.00	0.00	0.00	0.00
Ru	0.00	0.00	0.00	0.00	0.00	0.00	0.00
S	0.00	0.00	0.00	0.00	0.00	0.00	0.00
As	0.00	0.00	0.00	0.00	0.00	0.00	0.00
Sb	2.00	2.00	2.00	2.00	0.59	0.82	0.88
Te	0.00	0.00	0.00	0.00	1.41	1.18	1.12

1. 6007 stibiopalladinite
2. 6012   "
3. 6012   "
4. 6033B   "
5. 6027 ?
6. 6027 ?
7. UN 1974-6   + 4.3% Bi

APPENDIX 3

Compositions of laurite hollingworthite and Rh-Ir-As-S phases
----

	1	2	3	4	5	6	7	8
Ni	0.00	0.00	0.00	0.00	0.00	0.78	0.00	0.00
Fe	0.23	0.00	0.56	2.43	0.00	0.93	0.00	0.32
Cu	0.00	0.00	0.96	1.48	0.00	0.00	0.00	0.00
Pt	0.00	0.00	0.00	0.60	6.31	4.88	7.17	0.00
Ir	2.38	0.00	0.00	0.00	0.00	31.58	39.20	10.27
Os	3.39	8.52	0.00	0.00	2.02	0.00	1.10	2.69
Pd	1.31	0.00	3.37	0.00	0.00	0.00	0.00	0.79
Rh	2.69	0.00	49.17	45.80	44.00	19.03	10.97	12.54
Ru	52.87	53.07	0.00	0.00	0.00	3.00	4.41	31.14
S	35.18	38.41	15.51	15.55	15.24	12.87	12.76	26.42
As	2.92	0.00	30.43	33.01	32.43	26.93	24.42	15.83
Sb	0.56	0.00	0.00	1.13	0.00	0.00	0.00	0.00
Total	101.53	100.00	100.00	100.00	100.00	100.00	100.03	100.00

Number of atoms on the basis of 2 S+As+Sb

	1	2	3	4	5	6	7	8
Ni	0.00	0.00	0.00	0.00	0.00	0.03	0.00	0.00
Fe	0.01	0.00	0.02	0.09	0.00	0.04	0.00	0.01
Cu	0.00	0.00	0.03	0.05	0.00	0.00	0.00	0.00
Pt	0.00	0.00	0.00	0.01	0.07	0.07	0.10	0.00
Ir	0.02	0.00	0.00	0.00	0.00	0.43	0.56	0.10
Os	0.03	0.07	0.00	0.00	0.02	0.00	0.02	0.03
Pd	0.02	0.00	0.07	0.00	0.00	0.00	0.00	0.01
Rh	0.05	0.00	1.07	0.95	0.94	0.49	0.29	0.24
Ru	0.92	0.88	0.00	0.00	0.00	0.08	0.12	0.60
S	1.92	2.00	1.09	1.04	1.05	1.05	1.10	1.59
As	0.07	0.00	0.91	0.94	0.95	0.95	0.90	0.41
Sb	0.01	0.00	0.00	0.02	0.00	0.00	0.00	0.00

1. 6027 laurite
2. 6033B   "
3. 6007 hollingworthite
4. 6033B   "
5. 6033B   "
6. 6007 hollingworthite-irarsite group
7. 6007   "
8. 6007   ?

Compositions of pentlandite

	1	2	3	4	5	6
Ni	39.69	37.24	38.34	32.13	35.41	34.55
Co	0.80	0.77	0.89	1.13	0.56	0.94
Fe	24.66	26.98	26.16	26.95	30.41	29.19
Cu	0.50	0.00	0.00	6.37	0.00	0.00
S	32.49	33.11	33.67	31.91	33.60	33.35
As	0.79	0.34	0.00	0.34	0.00	0.00
Sb	0.00	0.00	0.00	0.00	0.00	0.00
Total	98.93	98.44	99.06	98.83	99.98	98.03

Number of atoms on the basis of 1 S+As+Sb

	1	2	3	4	5	6
Ni	0.66	0.61	0.62	0.55	0.58	0.57
Co	0.01	0.01	0.01	0.02	0.01	0.02
Fe	0.43	0.47	0.45	0.48	0.52	0.50
Cu	0.01	0.00	0.00	0.10	0.00	0.00
S	0.99	1.00	1.00	1.00	1.00	1.00
As	0.01	0.00	0.00	0.00	0.00	0.00
Sb	0.00	0.00	0.00	0.00	0.00	0.00

1. 6007
2. 6010
3. 6012
4. 6029
5. 6029
6. 6135

APPENDIX 5

Compositions of Ni and Ni-Co sulphides

	1	2	3	4	5	6
Ni	67.42	64.98	72.58	69.41	73.70	48.10
Co	0.00	0.00	0.00	0.00	0.00	16.67
Fe	0.21	0.50	0.00	0.24	0.35	0.00
Cu	0.00	0.00	0.00	0.00	0.00	0.00
S	31.58	31.55	27.17	25.09	27.26	25.94
As	0.00	0.00	0.40	0.75	0.00	9.32
Sb	0.00	0.00	0.00	0.00	0.00	0.00
Total	99.21	97.03	100.15	95.49	101.31	100.03

Number of atoms on the basis of 2 S+As+Sb

	1	2	3	4	5	6
Ni	2.33	2.25	2.90	2.99	2.96	1.76
Co	0.00	0.00	0.00	0.00	0.00	0.61
Fe	0.01	0.02	0.00	0.01	0.01	0.00
Cu	0.00	0.00	0.00	0.00	0.00	0.00
S	2.00	2.00	1.99	1.97	2.00	1.73
As	0.00	0.00	0.01	0.03	0.00	0.27
Sb	0.00	0.00	0.00	0.00	0.00	0.00

1. 5001 godlevskite
2. 5019   "
3. 6010 heazelwoodite
4. 6013   "
5. 6029   "
6. 6013

Compositions of Ni arsenides.

	1	2	3	4	5	6	7
Ni	60.71	64.47	66.60	60.31	64.87	64.46	51.52
Co	0.00	0.00	0.00	0.00	0.00	0.00	0.00
Fe	0.00	0.37	0.26	2.39	0.26	0.35	0.68
Cu	0.00	0.00	0.00	0.00	0.00	0.00	0.00
S	0.00	0.00	0.00	1.91	0.00	0.00	0.54
As	38.18	35.72	33.03	28.75	35.12	35.98	41.58
Sb	0.00	0.00	1.00	3.35	0.50	0.00	0.78
Total	98.89	100.56	100.89	96.71	100.75	100.79	95.10

Number of atoms on the basis of 2 S+As+Sb

Ni	4.06	4.61	5.05	4.36	4.67	4.57	3.04
Co	0.00	0.00	0.00	0.00	0.00	0.00	0.00
Fe	0.00	0.03	0.02	0.18	0.02	0.03	0.04
Cu	0.00	0.00	0.00	0.00	0.00	0.00	0.00
S	0.00	0.00	0.00	0.25	0.00	0.00	0.06
As	2.00	2.00	1.96	1.63	1.98	2.00	1.92
Sb	0.00	0.00	0.04	0.12	0.02	0.00	0.02

1. 6007 orcellite
2. 6012   "
3. 6029   "
4. 6029   "
5. 6029   "
6. 6033B   "
7. 6024 maucherite

APPENDIX 7

Compositions of chromite

	1	2	3	4	5	6
Cr_2O_3	40.98	39.74	52.97	58.87	49.72	39.42
Al_2O_3	29.29	6.13	19.13	9.79	20.29	6.14
Fe_2O_3	3.50	25.00	1.50	4.90	0.90	22.30
FeO	10.78	11.85	11.94	15.17	19.93	26.70
MgO	17.27	12.63	15.34	12.20	10.23	3.51
Total	101.82	95.35	100.88	100.93	101.07	98.07

Number of ions on the basis of 32 oxygens

	1	2	3	4	5	6
Cr	7.45	8.75	10.22	12.06	9.85	9.04
Al	7.94	2.01	5.50	2.99	5.99	2.10
Fe^{3+}	0.61	5.24	0.28	0.96	0.17	4.87
Fe^{2+}	2.07	2.76	2.44	3.29	4.17	6.47
Mg	5.92	5.24	5.58	4.71	3.82	1.52

Fe^{3+} calculated by charge balance

1. 5001c
2. 5001e
3. 6013c
4. 6013e
5. 6042
6. 6042

APPENDIX 8

Compositions of chlorite

	1	2	3	4	5
SiO2	33.19	30.45	30.40	36.07	34.11
Al2O3	13.69	19.21	12.76	7.78	11.56
Cr2O3	1.17	0.00	5.99	3.85	1.34
FeO	1.52	0.92	0.90	1.97	2.15
MgO	35.61	33.18	33.03	37.02	34.61
NiO	0.38	0.38	0.53	0.00	0.00
Total	85.56	84.14	83.61	86.69	83.77

Total Fe as FeO

1. 6012 chromite dunite
2. 6013 chromitite
3. 6027   "
4. 6033B dunite
5. 6024 vein

APPENDIX 9

Compositions of serpentine minerals.

	1	2	3	4	5	6	7	8
SiO2	41.90	35.91	32.03	41.19	42.38	37.35	39.66	34.19
Al2O3	0.00	0.00	0.00	0.38	1.31	0.77	0.00	0.00
FeO	8.09	4.22	7.27	2.15	1.66	4.55	1.10	0.39
MgO	50.88	40.08	39.43	38.94	39.19	37.75	39.52	1.50
NiO	0.24	0.25	0.33	0.33	0.00	2.02	1.97	37.25
Total	101.11	80.46	79.06	82.99	84.54	82.44	82.25	73.33

Total Fe as Feo

1. 6029 olivine
2. 6029 serpentine
3. 6042   "
4. 6135   "
5. 6024   "
6. 6024   "
7. 6012   "
8. 6033A   "